Title
Cyteine protease trafficking and function in Giardia lamblia

Author
Abodeely, Marla E

Publication Date
2006

Peer reviewed|Thesis/dissertation

Cysteine protease trafficking and function in *Giardia lamblia*

by

Maria E. Abodeely

DISSERTATION

Submitted in partial satisfaction of the requirements for the degree of

DOCTOR OF PHILOSOPHY

in

Biomedical Sciences

in the

GRADUATE DIVISION

of the

UNIVERSITY OF CALIFORNIA, SAN FRANCISCO

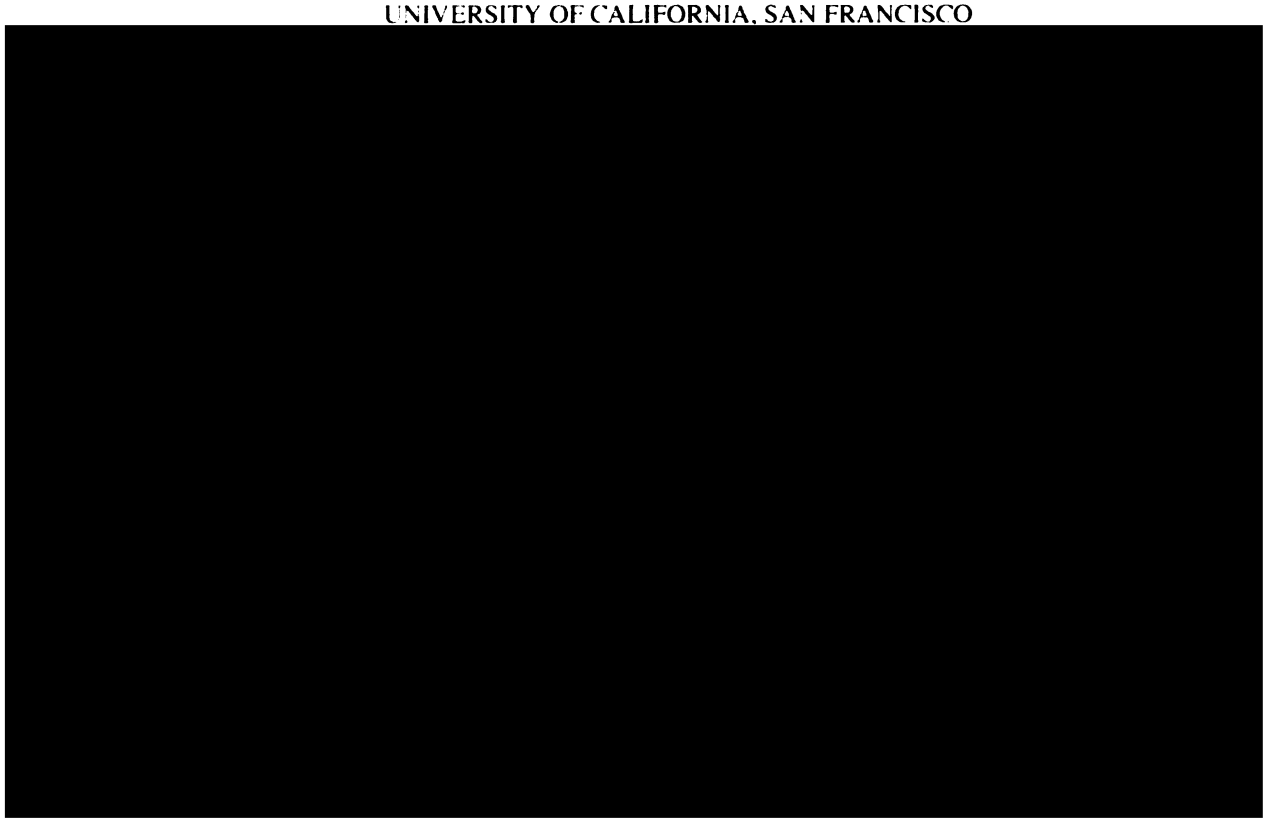

Acknowledgements

I define my experience in graduate school primarily by the relationships that I have formed during this very significant time in my life and not simply by the science, itself. There are so many people who have contributed to my scientific, professional and personal development during my time at UCSF that I can hardly find the space to thank you all.

First and foremost, I must first thank my advisor, Jim McKerrow. Seven years and three campuses after joining his lab, I was finally successful at putting together a story of which I am very proud and could not have done without his guidance. Jim is dedicated not only to discovering therapies for neglected diseases afflicting developing nations, but he is also dedicated to understanding the parasites themselves. He marvels at new discoveries that reveal how a parasite manages to survive and thrive in its host. His enthusiasm for science is contagious. Jim has also put together an equally enthusiastic group of scientists who are collaborative and view science and research as fundamentally fun.

To Rick Brown and Keith Mostov, thank you for always making time to advise me on this project.

I never imagined that my graduate experience would include someone like Mohammed "Saj" Sajid. I never would have imagined that I could be so fortunate. He taught me to think critically and creatively even when data seemed unexplainable. He encouraged me to step out on a limb and analyze my results from different perspectives with confidence and a sense of humor.

I have known Linda Brinen throughout graduate school as both a postdoctoral fellow and faculty member. I have always enjoyed and taken comfort in our discussions on science, politics, life and everything in between. She has been a true mentor and

friend.

Kelly Dubois and I are team *Giardia*. We have had a lot of fun brainstorming how this quirky organism works. Kelly and I had each other both to commiserate and, more importantly, to appreciate each other's successes. I want to wish her all of the best in her future adventures.

Zachary Mackey would probably never want me to say or write thank you, but since I have always loved to bug him, why stop now? I must say simply that Zac keeps me honest and has always helped me to remember my priorities. I have always admired his discipline and intellectual drive. I know there are many successes in his future. I would also like to give a special thank you to Chris Franklin who has taught me to embrace technology and pointed me in the direction of delicious Bay Area treats.

There are so many other members of the McKerrow Group, present and past, who have given me support over the years: Patricia Doyle, Juan Engel, Ivy Hsieh, Joey Hansell and her husband Peter, Stephanie Wang, Melaine Delcroix, Ryan Kells Swenerton, Jan Dvorak, Moumita and Anjan Debnath, Rachel Marion, Arthur Baca, Landys Lopez-Quezada and our own resident musician, Ben Kelly, to name only a few! I would also like to thank Conor Caffrey, who generously offered to read and edit the rough draft of my thesis. Before I even relocated to California, Conor taught me what a real St. Patrick's Day should be. My experience would not have been as productive or as memorable without you all.

Graduate school is a long and thorough process with its own set of trials and tribulations and of course it's rewards. I have met an unbelievable group of friends, who helped me to navigate obstacles at the bench, but who also reminded me of the rich world that existed around me. Melissa Lodoen, Maria Christophoru, Rebecca Blank and Luisa Stamm are among the scientists I respect most, and I feel very fortunate to be able to call them good friends.

To Sarah Sullivan Pulsifer, thank you for patiently listening to me and always

encouraging me even when Sunday walks became long distant phone calls. I feel very grateful and fortunate to have had your friendship.

I want to thank my grandparents, George and Sally Abodeely and David and Betty Atkinson, as well as my parents, William and Mary Ann Abodeely, and sisters, Alison and Rana Abodeely. Above all else, I want them to know just how much comfort I took in knowing that I could always count on their love and tremendous support. Thank you for encouraging me to find what I love and teaching me integrity, perseverance and patience to reach my goals. To my sisters, thank you for reminding me to laugh at life and myself while still being true to myself.

Finally, I must thank my husband, Matthew Trammell, for asking me whether I wanted to join him for a hamburger. Since then, my life has not been the same, and I am so thankful for that. Matt has been a loving husband, trusted friend and respected colleague. He has helped me to brainstorm obstacles at the bench while keeping my spirits up and my laughter forthcoming. My life would not have been as full or as much fun without you. Thank you.

Declaration

This dissertation is the result of my own work. Some figures have been included which resulted from the work of other members of the laboratory and these have been appropriately attributed in the figure legends and text.

Chapter three is based on data from a manuscript that will be submitted, titled, "A pluripotent compartment functions as ER and endosome/lysosome in *Giardia lamblia*". The following co-authors contributed helpful advice or reagents to this work: Kelly N. Dubois, Wanderley deSouza, Mohammed Sajid, Juan, C. Engel, Adrian Hehl, Ivy Hsieh. This work was done in collaboration with the lab of Adrian Hehl at the University of Zürich, Zürich, Switzerland. The Hehl lab provided antibodies against *Giardia* PDI2, clathrin, COPI and COPII. This work was also done in collaboration with the lab of Wanderley deSouza at the Universidade Federal do Rio de Janeiro, Rio de Janeiro, Brazil. The de Souza lab provided electron microscopy images of Glucose 6-phosphatase reaction in *Giardia lamblia*. Finally, I also thank Theodore Nash from the NIH for his kind gift of the *Giardia lamblia* transfection vector and Drs. CC Wang and Lei Li from the University of San Francisco for an altered version of the *Giardia lamblia* transfection vector.

This work was supervised by James H, McKerrow in the Department of Pathology at the University of California, San Francisco from October 2000 to November, 2006.

Cysteine protease trafficking and function in *Giardia lamblia*

by

Marla E. Abodeely

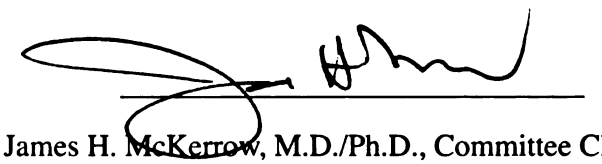

James H. McKerrow, M.D./Ph.D., Committee Chairman

Abstract

Giardia lamblia is one of the most common intestinal parasites worldwide and is the etiological agent of human *Giardiasis*, a major water-borne gastrointestinal disease. *Giardia*'s life cycle includes a binucleated trophozoite stage and an infective cyst stage. Protozoa utilize cysteine proteases as key factors for cellular functions. The major *Giardia* proteases are cathepsin B-like proteases, which are orthologous to mammalian lysosomal cathepsin B proteases and represent the earliest lineage of the cathepsin B proteases. The focus of this work was to define the subcellular localization and functional role of a major cysteine protease, *Gl*CP2, expressed by *Giardia.*

In order to investigate the functional roles of the *Gl*CPs, I utilized transfection, reporter constructs, functional protease assays, as well as immunofluorescence assays, confocal microscopy, affinity chromatography and mass spectrophotometry. In the vegetative trophozoite, I found that endocytosis and subsequent degradation of exogenous proteins occur in the ER-like compartment of an early diverging protozoan, which lacks peroxisomes, a classical Golgi and canonical lysosomes. I demonstrated that the *Gl*CPs function to degrade endocytosed host proteins in this ER-like tubulovesicular network (TVN). In addition, I found that the TVN dynamically fuses with clathrin-studded

vesicles at the cell periphery to receive endocytosed proteins. I also found that *Giardia* lacks several of the core endo- and exocytic Rab small GTPases that localize to the Golgi network, early and late endosomes in higher eukaryotic cells. *Giardia*, therefore, contains a transitional ER-like endomembrane structure, which predates compartmentalization of endocytic and lysosomal functions into organelles distinct from ER.

In addition, I showed a putative role for the *Gl*CPs during encystation. Previous work demonstrated that cysteine proteases are involved in encystation-specific vesicle (ESV) biogenesis, specifically cyst wall protein (CWP) processing. I co-localized *Gl*CP2 and CWPs to ESVs by transfection of *Gl*CP2-GFP fusion constructs, confocal microscopy and immuno-electron microscopy. Using affinity chromatography and mass spectrophotometry, I also investigated whether *Gl*CP2 interacts with other proteins during encystation.

This work provides insight into the early evolution of a protease trafficking pathway that continues to function in higher eukaryotes and contribute to the goal of validating cysteine proteases as a drug target for *Giardiasis*.

Table of Contents

Chapter One

An introduction to *Giardia lamblia* as parasite and living fossil

Giardia lamblia

Giardia lamblia (syn. *G. intestinalis, G. duodenalis*) is one of the most common intestinal parasites worldwide and is the etiological agent of human *Giardiasis*, a major water-borne gastrointestinal disease (1-3). *Giardia* is transmitted through exposure to fecally contaminated water or food and may lead to severe diarrhea, nausea, vomiting, and weight loss. Exposures commonly occur in restaurants, daycare facilities, and among travelers (1,3,4).

The simple *Giardia* life cycle includes a binucleate trophozoite stage and a tetranucleated protective cyst stage (Figure 1.1).

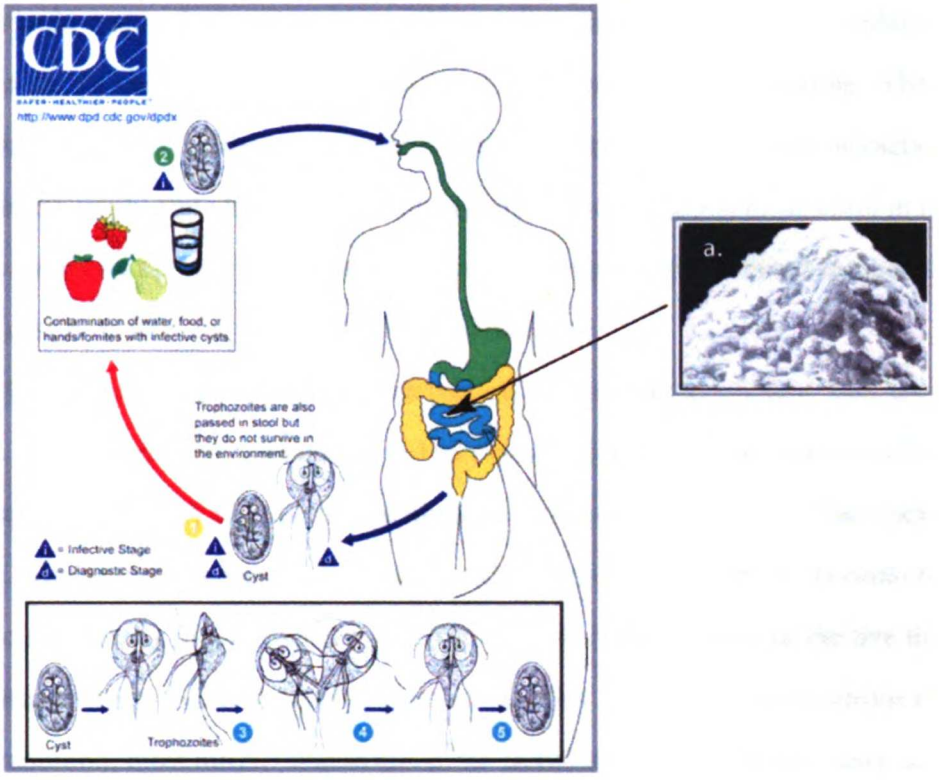

Figure 1.1. The Giardia lamblia life cycle. Giardia is transmitted by ingestion of infective cysts that may be found in fecally contaminated food or water (1 and 2). The protective cysts pass through the acidic stomach into the more basic upper small intestine, the duodenum, where two replicating trophozoites emerge from a single cyst (3, excystation). The trophozoites replicate asexually (4) to colonize the duodenum and use their adhesive disc to adhere to the intestinal wall (a). As trophozoites travel through the intestine, they are stimulated to produce a cyst wall (encystation) in order to survive in the environment outside of a vertebrate reservoir host (5).

The trophozoites replicate asexually in the lumen of the upper small intestine and differentiate into cysts that are then shed in the feces. The *Giardia* cyst wall is a 300nm thick fibrous structure of approximately 57% protein and 43% carbohydrate (5). Though little information is available about the cyst formation, it is the key barrier that has to be compromised to initiate a new infection. Fecal-oral transmission of the cysts between mammalian hosts leads to the spread of infection.

During ingestion, the cyst passes through the acidic environment of the stomach (pH3-4) to the basic environment of the small intestine (pH8-9). These environmental cues in a yet to be defined pathway stimulate a pair of replicating trophozoites to emerge from a single cyst in the host's upper small intestine, the duodenum. The trophozoites colonize the duodenum by attachment to the lumenal surface of the intestine. The adhesive disc located on the ventral side of the trophozoite mediates this interaction. In addition, the trophozoite has four pairs of flagella that are believed to function in motility. As *Giardia* travel through the intestine, they are stimulated by undefined mechanisms to initiate cyst formation for survival outside of the host.

Giardia is a single-cell protozoan parasite and considered to be a "biological fossil". Phylogenetic analyses based on 16S ribosomal RNA and on protein-coding gene sequences classify *Giardia* as one of the earliest known branches in the eukaryotic lineage, prior to the divergence of the plant and animal kingdoms (6-8). *Giardia* has a genomic complexity of approximately 12Mb with 4-8 copies of each of the five linear chromosomes and a GC content of approximately 46%. Few genes have introns (5,9-11). In addition, most mRNA transcripts in the trophozoite stage not only have unusually short 5' untranslated regions of only 1-6 nucleotides, but also short polyA tails (12). Interestingly, there is little evidence of capping and sequences resembling bacterial internal ribosome entry sites have been identified (13).

Unlike the other eukaryotic cells, the microaerophilic *Giardia* is distinguished by several non-eukaryotic properties. It is binucleated, but devoid of a nucleolus as well

as a classical Golgi apparatus (see below) and peroxisomes. In higher eukaryotes, the Golgi functions to enzymatically modify cargo proteins destined to function in different cellular compartments or for secretion. The classical Golgi network morphology consists of a series of flattened sacs called cisternae, which have not been observed in *Giardia* (2). Furthermore, several Golgi-associated enzymes and Golgin (the Golgi structural component) have not been identified in the recently completed *Giardia* genome. Despite lacking a discernible Golgi, *Giardia* is able to conduct endocytic and exocytic processes (14). In the vegetative trophozoite, the exocytic system functions as a constitutive secretory pathway to carry variant surface proteins (VSPs) to the plasma membrane (15). VSPs may serve to help the parasite evade the host immune system. Interestingly, in the encysting trophozoite, the exocytic pathway behaves as a regulated secretory pathway in which external stimuli through uncharacterized signaling pathways, initiates formation of encystation-specific vesicles (ESVs) to carry the newly synthesized cyst wall proteins (CWPs) to the cell surface where they are secreted and assembled into the cyst wall (16,17).

Does *Giardia* have a Golgi?

An ongoing debate is whether the nascent ESVs comprise a transient Golgi that is developmentally regulated in the encysting cell. Studies have demonstrated developmental regulation of ESV biogenesis (18-20) and transcription and translation of CWP in encysting cells (10,11,17,21,22). How does *Giardia* maintain the endomembrane system and secretory pathways without a Golgi and, secondly, are Golgi functions carried out by other compartments in the *Giardia* cell? This quandary leads to the fundamental question of what defines the Golgi as an endomembrane compartment? The CWPs contain signal sequences that direct the proteins to the regulated secretory pathway via entry into an ER-like compartment where they are packaged into budding vesicles. The CWP-containing budding vesicles, ESVs, undergo a dynamic maturation process. In the early stages of ESV biogenesis, Marti *et al.*, (2003) observed that early

ESVs are located closer to the perinuclear region, co-localizing with antibodies to the small GTPase, sar1p, which is associated with COPII coatomer and found on the ER-like membranes in vegetative cells. In mammalian systems, COPII functions in ER to Golgi anterograde transport (23,24). Maturing ESVs are differentially associated with Giβ-COP1 and GiYip, the *Giardia* orthologues of the respective mammalian coatomer protein COP1 and yeast Yip1p. In mammalian systems, COP1 functions in retrograde transport pathways, recycling ER resident proteins from the Golgi to the ER. More recently, COPI has been implicated in protein trafficking traversing the cisternae of the Golgi network in anterograde pathways (24). In yeast, Yip1p was initially identified by its interaction with the Ypt1p (the yeast Rab1 small GTPase). It localized to the ER membrane and was implicated in ER to Golgi trafficking. As in yeast, *Gi*Yip one is also observed to associate with the nuclear envelope/ER membrane in vegetative trophozoites, while *Gi*β-COP1 is localized toward the periphery of the cell near the peripheral vesicles (PVs) (25). The association of the coatomer and small GTPases proteins with ESVs is significant as these proteins are known to function in the Golgi network in higher eukaryotic systems, suggesting Golgi-like characteristics of ESVs. In support of this concept, most ESV biogenesis and trafficking is sensitive to Brefeldin A (26). It is noteworthy that the VSG constitutive pathway is also sensitive to Brefeldin A suggesting that some Golgi functions are present in this life stage though a distinct 'classical' Golgi structure has not been detected. Protein trafficking in both life stages is insensitive to the microtubule depolymerizing drug nocodazole, which disrupts Golgi morphology in other eukaryotic systems. In the final stages of *in vitro* encystation, the maturing ESV in proximity to the periphery of the cell is coated with *Giardia* clathrin, GiCLH, which is concurrently associated with the PVs. This observation suggests that the ESVs do indeed undergo a maturation process and that this process may parallel the maturation process observed between the cis-, medial- and trans-Golgi cisternae (Figure 1.2).

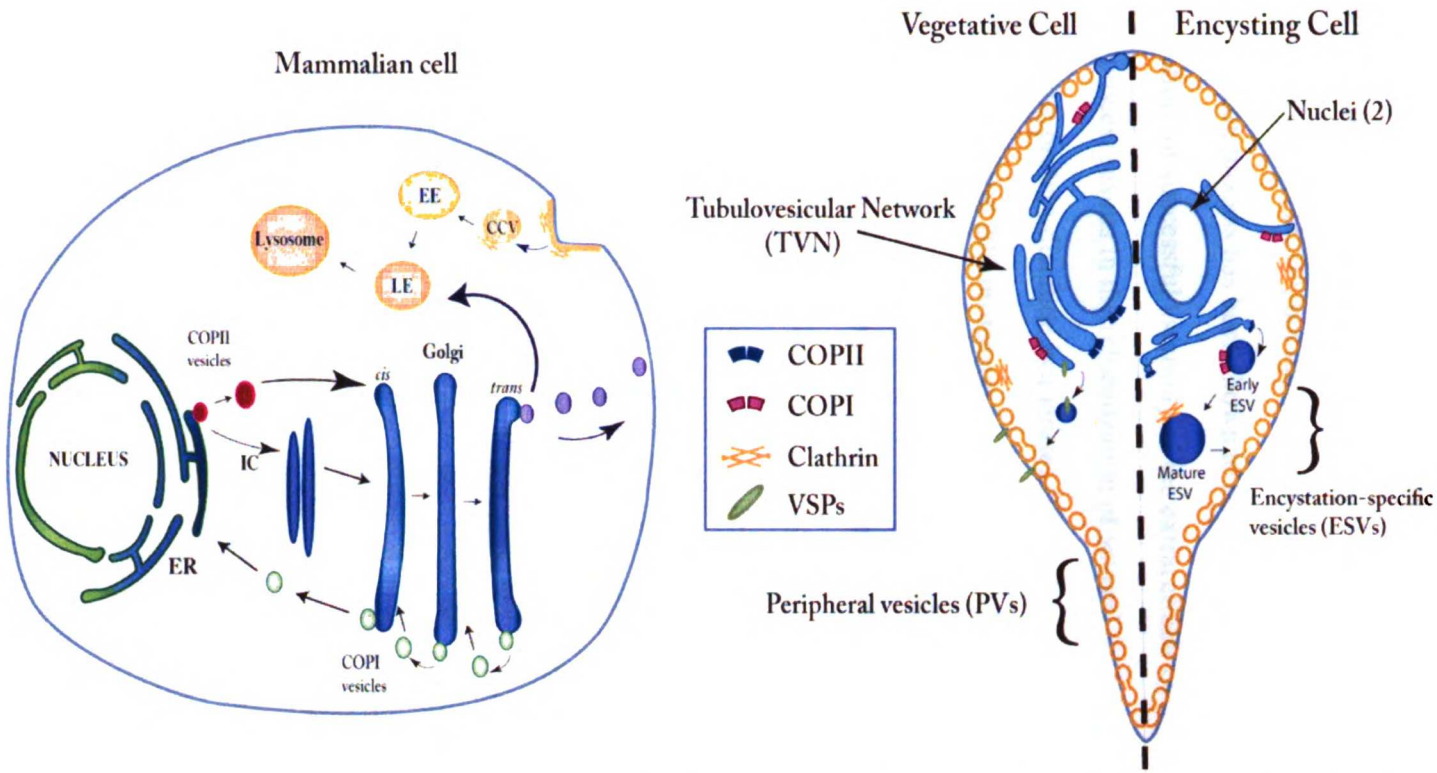

Figure 1.2. The endomembrane systems of a mammalian cell and a Giardia trophozoite. In mammalian cells, anterograde transport of endomembrane and secreted proteins is regulated by COPII from the ER to the intermediate compartment (IC) to the Golgi network. Retrograde protein traffick transversing the Golgi (trans to cis) and Golgi to ER is mediated by COPI. The binucleated Giardia trophozoite has a simple endomembrane system that includes a nuclear envelope, ER-like tubulovesicular network (TVN), peripheral vesicles (PVs) and encystation-specific vesicles (ESVs) under encysting conditions. The trophozoite undergoes both vegetative growth in the host (left of the dashed line) and encystation in preparation for exiting the host (right of the dashed line). During vegative growth, the exocytic pathway functions constitutively to traffic VSPs to the plasma membrane. During encystation, the exocytic pathway functions as a regulatory pathway to traffic the newly synthesized cyst wall proteins to the cell periphery for secretion and cyst wall formation. COPII is found localized to the ER-like TVN and maybe involved in VSP and CWP packaging for secretion. COPI is found localized to an endomembrane compartment underneath the clathrin-studded PVs in vegetative trophozoites and to early ESVs in encysting cells. In both life stages clathrin is observed at the PVs and associated with mature ESVs in encysting cells.

Protein quality control in *Giardia*

In addition to having Golgi-like properties, ESVs have also been observed to have ER-like properties. CWPs undergo a maturation process to ensure cyst wall synthesis, including phosphorylation (27), reshuffling of disulfide bonds (28) and processing (11,21), not unlike proteins that traverse the Golgi cisternae. This maturation process has been shown to be essential and must be completed prior to secretion for successful assembly of the extracellular cyst wall (16,17). Furthermore, this process results in the relocalization of several *Giardia* ER proteins to ESVs, including protein-disulfide isomerases (PDI) (29), the heat shock protein Bip/Hsp70 (GiBip) (30) and 20S proteasome subunit (31). In vegetative cells PDI is an ER marker, though it is not surprising that it is found associated with ESVs since CWP1 and CWP2 form heterodimers mediated by disulfide bonds (28). Interestingly, DTT treatment of encysting cells inhibits CWP processing and cyst wall formation (32,33). In previous work, GiBip had been identified and localized to the perinuclear and ER-like compartment of vegetative cells. Hehl *et al.,* (2006) proposed that developmentally regulated relocalization of GiBip and the *Giardia* 20S proteasome subunit to the lumenal and cytosolic side of ESVs, respectively, reflects the need for CWP quality control. Bip/Hsp70A is known to function in ER-associated quality control to rid the cell of improperly folded proteins by exporting them out of the ER and secretory pathway into the cytosol for targeted degradation by the cytosolic proteasome (34). Incidentally, both PDI and GiBip contain the conserved ER-retrieval sequence KDEL. The proteasome has been shown to relocalize to the ER membrane in higher eukaryotic cells. Since there is a dramatic increase in cyst wall protein synthesis, Stefanic *et al.,* (2006) suggest that the GiBip and *Giardia* proteasome subunit function to eliminate misfolded and/or unprocessed CWPs from the ESVs to ensure the essential process of cyst wall formation. A classical Golgi marker in higher eukaryotes, C (6)-NBD-ceramide, which shows high affinity for Golgi membranes, did in fact label ESVs although it was also observed to

label the perinuclear/ER region (35). These data give us insight into the nature of ESVs though it remains unclear as to whether ESV biogenesis is due to *de novo* synthesis of an "encystation-specific" Golgi or, alternatively, is simply the reorganizing and restructuring of compartments that already exist in the vegetative cell.

The mitochondria controversy

Until recently, *Giardia* was grouped along with other amitochondrial eukaryotes in the Archezoa kingdom (36). Archezoa contain the most primitive ancient extant eukaryotes, most of which do not have classical mitochondria. However, a series of recent discoveries have started to paint a different picture. Many of the archezoal parasites have been found to have either a set of mitochondrial enzymes and/or have remnants of a mitochondrial structure. For example, the microsporidian obligate intracellular parasite, *Trachipleistophora hominis*, and the protists, *E. histolytica* and *T.vaginalis* have each been shown to contain either mitosomes or hydrogenosomes, which are mitochondrial-like organelles often referred to as mitochondrial "relics" (37-41). These remnant organelles along with chloroplasts (42) are considered to be part of the mitochondrial family of common ancestral descent (43-47). Hydrogenosomes are hydrogen-producing, double-membraned structures that function in the assembly of iron-sulfur complexes into apoproteins, and are thought to be a type of anaerobic mitochondria (46). First discovered in *E. histolytica* by Tovar and colleagues (1999), mitosomes also comprise a double membrane and Fe-S cluster biogenesis and assembly machinery. There is now recent evidence that *Giardia* does in fact have a mitosomes and may have once had mitochondria, but that they evolved their morphology and function to accommodate *Giardia* in the current ecological niche it occupies. The idea that archezoal lineages diverged from the eukaryotic branch before the mitochondrial symbiotic event and that archezoal *Giardia* is a direct descendent of a premitochondrial eukaryote has been significantly challenged.

Giardia is often referred to as an anaerobe, but it is in fact a microaerophilic

organism being able to survive in a very low oxygen environment. This may explain why the absence of mitochondria was not surprising at first and why it may have mitochondrial remnants, the mitosomes, in place of classical mitochondria. In higher eukaryotic organisms, mitochondria are described as cellular power plants since they serve as the primary source of cell's energy, ATP, through an oxygen-dependent process called oxidative phosphorylation. Mitochondria are found in the hundreds to thousands dispersed throughout of the cytoplasm and aside from the nucleus, they are the only organelles in animal cells to have a double membrane. In addition to ATP synthesis, mitochondria have their own DNA and several other unique pathways, including amino acid synthesis, as well as the biogenesis, assembly and maturation of iron-sulfur clusters (48). The mature Fe-S clusters are incorporated into functional redox and electron transport proteins either in the mitochondria or transported to the cytoplasm for protein complex formation.

Though the *Giardia* cell is microaerophilic, it still requires energy in the form of ATP as in all cells. *Giardia* synthesizes ATP using cytosolic Fe-S-containing proteins in anaerobic pathways (49,50). Among these Fe-S cluster containing proteins are hydrogenases (46,51), ferredoxins and pyruvate:ferredoxin oxioreductase (46,49). Interestingly, orthologues of two enzymes responsible for Fe-S cluster biogenesis were identified in *Giardia*, cysteine desulferase (IscS) and a scaffolding protein (IscU). Using immuno-electron microscopy, Tovar *et al.*, (2003), observed that *Gi*IscS and *Gi*IscU co-localized to the inner membranes of the double-membraned tiny sacs throughout the cytoplasm. They proposed that the observed tiny sacs (~24) were, in fact, the mitochondrial equivalent in this protist and referred to them as mitosomes. In a separate set of experiments, Lloyd and colleagues (2002) used mitochondrion-specific dyes to demonstrate that discrete cytoplasmic structures in *Giardia* have an electron potential, characteristic of mitochondria and hydrogenosomes. Additional studies are needed to determine whether the structures Lloyd *et al.*, (2002) identified the mitosomes that Tovar

et al., (2003) observed. Furthermore, genes for chaperonin 60 (cpn60) (52) and valyl-tRNA synthetase (53) otherwise found in mitochondria were detected in the nuclear DNA of *Giardia*. Interestingly, the *Giardia* cpn60 gene is most closely related to a homolog in alpha-proteobacteria. Alpha-proteobacteria is the closest extant relative to prokaryotes that gave rise to mitochondria (54).

In summary, these findings have led many to conclude that *Giardia* did at one time have mitochondria. Nevertheless, some researchers in the field question the hypothesis that the mitosome of *Giardia* is in fact a mitochondrial relic, and that it diverged from the eukaryotic plant after an endosymbiotic event. Researchers point to controversial experimental evidence that the cpn60 protein does not localize to the mitosomes in *Giardia*. Also, phylogenetic analyses using ribosomal RNA (6) and elongation factors 1 and 2 (8), place the emergence of *Giardia* before the mitochondrial transfer event. In any case, this protist can still be considered as one of the earliest eukaryotic cells and may serve as a model system to study organelle compartmentalization, as well as protein molecular evolution regardless of whether mitosomes have evolved by lateral gene transfer, a separate endosymbiotic event or are simply reduced mitochondrial relics.

Chapter Two

Clan CA cysteine proteases in *Giardia*

Cysteine protease nomenclature

Isolated in 1879 from the tropical fruit *Carica papaya*, papain was the first cysteine protease to be identified and, also the first cysteine protease to be structurally solved (55). Proteases are referred to as biological catalysts due to their facilitating efficient cleavage of peptide bonds in proteins or peptides at rates up to one million times a second (56). There are four major categories of proteases, aspartyl-, metallo-, serine-, glutamate and cysteine-proteases, named according to the key residue(s) or metal ion(s) that participate directly in the catalytic mechanism. Cysteine proteases are defined by their catalytic mechanism that employs an indispensable cysteine residue, such that the sulfur of the cysteine sulfydryl group is the nucleophile involved in peptide bond cleavage.

In addition to classification by the catalytic residue, proteases may also be defined by the type of reaction they catalyze. Proteases may function as exopeptidases or endopeptidases, or both. Exopeptidases hydrolyze amino acid (s) or peptides from either the amino or carboxy terminus and are respectively referred to as aminopeptidases and carboxypeptidases. Endopeptidases cleave peptide bonds within peptides or proteins. In a major effort to refine the protease classification system, Barrett and Rawlings developed a system located at the MEROPS website (www.merops.sanger.ac.uk). Under MEROPS, proteases are classified into clans, families and subfamilies according to the known crystal structures (when available) and sequence homology spanning the catalytic residues (57,58). In this system, each of the mechanistic classes is divided into clans that share a common ancestry and are proposed to be the product of convergent molecular evolution (56). Clan designations contain two letters: the first letter corresponds to the catalytic type with the exception that the letter P is used when a clan is composed of more than one catalytic type. To date, cysteine proteases are organized into clans as follows: CA, CD, CE, CF, CH, CL, C-, PA(C), and PB(C) (www.merops.sanger.ac.uk) (Figure 2.1).

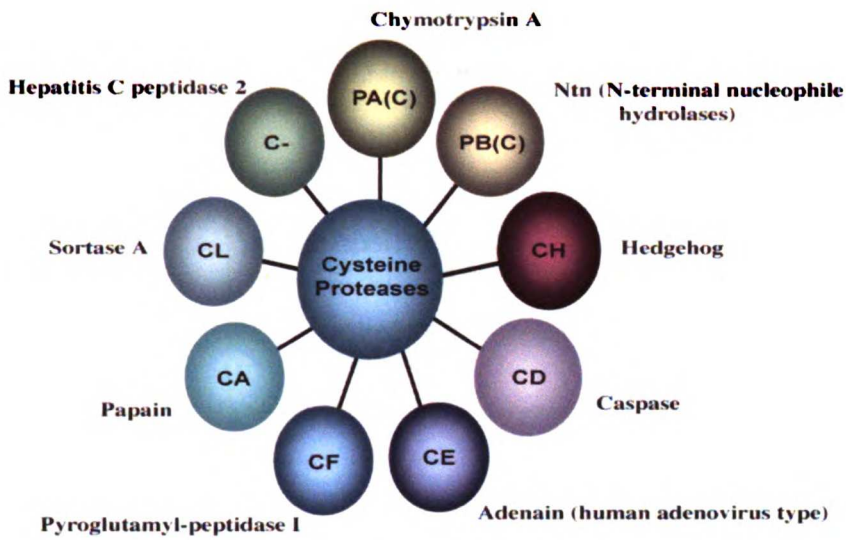

Figure 2.1. Schematic of the cysteine protease superfamily. To date, parasite cysteine proteases are restricted to clan CA (papain). Giardia lamblia proteases investigated in this work belong to clan CA (papain-like).

Among parasites to date, cysteine proteases are restricted to clan CA (for which the template enzyme is the aforementioned plant enzyme papain) and clan CD (for which the template enzyme is human caspase 3). Clan CA is the larger of the two containing 32 families whereas clan CD consists of five families. I will focus on clan CA family C1 subfamily C1A enzymes, specifically cathepsin Bs. The C1A subfamily includes secreted and lysosomal proteases such as cathepsins B, C, L, H, K and O (Figure 2.2).

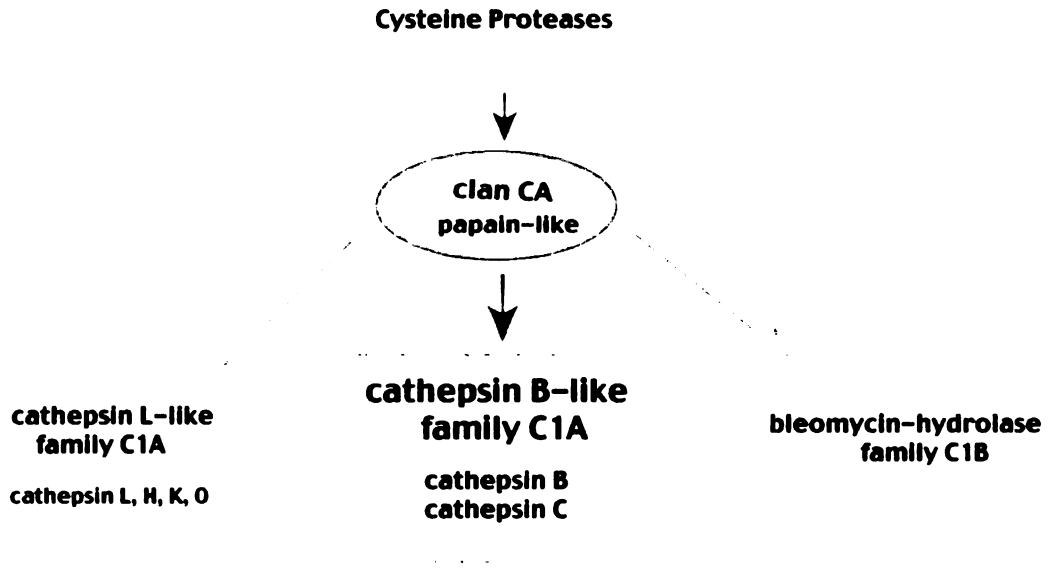

Figure 2.2. Schematic of clan CA family C1 subfamily C1A enzymes. The C1A subfamily includes secreted and lysosomal proteases.The focus of this work is on the cathepsin B-like cysteine proteases in Giardia lamblia.

Mechanism of action and specificity

Clan CA proteases utilize the sulfhydryl (or thiol) functional group of the active site cysteine residue (Cys25, mature papain numbering system) to cleave proteins and peptides (Figure 2.3). This cysteine is thus referred to as the "active site" cysteine to distinguish it from other non-catalytic cysteine residues within the protein. The sulfhydryl group has an increased nucleophilicity (attraction to the electrophilic carbonyl carbon of the scissile peptide bond) due to close proximity to another conserved, active site amino acid residue, histidine (His159). The functional side groups of the active site cysteine and histidine form the catalytically active thioloate-imidazolium charge relay dyad (Figure 2.4).

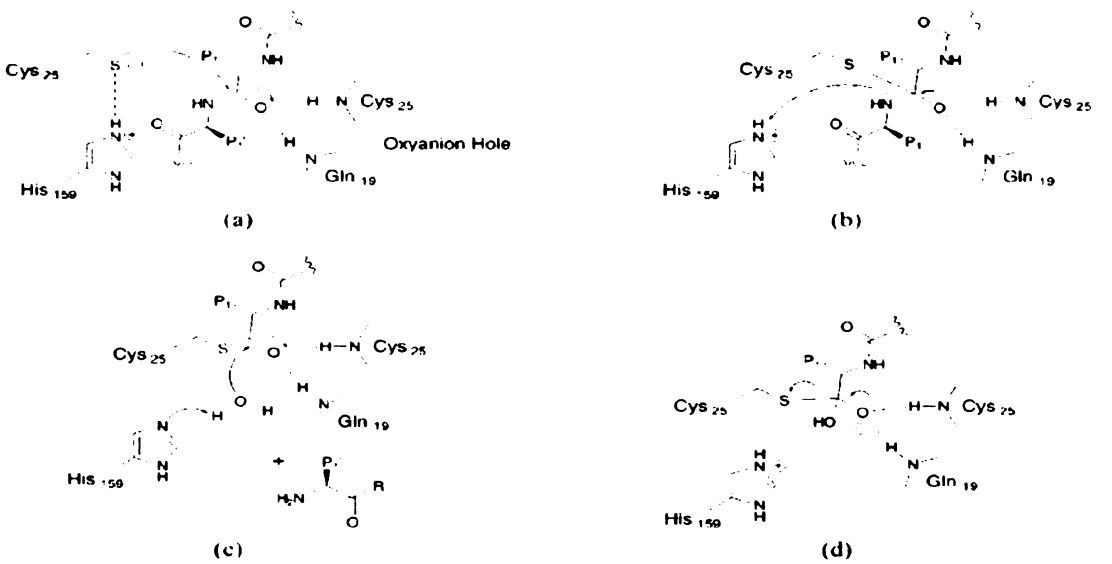

Figure 2.3. Catalytic mechanism of proteolysis by cysteine proteases. (Sajid and McKerrow, 2002). Due to the close proximity of the imidazole side group of the Histidine (His 159), the sulfhydryl group of catalytic cysteine (Cys25) is a reactive nucleophile (a). A transient covalent tetrahedral intermediate is formed between the enzyme and substrate (b). An amino leaving group is generated by the transfer of a proton from His 159 to the intermediate resulting in enzyme acylation (c). The final step is hydrolysis resulting in the release of the product acid of the substrate and a free enzyme (d).

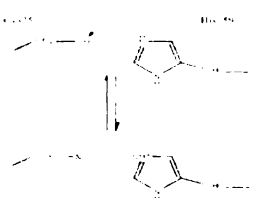

Figure 2.4. Thiolate-imidazolium charge relay dyad (Sajid and McKerrow, 2002).

In some cysteine proteases, a third residue, an asparagine/aspartic acid (Asn/Asp 175), can serve to stabilize and orient the imidazole functional group of the active site histidine, thereby maintaining and maximizing the nucleophilicity of the sulfur of the sulfhydryl. During catalysis, the active site cysteine forms a transient covalent anionic-tetrahedral intermediate with the substrate that is stabilized by a highly conserved glutamine residue (Gln19); the pocket formed is referred to as the oxyanion hole. Catalysis results in enzyme acylation and the release of the carboxyl portion of the substrate.

Domain structure and function

Cysteine proteases are synthesized as precursor enzymes or preproenzymes. The "pre" refers to the signal sequence, the hydrophobic nature of which directs the protease into the endoplasmic reticulum (ER) to be co-translationally translocated. The propeptide

acts as an internal chaperone to assist in both protein folding of the mature catalytic domain and as a reversible cognate inhibitor of the catalytic domain to prevent undesired enzymatic activity (59,60). Recent studies have also suggested that protease prodomains have roles in post-Golgi intracellular protein trafficking (61-63). Finally, the third domain of the protease gene product is the mature or catalytic domain, as it is functions directly in peptide substrate hydrolysis. In some cases, the third domain has a C-terminal extension that has postulated roles in intracellular trafficking, modulating the substrate specificity, inhibiting the activity of the enzyme, and diverting the host's immune system (64). However, in plants and trypanosmatid protozoa (for example, *Leishmania*), the functions of such C-terminal extensions are unknown (65-67).

The primary amino acid sequence of the catalytic domain dictates its molecular structure and those regions of the protein that directly interact with a substrate/inhibitor. The interaction between a protease and a substrate is illustrated schematically in Figure 2.5 and is based on the nomenclature originally described by Schechter and Berger (1967).

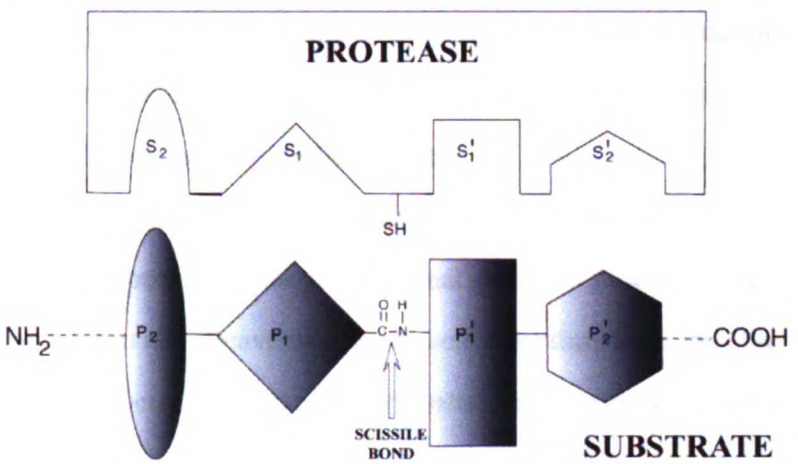

Figure 2.5. Nomenclature of the enzyme-substrate interaction. (Sajid and McKerrow, 2002). The protease subsite amino acid residues (P) and the substrate amino acid residues (S) are designated as P1', P2',...Pn' and S1', S2',...Sn' to the right of the sulfhydryl of the catalytic cysteine (SH) and the scissile bond (arrow), respectively. To the left of the catalytic cysteine and scissile bone, the residues of the protease and substrate are designated as P1, P2,...Pn and S1, S2,...Sn, respectively.

In this representation, the regions of the protease that directly interact with the substrate

are referred to as subsites: unprime S and prime S′ depending on whether they are positioned to the conventional left (amino) or right (carboxy) of the active site cysteine. The corresponding subsites of the peptide substrate are referred to as an unprime and prime and are given the letters P and P′, respectively. Cysteine proteases can vary in their substrate preferences among the different clans and families. For example, clan CA enzymes show substrate specificity primarily at the S_2 subsite while the substrate specificity of clan CD is defined by the S_1 subsite (58). Clan CA enzymes generally prefer hydrophobic side groups, which in most cases is as a direct result of a serine residue (Ser205) present at the bottom of the S_2 subsite or pocket. The preference for hydrophobic residues in the S2 pocket helps to explain why clan CA enzymes are inhibited by E64 and its derivatives. The fungal metabolite E64 (*L-trans*-epoxysuccinyl-leucylamide-(4-guanido)-butane) is an irreversible inhibitor of papain family enzymes. Cathepsin B sensitivity to E64 is mediated by a peptidyl moiety on the inhibitor that binds to the cathepsin B unprime subsites in a similar orientation as its propeptide (68,69). Interestingly, in addition to hydrophobic residues, vertebrate cathepsin B can accommodate positively charged residues such as arginine due to a glutamic acid or aspartic acid at the base of the S2 pocket.

Though cathepsin B, like most members of the family C1, is primarily thought of as an endopeptidase, it has an additional ability to function as an exopeptidase (70). Cathepsin B can also cleave two amino acids at a time from the C-terminus of the substrate and, therefore, is capable of functioning as a peptidyl dipeptidase. This activity is imparted by a unique 20 amino acid peptide loop located between the catalytic cysteine and histidine in the catalytic domain (70,71). The peptide loop contains two conserved histidine residues that function to anchor the carboxylate of the S2′ amino acid group of the substrate so that a dipeptide may be cleaved from the protein. The peptide loop is referred to as the 'occluding' loop as it partially occludes the primed side (toward the C-terminus) of the active cleft. The dual enzymatic activities of cathepsin B may reflect the

diverse responsibilities it has in biological functions.

Functions of vertebrate cysteine proteases

Vertebrate family C1 proteases, including cathepsins B, C, H and L primarily function in degradative roles in lysosomes (58). Some lysosomal proteases may also function outside of the lysosome such as in peptide processing for MHC II (72-75) and surfactant-associated protein C processing (76). Cathepsin B is one of the most abundant lysosomal enzymes (77). It also functions in trypsinogen activation in the pancreas (78), and in TNF-alpha-induced apoptosis in hepatocytes. Apoptosis is induced by cleaving Bid, thereby resulting in mitochondrial protein C release and subsequent caspase activation (79,80). In human disease, cathepsin B is associated with pancreatitis due to increased levels of active trypsinogen (78) and cancer invasion (81). Elevated cathepsin B expression, and activation at the cell surface, has been linked to malignant progressions in colon carcinomas, glioblastomas, breast carcinomas and prostate cancers (82). Cathepsin B has been observed at the invasive edge of the tumors where it may participate in degrading extracellular matrix proteins (83-87).

Parasite cysteine proteases

Cysteine proteases are the dominant protease activity in all parasites studied to date. This is in contrast to vertebrates where serine proteases predominate in the genome (56). The parasite cysteine proteases are functionally similar to vertebrate cysteine proteases and also perform a variety of diverse cellular and extracellular functions that contribute to the life cycle and pathogenesis of the parasite. Parasite cysteine proteases facilitate tissue/cellular invasion, immunoevasion, nutrition, encystment and excystment. For example, *Entamoeba histolytica,* the etiological agent of human amoebiasis, uses surface-associated cysteine proteases to mediate extracellular matrix degradation and invasion through the intestinal wall to access the bloodstream (88-91). The cysteine proteases of *Leishmania mexicana*, the causative agent of South American cutaneous leishmaniasis, facilitate the successful invasion and colonization of host macrophages

(92).

In addition to their involvement in invasion, parasite proteases also serve to evade the host immune response. One common component of the host defense verses parasite is the complement pathway, which functions as a biological cascade leading to inflammation, phagocytosis, cytolysis and ultimately pathogen clearance. Cysteine proteases from the protozoan parasite, *Trichomonas vaginalis*, are implicated in C3 degradation, inactivating a key component of the complement system (93). Likewise, extracellular cysteine proteases of *Entamoeba histolytica* degrade immunoglobulin A and the proinflammatory complement factors, C3a and C5a (94).

Cysteine proteases are also responsible for the provision of absorbable nutrients. The causative agent of malaria, *Plasmodium falciparum*, uses erythrocytic hemoglobin as a major nutritional source and its degradation is mediated in large part by cysteine proteases within the food vacuole (95,96). This is also true in the adult bloodfluke, *Schistosoma mansoni*, which utilize a number of cysteine proteases to degrade hemoglobin (97,98).

Finally, cysteine proteases have been reported to function in development and differentiation, including encystation and excytation of protozoa involving cyst wall formation and degradation essential for pathogen survival outside of the host. In *Entamoeba invadens*, a model to study excystation and encystation in *E. histolytica,* inhibitors of cysteine proteases arrest both processes, although the exact mechanisms remain to be determined (99,100). The protist, *Sterkiella histriomuscorum*, requires cysteine protease activity only during excystation (101). Interestingly, the cathespin B-like protease of *S. histriomuscorum* is most similar to *Giardia* cathepsin B proteases by sequence homology including absence of an occluding loop. As discussed below, *Giardia* cathepsin B activity has also been linked to excystation (102).

Cysteine proteases in *Giardia lamblia*

In *Giardia*, Ward *et al.*, (1997) demonstrated that family C1 activity is required

for excystation of *Giardia,* by which replicative trophozoites are released from the cyst into the intestinal lumen. Incubation with the cysteine protease inhibitors E64 or Mu-Tyr-(OME)hPhe-FMK inhibited cyst rupture in *G. muris* in a dose-dependent manner. The N-terminal protein sequence of the most abundant cysteine protease was identified using a biotinylated inhibitor, Z-F-A-FMK, in combination with streptavidin-sepharose chromatography. By designing degenerate primers corresponding to this N-terminus and to a conserved region spanning the active site asparagine of the cathepsin Bs, Ward *et al.,* (1997) identified and cloned three *G. lamblia* cathepsin B-like cysteine protease genes (*Gl*CP1, *Gl*CP2 and *Gl*CP3). The N-terminus of the cysteine protease catalytic domain sequence showed 100% identity to *Gl*CP2 and all three enzymes were assigned to family C1A within clan CA due to their sequence homology to the template enzyme, papain. Interestingly, whereas *Gl*CP1 has a glutamic acid in its predicted S2 pocket, *Gl*CP2 and *Gl*CP3 have a glutamine, suggesting that *Gl*CP1, like mammalian cathepsin B may accommodate an arginine in the S2 pocket whereas *Gl*CP2/3 may not. The cathepsin B of the hookworm, *Ancylostoma*, also has a glutamine at the predicted bottom of the S_2 pocket implying cathepsin L substrate specificity and not allow binding of basic amino acid residues (56). While cathepsin L-like in substrate specificity, they are clearly cathepsin B proteases by sequence homology. *Gl*CPs are optimally active at pH7-8 (Sajid, M and Dubois, K personal communication), in contrast to mammalian lysosomal cathepsin B that is optimally active at acidic pH 4-5 (103).

*Gl*CPs possess endopeptidolytic activity. Because they lack an occluding loop, the signature dipeptidyl carboxypeptidase (exopeptidase) activity of vertebrate cathepsin B is absent (56,102). Other parasite cathepsin B-like proteases retain the occluding loop suggesting that *Giardia* either lost the loop or that the loop evolved later. Since it is one of the earliest lineages in the eukaryotic tree, *Giardia* cathepsin B-like proteases may represent one of the earliest cathepsin B lineages by phylogenetic analysis (56,58).

In addition to cysteine protease involvement in excystation, Touz *et al.,* (2002)

showed that cysteine proteases of *Giardia* also function in the cyst wall formation, a process referred to as encystation. Cysteine protease inhibitors such as E64d (cell permeable E64 analogue) interfered with the processing of cyst wall protein 2 (CWP2) secretion, and cyst wall formation. Using affinity chromatography with the inhibitor cystatin, a cathepsin C-like protease was identified from encysting *Giardia* lysates. Because CWP2 processing requires an endopeptidase activity (104) yet cathepsin C proteases exclusively function as exopeptidases (removing dipeptides sequentially from the N-terminus), the exact role of this protease is still uncertain. In a recent study, Dubois *et al.*, (2006) have identified 20 additional cysteine proteases, which are classified into three main groups: cathepsin K/L-like, cathepsin C-like and cathepsin B-like. By quantitative PCR, the cathepsin B-like *Gl*CP2 was found to be the major protease expressed in both stages of the life cycle with increased expression during encystation. This suggests that *Gl*CP2 may also have a crucial role in encystation.

GlCP2 function in endocytosis

A key event in the evolution of eukaryotic cells was compartmentalization of cellular functions within distinct organelles responsible for protein synthesis, sorting, secretion, Endocytosis, and degradation (6). However, it is clear from ultrastructural and biochemical analysis of many eukaryotic cells that these functionally distinct compartments often share common aspects of biogenesis and function (105). Evolutionarily, *Giardia* is as far from yeast as yeast is far from humans. Despite this evolutionary distance, *Giardia* contain many of the same organelles as higher eukaryotic cells including nuclei, a glycogen-rich cytoplasm, acidified peripheral vacuoles/vesicles (PVs), which are reminiscent of lysosomes and an ER including segments decorated with ribosomes (19). In addition, *Giardia*'s genome contains orthologues to many of the endomembrane and endocytic components found in higher eukaryotes, such as adaptins, coatomer, and Rab GTPases (14,26,33,106-108). *Giardia* emerges from its protective cyst in the upper intestine and then adheres to the intestinal endothelium via

its adhesive disc where it opportunistically scavenges nutrients by endocytic pathways. In this study, we report that fluorescent proteins are endocytosed by *Giardia* into a labyrinthine endocytic compartment having ER-like characteristics that we refer to as the tubulovesicular network (TVN). The TVN is an extensive endomembrane compartment extending from the nuclear envelope to the PVs at the cell periphery (109). In additional studies using electron microscopy tomography and three-dimensional reconstruction of cells stained with an ER marker, we observed direct focal fusions between the TVN and the PVs. *Giardia*'s cathepsin B-like cysteine proteases localize throughout TVN, where they actively degrade fluorescent endocytosed proteins. The *Gl*CPs were not localized to PVs as previously expected. In summary, we propose that ER-like TVN is a site of both anabolic protein biosynthesis and is part of the endocytic system, as a site of protein degradation. Several studies in mammalian and other eukaryotic systems have also put forth evidence to characterize the pluripotent nature of the ER, including its roles in MHC class I function, phagocytosis, and the entry of toxins and viruses (110-113).

More detailed characterization of *Giardia*'s endomembrane system remains to be done in order to gain greater insight into the maintenance and functioning of basic cellular processes that contribute to pathogenesis. Endomembrane systems in higher eukaryotic organisms utilize Rab proteins to functionally define endomembrane compartments. Rab proteins localize to specific organelles, but also to localize to equivalent membranes in different organisms. I performed a genome survey in the recently completed *Giardia* genome to identify Rab proteins and compare their number and function with other eukaryotic cells *vis a vis* the primitive endomembrane network of *Giardia*.

The work presented in this thesis examines *Giardia* cell biology as it pertains to *Giardia* as a pathogenic organism and as an ancient eukaryotic system. I propose that *Giardia* has an endomembrane compartment that predates organelle compartmentalization of the ER, endosome, and lysosome, which we will be designated as the tubulo-vesicular

network (TVN). I will show that *Giardia*'s cathepsin B-like cysteine proteases, which are orthologues of mammalian lysosomal degradative proteases, localize to the ER-like TVN where they function in *Giardia*'s endocytic pathway by degrading endocytosed proteins. Finally, I initiated studies that will contribute to more detailed molecular characterization of *Giardia*'s endocytic and exocytic pathways including the identification of at least 10 putative ER-endosome associated Rab-like proteins as well as the identification of putative trafficking partners for *Gl*CP2.

Chapter Three

Giardia ER also functions as an endosome/lysosome

Introduction

A key event in the evolution of eukaryotic cells was compartmentalization of cellular functions within distinct organelles responsible for protein synthesis, sorting, secretion, endocytosis and degradation (6). However, it is clear from ultrastructural and biochemical analysis of many eukaryotic cells that these functionally distinct compartments often share common aspects of biogenesis, function and, in some cases, a common tubulovesicular network (105). For example, one recent and ongoing debate concerns the proposed role of the endoplasmic reticulum (ER) in phagocytosis (111,113). Based on the presence of ER markers at the initial stage of phagosome formation in mammalian macrophages, a role for the ER in direct uptake of material from the extracellular environment via fusion with the plasma membrane was proposed (111). Touret et *al.*, (2005) however, found no evidence for a direct ER to plasma membrane communication in either macrophages or dendritic cells. Nevertheless, the concept of pluripotent functions for the ER was left unresolved, and the logic of an ER function in phagocytosis or endocytosis was emphasized, particularly in regards to antigen processing for MHC class I presentation. Furthermore, there are intriguing examples of exogenous toxins and viruses entering mammalian cells via the ER (110,112). Clues from early diverging eukaryotic cells could provide valuable insights on how cell compartmentalization and discrete organelle function evolved.

Giardia has a simple life cycle that includes a replicating trophozoite stage and, under certain environmental conditions, an infectious environmentally resistant cyst. The cyst form allows the replicative trophozoite to persist under conditions of desiccation outside the host and in harsh chemical environments like the host stomach. Following passage through the acidic stomach into the alkaline duodenum, the trophozoite form excysts and resides in the upper small intestine of its vertebrate host where it opportunistically scavenges nutrients by endocytic pathways; the exact natures of which are unknown.

The vegetative trophozoite form of *Giardia* lacks aspects of the compartmentalization and diversity of higher eukaryotic cells. In many eukaryotic cells, all secretory and several organelle-resident proteins are initially delivered by co-translational translocation to the ER lumen, prior to maturation and subsequent targeting to the Golgi apparatus (105). In *Giardia*, no morphologic equivalent of the classic mammalian cell Golgi apparatus has been identified, and the transient secretory pathway for cyst wall synthesis is only induced under specific conditions (114-116). *Giardia* does contain two nuclei, a glycogen-rich cytoplasm, acidified peripheral vacuoles (PVs) and a labyrinthine tubulovesicular network (TVN), segments of which are decorated with ribosomes (109,117,118). *Giardia* also contains a multigene family of cysteine endoproteases that are orthologous to cathepsin L and cathepsin B found in lysosomes of higher organisms and therefore are useful markers of cell compartments where protein degradation takes place (102,119), (*Giardia* genome project, gmod.mbl.edu). Due to the availability of few established ER/endocytic subcompartment markers and the lack of classical genetic techniques, the discrete endocytic pathway of *Giardia* has not been fully characterized. Despite reports of preliminary efforts, RNAi has not been established as a reliable and consistent genetic approach (120). In spite of these limitations, we were able to use reporter gene constructs, organelle-specific markers and functional protease cytochemistry to show that endocytosis and degradation of exogenous proteins takes place not in the acidified PVs, but in the ER-like TVN. In accordance with its primitive lineage, *Giardia*'s transitional endomembranous structure predates compartmentalization of endocytic/lysosomal functions into organelles distinct from the ER. These observations have important implications for recent theories of pluripotent mammalian ER function, including its role in phagocytosis, entry of toxins and viruses and MHC class I function.

Results

Proteins and Fluospheres are endocytosed by Giardia trophozoites at the periphery of the cell and rapidly traverse a tubulovesicular network (TVN) that extends to the perinuclear region

By confocal microscopy, the intracellular localization of fluorescein-labeled albumin and casein was first ascertained following a 30-minute incubation of labeled proteins with *Giardia* in culture (Figure 3.1A, left and middle panels).

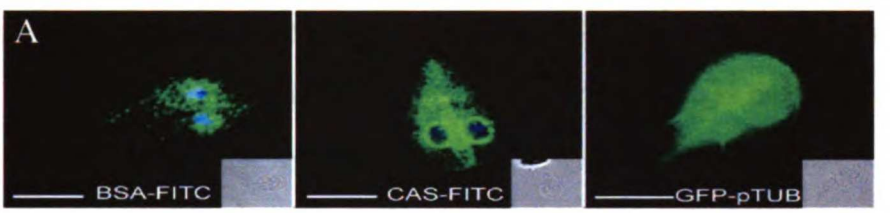

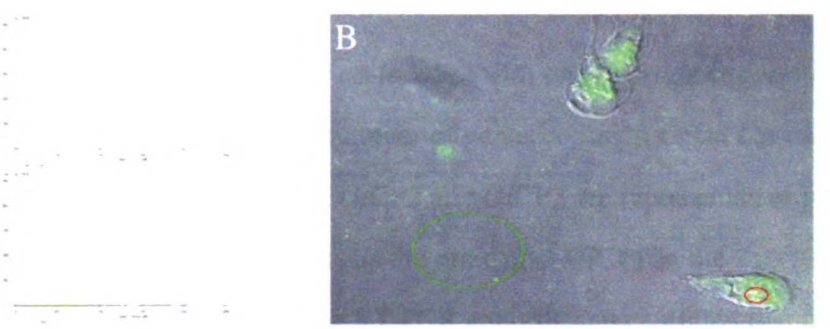

Figure 3.1. Proteins were rapidly endocytosed by trophozoites into a tubulovesicular network (TVN) and the perinuclear region. In panel A, endocytosis of albumin (BSA-FITC, left panel), and casein (casein-FITC, center panel) resulted in a fine "vesicular" pattern in the cytoplasm and intense perinuclear localization. DAPI (blue) highlighted the nuclei of Giardia. The perinuclear localization was more apparent with casein due to the specific optical cut that included the nuclei. Transfection with the empty GFP vector (right panel) resulted in cytoplasmic localization that was not specific to any cellular compartment (Bars, 5μm). In panel B, the kinetics of biotin-conjugated Fluosphere uptake were tracked by monitoring the increase in relative fluorescent units (RFU) in the perinuclear region of a cell (red circle, upper graph) compared to the background level of fluorescence (green circle, lower graph). The green line in each graph corresponds to fluorescence intensity over time (The gray line represents background intensity).

Live cell imaging (Supplemental data S3.1 http://www.ucsf.edu/mckerrow/giardia.html) verified that uptake is extremely rapid; cells were saturated with fluorescent biotin-conjugated Fluospheres within 40 seconds following initial uptake (Figure 3.1B). Interestingly, during live cell imaging, the initial Fluosphere signal was observed near the site of flagellar attachment in the region of the ventral groove (Figure 3.1B) (118). This was followed by rapid distribution throughout the labyrinthine TVN with accumulation in the perinuclear region. Diffusion of the fluorochrome following protein degradation did not occur, as no difference in fluorescence localization was observed upon pretreatment with a protease inhibitor cocktail. This is in contrast to the diffuse cytosolic, non-compartmental localization seen with GFP lacking a signal peptide (Figure 3.1A, right panel). Treatment of trophozoites with sodium azide, cytochalasin D or incubation at 4°C inhibited protein uptake (data not shown).

Cathepsin B-like proteases co-localize with and degrade endocytosed proteins in the TVN

Giardia contains a number of genes coding for clan CA cathepsin B-like cysteine proteases of which *Gl*CP1, *Gl*CP2 and *Gl*CP3 are representative members (119). Though previous northern blot analysis did not detect *Gl*CP1 in the vegetative trophozoites, recent studies using more sensitive RT-PCR analysis demonstrated that the genes encoding *Gl*CP1, *Gl*CP2 and *Gl*CP3 are each expressed during vegetative growth (data not shown). C-terminal fusion GFP reporter constructs indicated that each of *Giardia* cathepsin B-like proteases were present in both the peripheral TVN as well as the perinuclear region and co-localized with endocytosed rhodamine-conjugated albumin and DQRed BSA (Figures 3.2A, S3.3, S3.4 http://www.ucsf.edu/mckerrow/giardia.html). To ensure that the GFP constructs did not mislocalize due to misfolding or due to the presence of the GFP reporter protein, cathepsin activity, identified by *in situ* cleavage of the MNA-derivatized peptide substrate, was localized to the same region of the cell (Figure 3.2B).

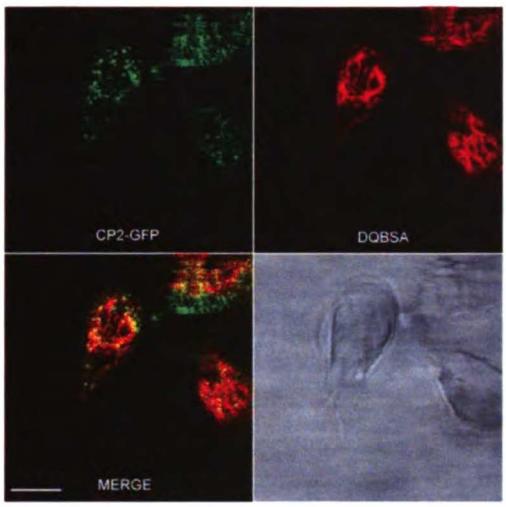

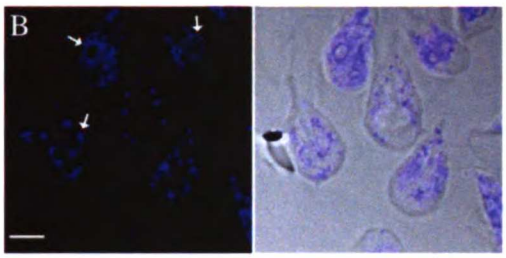

Figure 3.2. Giardia orthologues of mammalian lysosomal proteases were active in the endocytic TVN where they co-localized with endocytosed proteins. In panel A, the cathepsin B-like protease GlCP2-GFP (green, Giardia orthologue of mammalian lysosomal proteases) co-localized with endocytosed albumin (red, DQRed BSA) during live cell imaging. The merged image shows overlap (yellow) in the perinuclear region of the trophozoite (left cell; Bar, 5μm). In panel B, cathepsin B-like cysteine protease activity detected by fluorescent substrate cleavage (Z-RR-MNA). This activity is seen in the TVN in a different optical cut but is particularly intense in the perinuclear region (short arrows; Bar, 5μm).

In situ MNA cleavage, indicated by coupled fluorescent activity, was completely inhibited by treatment with the cysteine protease inhibitors E64d and K11777 (data not shown). This activity correlated with the localization and degradation of endocytosed proteins. Functional assays shown in Figure 3.3A confirmed that endocytosed casein was degraded and this degradation is inhibited by the known cysteine protease inhibitors E64d, K11777 and WRR477. Replacing casein-FITC with BSA-FITC in this assay yielded equivalent results (data not shown). Interestingly, our findings indicate that the pH optimum of the *Giardia* cathepsin activity was 6-7, notably higher than their mammalian orthologues that have an acidic pH optimum of 5-6 and function in acidified lysosomes (Figure 3.3B) (121).

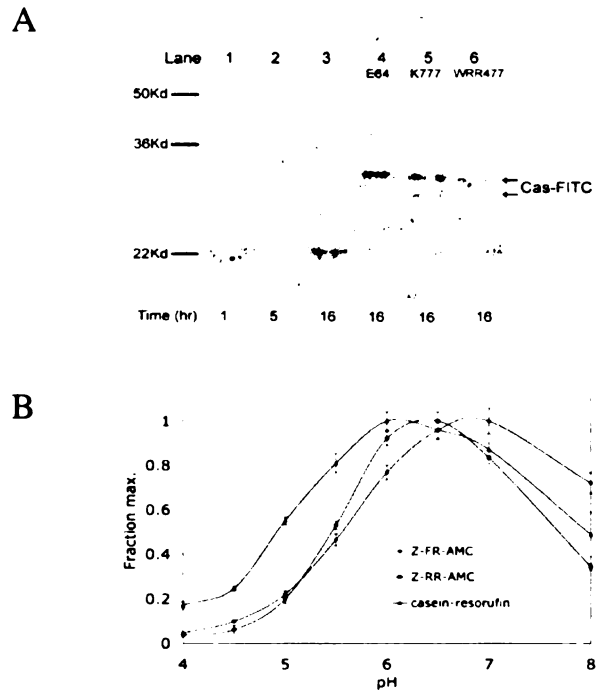

Figure 3.3. Giardia cysteine proteases degraded endocytosed proteins and were optimally active at a higher pH than their mammalian orthologues. In panel A, cysteine proteases degraded endocytosed casein-FITC. Cells were pulsed for 30 minutes with substrate and chased with fresh media for the times indicated. Cell lysates were examined. Lanes 1, 2 and 3 shows loss of substrate in the cells following 1, 5 and 16 hours of incubation. In the presence of three known cysteine protease inhibitors (10μM) (Lanes 4, 5 and 6) casein degradation was blocked (arrows). Panel B shows the pH profile of Giardia lamblia cathepsin B-like cysteine protease activity against the fluorogenic substrates Z-FR-AMC and Z-RR-AMC and against the macromolecular substrate casein-resorufin. The pH optimum was 6-7 for activity against all substrates.

The Giardia TVN contains active cysteine proteases, ER markers and is distinct from the acidified peripheral vacuoles (PVs)

The acidified PVs (as demonstrated by acridine orange staining) were previously thought to represent a lysosome-like compartment where endocytosed proteins are degraded (109). The PVs were identified by accumulation of Lucifer yellow, a classical marker for PVs (Figure 3.4A, shown in yellow) (109), and unexpectedly contained abundant clathrin, which co-localized with Lucifer yellow (Figure 3.4B, shown in red and green, respectively with a yellow merge). A concentration of PVs was observed near the site of flagellar attachment in the region of the ventral groove (Fig 3.4A and 3.4C). PVs were clearly distinct from the labyrinthine TVN that contains a cathepsin B-like protease shown by the *Gl*CP2-GFP reporter construct (green) (Figure 3.4C). The TVN again demonstrated ER characteristics where the *Giardia* ER marker, protein disulfide isomerase 2 (PDI2, shown in red) (29) co-localized with *Gl*CP2-GFP (Figures 3.5A and 3.5B). The tubulovesicular nature of the TVN is highlighted by cysteine protease activity, which co-localized with PDI2 (Figure 3.5C). Antibodies against HSC70, an ER-resident protein, and the ER-retention signal (KDEL) also localized to the TVN and particularly to the perinuclear compartment (Figure S3.5).

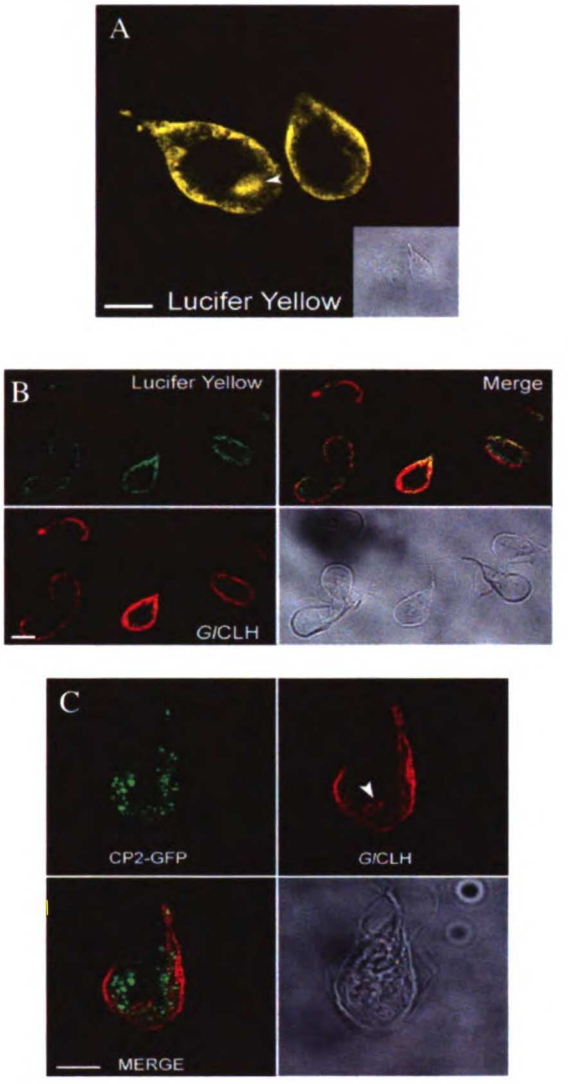

Figure 3.4. The acidified clathrin-rich PVs did not contain lysosomal protease orthologues in Giardia trophozoites. In panel A, Lucifer yellow staining (yellow) highlights the acidic nature of the peripheral vacuole network aside from the cell periphery. PVs are also abundant in an area of the cell near the flagella origin (white arrow head; Bar, 5μm). Panel A shows the clathrin (red) and Lucifer yellow (green) overlay at the PV network. Merge is yellow (Bar, 5μm). In panel B, cathepsin B-like cysteine protease GlCP2-GFP (green) marks the endocytic TVN of Giardia. This network is distinct from the peripheral vacuole network marked by clathrin (red). Clathrin also highlights the abundance of PVs near the site of flagellar attachment (white arrow head; Bar, 5μm).

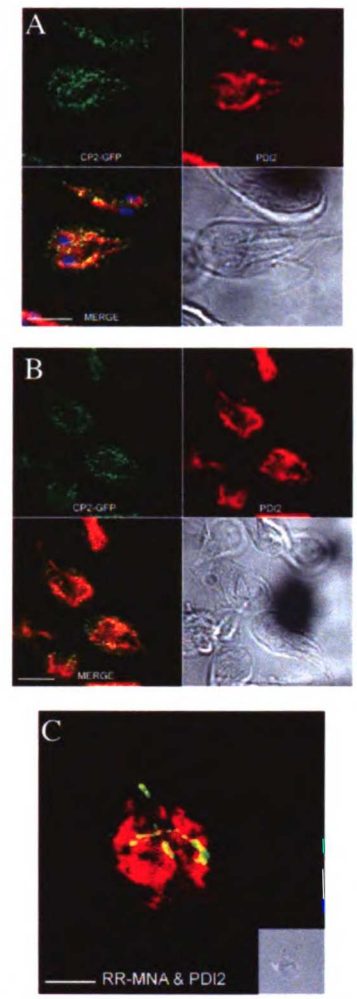

Figure 3.5. The perinuclear region and TVN shown in Figures 3.1-3 are ER-like, as shown by the markers PDI2, KDEL and HSC70. GlCP2-GFP and GlCP protease activity co-localized with PDI2. KDEL was localized more prominently in the perinuclear region while HSC70 and PDI2 were more dispersed throughout the TVN (Figure S3.5). In panel A, cathepsin B-like cysteine protease GlCP2-GFP (green) co-localized with PDI2 (red), extending throughout the TVN. Merge is yellow (Bar, 5μm). Panel B shows a three-dimensional projection of a six image Z-series of cells expressing GlCP2-GFP (green) and probed for PDI2 (red). Co-localization (yellow) is notable in the TVN (Bar, 5μm). Panel C shows a three-dimensional projection of cysteine protease activity against the substrate Z-RR-MNA (green) co-localized (yellow) with PDI2 (red) in the perinuclear region and in the posterior TVN. The projection highlights the continuous and tubulovesicular nature of the TVN (Bar, 5μm).

Ultrastructural analysis confirms that the TVN has properties of ER and identifies foci of ER fusion with PVs

Sequential confocal images of the TVN along the Z-axis and ultrastructural analyses were both consistent with a complex branching tubular network, appearing at times "vesicular" depending on orientation of the optical cut (Figures 3.5C, 3.6A, S3.6 and S3.7). This morphology was consistent with previous reports of the *Giardia* ER and was confirmed by co-localization of ER markers. *Giardia*'s ER network at the ultrastructural level appears to be slit-like and is highlighted by the glucose-6-phosphatase (G6P) reaction (Figure S3.6) (109) (35).

While primarily PVs are differentially labeled with acid phosphatase, G6P and acid phosphatase activities overlap, especially at focal points of ER-PV fusion (109) (35). Ultrasmall (≤5nm) albumin-conjugated gold particles were endocytosed by *Giardia* and distributed throughout the TVN, including the perinuclear region (Figure 3.6A),

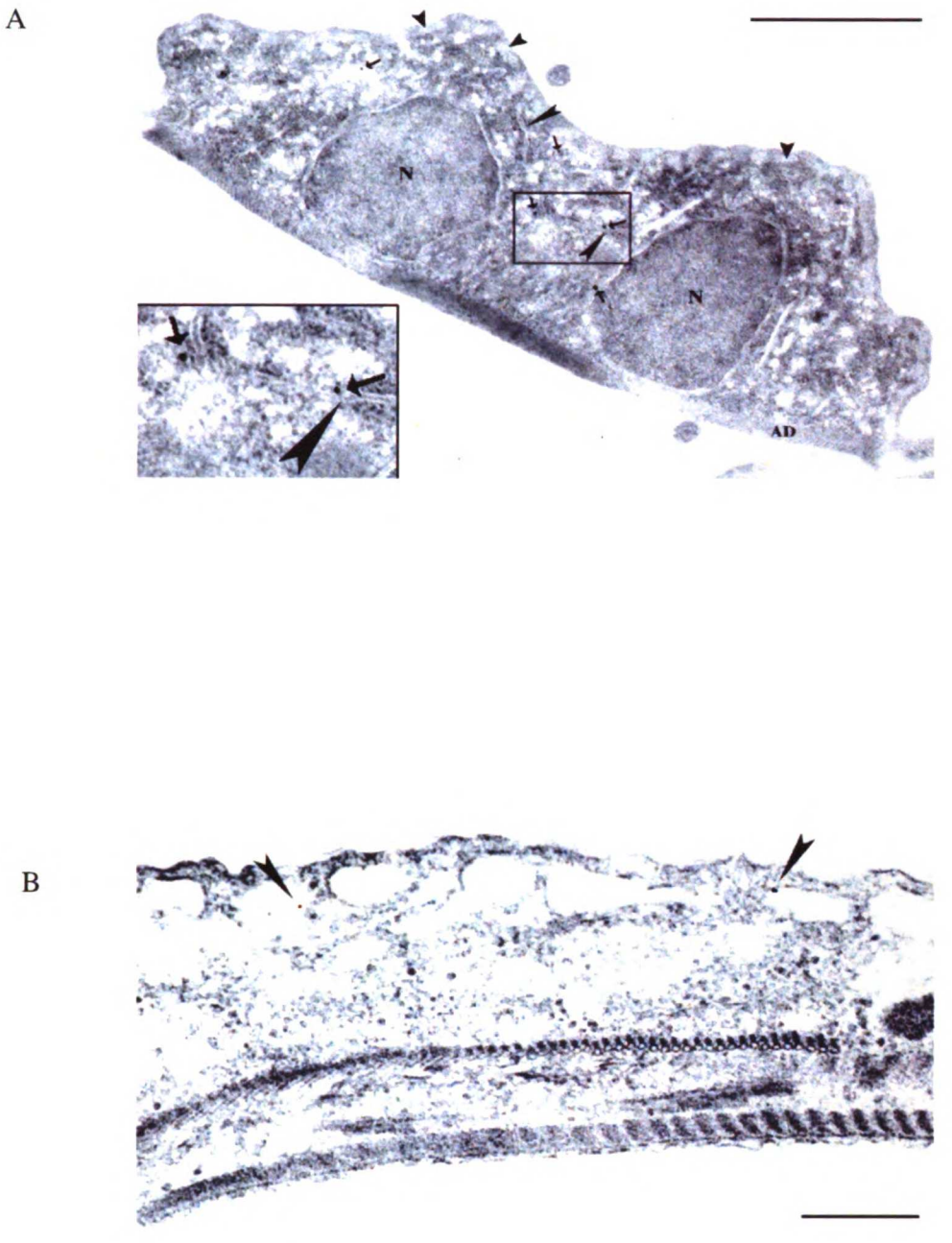

Figure 3.6. Ultrastructural analysis revealed that gold particles were endocytosed into the TVN. In panel A, endocytosed albumin-coated ultrasmall (≤5nm) gold particles (short arrows) localized to both the TVN (elongated arrow heads) including the perinuclear region (see inset). This correlated with the endocytic pattern seen by confocal analysis in Figures 3.1-4 (short arrow heads denote PVs; N = nucleus, AD = adhesive disc; Bar, 1μm). In panel B, endocytosis of larger albumin-coated gold particles (10nm) (elongated arrow heads) was arrested in the PVs (Bar, 200nm).

consistent with results of confocal microscopy. Larger (10nm) gold particles entered the PVs but progressed no further (Figure 3.6B). While at first surprising given the slightly larger diameter of the 10nm particle, this result is not unexpectant due to the increased charge and relative mass of the larger gold particle. Three-dimensional reconstruction of G6P distribution provides a detailed view of the tubular network of ER and confirms focal fusion between ER and PVs (Figure 3.7) (109).

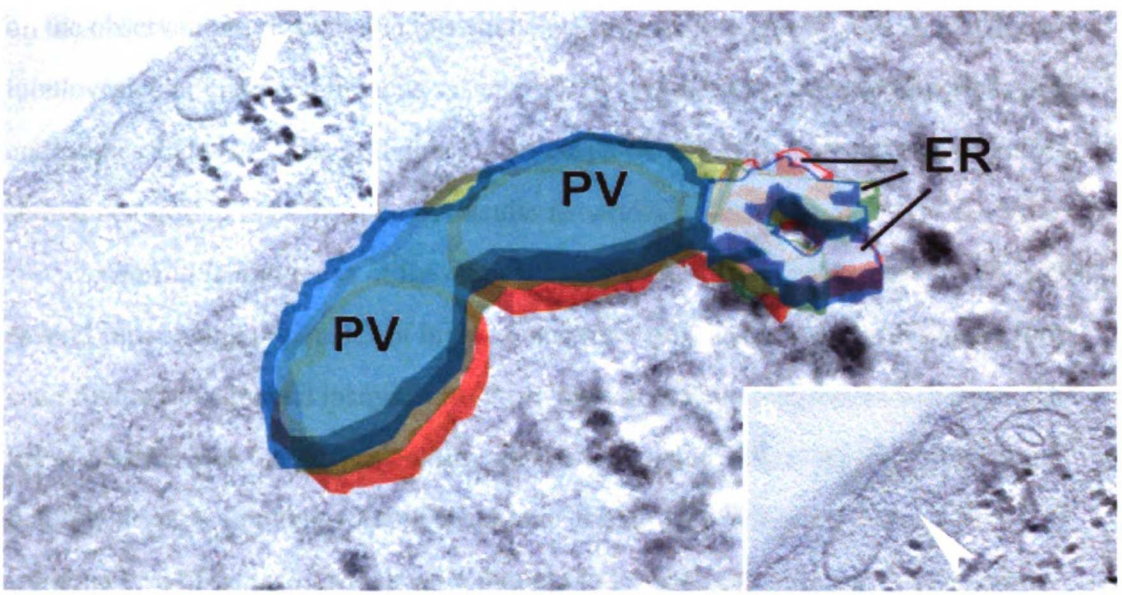

Figure 3.7. Identification of sites of fusion between the TVN and PVs. To visualize interactions of intracellular structures obtained from the EM tomography, data were analyzed further using Openlab software (Improvision Ltd., England). To obtain a pseudo 3D view, 3 consecutive 0.25μm thick images were merged. Fusion between a large peripheral vacuole and the branching ER-like TVN (identified by the glucose-6-phosphatase reaction product, black) was observed (inset a, white arrowhead, bottom z-stack slice). Fusion between two adjacent PVs is also seen (inset b, white arrowhead, top z-stack slice). Each subsequent section is represented by a different color (red, green, and blue). The TVN is outlined with color, while PVs are filled.

Discussion

The endoplasmic reticulum (ER) was first identified and characterized in mammalian cells by Keith Porter (122). Accordingly, our current concepts about the function and compartmentalization of the ER derive primarily from studies with mammalian cells and yeast. The ER is a labyrinthine tubular endomembrane system that co-evolved with the nucleus and serves as a conduit for newly translated proteins, a subset of which will be sorted by the Golgi apparatus to other membrane-bounded organelles such as lysosomes and secretory granules (105,123,124). Based on the observations presented in this study, we propose that *Giardia* ER is actually a tubulovesicular endomembranous system (TVN) in which the disparate functions of ER, endosomes and lysosomes of higher eukaryotes have not fully diverged and, therefore, should be referred to as the tubulovesicular network (TVN).

Giardia lamblia, one of the earliest branches of the eukaryotic tree (6,30), lacks several functioning organelles of higher eukaryotes and, as an early evolutionary form, can provide fundamental insights into the evolution of cell compartmentalization. The ER of *Giardia* was first identified through localization of BIP, an HSP70 homolog that functions as a protein-folding chaperone (123). This helped to distinguish the ER from the PVs of *Giardia,* which were thought to be secretory granules, endosomes or lysosomes (2). In this present study, the PVs were marked both by intense Lucifer yellow and abundant clathrin antibody labeling (Figures 3.4A and 3.4C, white arrowheads). This is the first reported observation that *Giardia*'s PVs contain clathrin. The presence of clathrin on PVs may at first seem surprising given their relatively large size (50-200nm). However, a clathrin heavy chain isoform in mammalian myocytes was also found on large vesicular compartments (125).

By video microscopy, endocytosed proteins and Fluospheres primarily appear first in a "hot spot" corresponding to a region near the flagellar attachment site (126). This region appears to be abundant in clathrin-containing acidic PVs (Figures 3.4A and 3.4C,

white arrowheads). In other protozoan parasites, particularly the kinetoplastids, secretion and endocytosis are polarized, occurring only at a region known as the flagellar pocket (127). Therefore, it is possible that *Giardia* most efficiently (though not exclusively) takes up extracellular material at a similar region where the action of flagellar movement may optimize "sampling" of the environment. The observation by electron microscopy that 10nm gold particles only enter PVs (Figure 3.6B) suggests that the clathrin-rich peripheral vesicle network may be the initial site of uptake followed by rapid dynamic fusion with the TVN leading to the transfer of endocytosed material. This model is consistent with previous ultrastructural observations that showed fusion of PVs with the plasma membrane (126). Tomographic electron micrographs also confirm foci of fusion of TVN with PVs in vegetative trophozoites suggesting that direct delivery of endocytosed material from PVs to the TVN could occur (Figure 3.7).

It has been proposed that the ER is an extremely dynamic organelle (124,128); its size and shape can undergo drastic changes to meet the needs of ER-related functions. The focal fusions noted between TVN and PVs in vegetative trophozoites and the appearance of the PVs as either spherical organelles or a fused network, might both be reflections of dynamic changes occurring within the endomembranous system of *Giardia* (summarized in Figure 3.8).

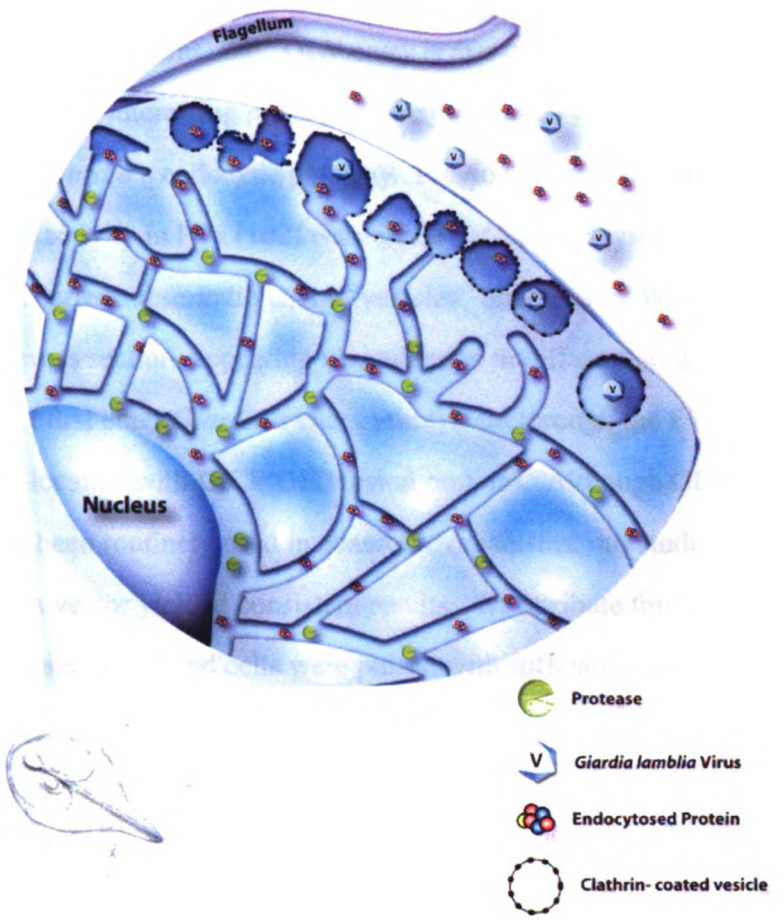

Figure 3.8. Model of endocytic network of Giardia trophozoites. Active proteases reside in the TVN where endocytosed proteins are degraded. PVs contain clathrin and are the site of initial uptake. Membrane fusions between PVs as well as between PVs and the TVN are dynamic. Giardia virus subverts this network for entry into the cell (Schematic designed by Chris Franklin for manuscript) (129).

Furthermore, rather than serving as lysosomes at the end of a typical mammalian cell endocytic pathway, the acidified clathrin-rich PVs may either denature recently endocytosed proteins, facilitating degradation by proteases in the "downstream" TVN; or neutralize the alkaline secretions of the pancreas present in the mammalian duodenum where *Giardia* trophozoites reside and replicate. Circumstantial support for this proposed

pathway of protein uptake by *Giardia* comes from a study of the uptake of *Giardia lamblia* virus (GLV), a double stranded RNA virus that is first translocated to the PVs after binding to the plasma membrane. GLV entry is arrested in the PVs of sodium azide-treated cells (129). In an interesting parallel to entry of some viruses into mammalian cells, GLV exploits *Giardia*'s endocytic pathway. Previous conclusions of the presence of cysteine protease activity in PVs (102) were made before the availability of ER and PV markers. Based on current observations, the "vesicles" observed by Ward *et al.*, (1997) are likely TVN in cross section, appearing vesicular due to diffuse fluorescent signal.

Proteins that first enter *Giardia*'s endocytic system through the PVs concentrate in the TVN and co-localize with *Gl*CP-GFP fusion proteins. Although GFP reporter constructs have not been routinely used in anaerobic organisms, our studies with the pGFPpac expression vector yielded consistent results. We attribute this to the fact that the *Giardia* is microaerophilic and cells were pulsed with sufficient oxygen levels prior to GFP visualization. Cathepsin proteolytic activity, confined to lysosomal organelles in other eukaryotes, is distributed throughout *Giardia*'s TVN, extending from the peripheral TVN to the perinuclear region (Figure 3.2B and 3.5C). In keeping with the localization of *Giardia* cathepsins in a pH neutral compartment, the pH optimum of the *Giardia* cathepsin enzymes are shifted towards neutral pH (6 –7). The orthologous proteases of mammalian lysosomes have a strictly acidic 5 - 6 pH optimum (121).

The observation that the *Giardia* ER functions in endocytosis and degradation of proteins has bearing on the recent debate concerning the role of the ER in mammalian macrophages. Gagnon *et al.*, (2002) proposed that the ER plays a pluripotent role, including direct involvement in formation of the phagosome at the early stages of macrophage phagocytosis. Specifically, they proposed a direct fusion of the ER to the plasma membrane to initiate this process. In support of this model, they demonstrated that ER proteins are enriched in phagosomes. In contrast, however, Touret *et al.*, (2005) could not verify a physical continuity between the ER and the plasma membrane using a

combination of biochemical fluorescent imaging and electron microscopy. Nevertheless, these latter authors pointed out the appeal of ER-mediated phagocytosis as an explanation of how phagocytes are able to internalize multiple large particles without large decreases in surface area. Furthermore, such a model provides a conceptual framework for understanding how antigens might be presented by MHC class I molecules when peptide loading takes place in the ER lumen. In light of this debate, two observations made in this study are noteworthy. First, the TVN of the protist *Giardia lamblia* serves as both a site of protein synthesis, endocytosis and degradation of material from the extracellular milieu. Second, a direct fusion of the ER in *Giardia* with the plasma membrane was not seen, rather the clathrin-rich PV network appears to be the initial site of endocytosis (Figure 3.8). Gagnon *et al.*, (2002) in fact suggested that the ER fuses with plasma membrane at phagocytic cups in an area of plasma membrane known to contain endocytic membranes, and perhaps even clathrin. Therefore, the observation that *Giardia* may endocytose proteins into clathrin-coated peripheral vacuoles that then fuse with the ER may be more analogous to the proposed model of phagocytosis than first appears.

This study raises the question of how a single compartment could function as a site of protein catabolism as well as a pathway for import and sorting of newly translated proteins. There is evidence of some polarized compartmentalization within the *Giardia* ER in that ribosomes are attached to the ER predominantly in the perinuclear region where most KDEL (ER retention signal) localization is also seen (Figure S3.5) (19). The chaperones PDI2, which also contains an ER retention signal (29), and the BIP homologue HSC70 are dispersed throughout the TVN including near the periphery of the cell. Nevertheless, cathepsin B GFP reporter constructs and functional protease activity (Figures 3.1 and 3.2) are both present in the perinuclear region as well as in more peripheral regions of the TVN. *Gl*CP2-GFP localization appeared marginally more punctate than the localization patterns of *Gl*CP1 and *Gl*CP3 (Figure S3.3 and data not shown), which may suggest some degree of spatial regulation. However, the exact nature

of compartmentalization, if it exists in the TVN, is not clear. One possible mechanism to protect newly translated proteins from the action of proteases functioning in the ER is sequestration by chaperones (130-132). Like other eukaryotic cells, *Giardia* contains a number of well-characterized chaperones, including PDI2 and HSC70 (http://gmod.mbl.edu). Newly translated peptide chains are rapidly enveloped and protected by chaperones as they thread into the ER lumen (124). This may allow functional separation of protein degradation and folding/transport of newly translated proteins in the same membrane-bound compartment in *Giardia*. Separating anabolic and catabolic ER functions might also be aided by the fact that newly folded globular proteins should be less efficiently cleaved in contrast to endocytosed, denatured proteins that have passed sequentially through the host's acidic upper digestive tract and acidified *Giardia* PVs.

The ancient "functional" compartmentalization of the TVN seen in *Giardia* may have parallels in higher eukaryotes, for example in the delivery of exogenous oligopeptides to the ER of MHC class I-presenting cells (72). Day *et al.*, (1997) found that after a brief incubation of antigen-presenting cells with fluorescein-labeled peptides in the medium, the peptides are detected within the ER bound to MHC class I molecules. Such ER internalization of exogenous peptides is blocked by pinocytosis inhibitors and occurs without traversing the Golgi or the cytosol. Most importantly, in cells lacking MHC class I, peptides are delivered to the ER but then are quickly removed. The authors speculated that this was due to the action of resident ER proteases (72). There are other examples of direct delivery of extracellular material to the ER in higher eukaryotic cells including endocytosis of AB5 toxins (112) and SV40 variants (110,133). We propose that both MHC class I retrieval, and thus protection of exogenous peptides, and the proposed chaperone-mediated protection of newly translated peptides in *Giardia*, represent related examples of a functional ER compartmentalization that has its origin in primitive ancestors of the modern eukaryotic cell.

Chapter Four

The simplicity of the *Giardia* endomembrane system is reflected in the simplicity of the Rab GTPase family

Introduction

Small, monomeric GTPases are a class of proteins that function in a variety of fundamental cellular processes in organisms as diverse as humans, yeast and *Giardia*. The Ras superfamily of small GTPases are classified by primary sequence into five families: Ras/Rac, Rho, Ran, Arf/Sar, and Rab/Ypt (mammalian)/ (yeast) (Figure 4.1) (134-136).

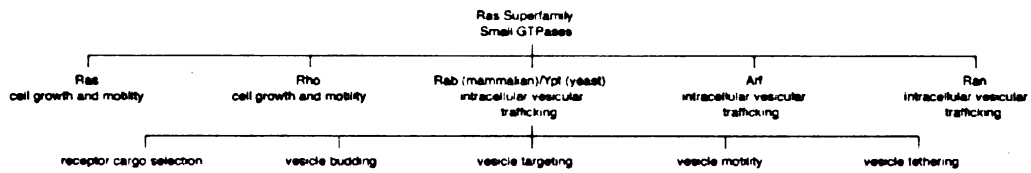

Figure 4.1. The Ras superfamily of small GTPases is composed of the Ras, Rho, Arf, Ran and Rab families. The Rab-like small GTPases are involved in a diverse array of cellular functions,including receptor cargo selection, vesicle budding, vesicle targeting, vesicle motility and vesicle tethering.

The Ras and Rho families are known to be the signaling nodes and regulators of extracellular-stimuli that mediate multiple catalytically distinct downstream effectors to control gene expression and regulate such processes as cell proliferation, differentiation, polarity, motility and survival (137). The Ran, Arf/Sar, and Rab/Ypt families function in several aspects of intracellular vesicular and tubulovesicular trafficking (138,139). The Rab/Ypt family is the largest of the monomeric small GTPase families (140). The number of Rabs was once thought to be indicative of organismal and tissue complexity since *Saccharomyces cerevisiae* have 11, *Trypanosoma brucei* have 16, *Caenorhabditis elegans* have 29, and humans have close to 70 Rab proteins. However, recent studies have identified 65 and 105 Rab proteins in the single-celled protists *Trichomonas vaginalis* and *Entamoeba histolytica*, respectively (141,142). The number of Rabs an organism encodes may instead be indicative of the demands imposed by their ecological

niche(s) and unique survival requirements. In this case, Rab complexity may be linked the amoeboid life stages of *T.vaginalis* and *E. histolytica*.

Rabs orchestrate several functions in the exocytic and endocytic pathways such as receptor cargo selection, vesicle budding, motility, tethering and fusion (138). GTPases play crucial roles in these processes and their ability to regulate fundamental cellular pathways is not only often the rate-limiting step, but also their activity is tightly correlated to their inherent nature as "molecular switches". GTPases alternatively bind guanosine diphosphate (GDP) and guanosine triphosphate (GTP) correlating to deactivated and activated states, respectively, coupling GTP loading and GTP hydrolysis to a specific cellular function.

Rabs of different organisms usually have equivalent membrane localizations and are functionally conserved. Structurally, Rabs are highly conserved by sequence and by corefolds through evolution. By sequence homology studies, Rabs were found to share very similar domains. The four characteristic Rab sequence domains include the switch regions (G1-G3, G for guanine), the family motifs (F1-F5), the subfamily motifs (SF1-4) and the C-terminal hypervariable domain (143). The switch regions I and II sequence elements bind GTP and GDP and are also the only sequence elements that change conformation upon nucleotide binding and contribute to downstream effector protein recognition (144). The family and subfamily motifs are also highly conserved and not only distinguish the Rab subfamily from the other Ras superfamily members but also define a conserved binding surface that are thought to bind various effector and regulatory proteins to mediate different cellular functions (143). Finally, the C-terminal hypervariable domain, which is the most divergent and unstructured, are generally defined by two cysteine residues which are modified by prenylations (143). The aforementioned conserved domains and motifs appear to be unique signatures among the different Rab proteins and are postulated to be involved in Rab targeting to resident membranes.

As "molecular switch" proteins, Rabs are understood to be temporal regulators, but recent studies have shown that they should also be considered as spatial regulators. Within the endocytic pathway, GTP-bound Rabs take on particular conformation and recruit effector proteins to organize specific, functional microdomains on organelle membranes. For example, the Rab subfamily member, Rab5A, is able to recruit up to 30 effector proteins to the early endosome (138). Ongoing studies are trying to determine effector proteins for other Rabs in order to delineate the endosomal system organization. What is clear is that organelle identity is now uniquely tied to the resident Rabs with which it associates. The evolution of compartmentalization and organelle identity was first thought of in terms of efficiency. From an evolutionary standpoint, compartmentalization provided a way to organize enzyme systems involved in a shared biochemical pathway so that they may be in close spatial proximity and so function efficiently. Subsequently, this enabled the many hundreds of biochemical pathways occurring within a cell to function simultaneously. Organelle identity is now also being defined by protein interactions on the membrane surface not just by the enzymes within the membrane and within the organelle itself. As a unique consequence, Rabs have become an important tool as markers to identify and define organelles within uncharacterized endomembrane systems in ancient eukaryotic organisms such as protists, *Trypanasomes*, *Entameoba* and *Giardia* (107,145,146).

With the completion of the *Giardia* genome project (http://gmod.mbl.edu), the *Giardia* genome has been found to contain many of the same genes for endomembrane trafficking as higher eukaryotic cells. Interestingly, the gene for mannose 6-phosphate transferase, early endosome antigen 1 (EEA1) and the genes for GRASP or Golgin, the structural components of the Golgi network (102) (Abodeely unpublished data) were not identified in the *Giardia* genome. Despite the absence of these central components of mammalian endocytic and secretory pathways, *Giardia* does have an endomembrane system which functions in exocytic and endocytic processes (14,129) (Abodeely, M *et*

al., manuscript submitted}. In studies examining how *Giardia* takes up and degrades proteins in its vertebrate host small intestine, a key discovery was the relative lack of compartmentalization of the endomembrane system of *Giardia*. Is the simplicity of this system reflected in the lack of Rab diversity?

Previous studies to uncover Rab proteins in *Giardia lamblia* revealed 8 genes encoding Rab proteins (107,108). By sequence homology, four (Rab1, 2A, 2B, and 11) can be classified into 3 Rab subfamilies, which represent the core group of endo- and exocytic Rab proteins. The additional four Rab sequences also code for Rab-like small GTPases, however their sequences are highly divergent from the core group of Rab subfamilies. These *Giardia* Rabs were assigned the following designations RabA, Bt, D, and F according to convention. These surveys were conducted before the completion of the *Giardia* genome (107,108); therefore, my study sought to confirm, update and uncover any additional Rab genes within the completed *Giardia* genome that would reflect or validate the model of *Giardia*'s endomembrane system.

The Rab proteins represent the largest of five families that comprise the Ras superfamily of small GTPases (147). Since Rabs have been shown to both localize to equivalent membranes and perform similar functions within different organisms (137), Rabs are a valuable and validated tool that can be extrapolated to characterize intracellular compartments of the pathogenic protist, *Giardia lamblia*. This approach has been successfully employed with other human pathogenic protozoans such as *Trypanasoma brucei* (148), *Trichomonas vaginalis* (142) and *Entamoeba histolytica* (149); though additional work is required for the detailed characterization of these systems. Characterization of the endomembrane systems of these protozoan pathogens will not only lead to identification and development of more specific, directed therapies (150), but also help us to understand essential cellular processes, such as endocytosis and exocytosis in the aforementioned higher eukaryotic organisms.

Results

The Giardia lamblia Ras Superfamily has 10 Rab family members

By BLAST searches and phylogenic analyses, fourteen *Giardia lamblia* genes that have significantly high sequence homology to members of the Ras superfamily were identified. By sequence homology the fourteen genes identified are as follows: 2 were found to be Arf-like, 1 was found to be Ran-like, 1 was found to be Ras/Rho-like and 10 sequences belonging to the Rab family (Figure 4.2, Table 4.1).

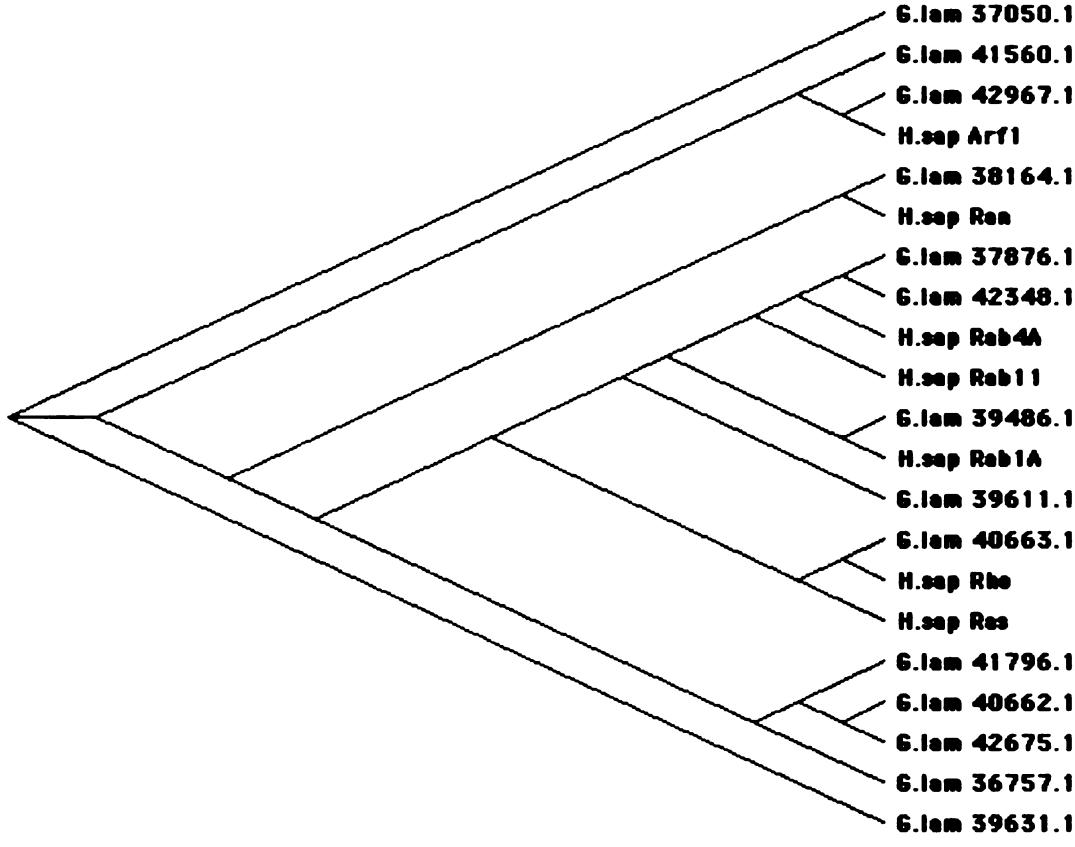

Figure 4.2. Phylogeny tree shows the relationship between the Ras Superfamily members and the 14 identified Giardia Ras-like sequences.

Pfam domain	Putative Giardia orthologue	Length (aa)	Closest Rab Orthologue	Previously Identified	Alternative Accession No.	References
Ras	EAA39486	212	Rab1	GiRab1	AAG12239	1,3,5
Ras	EAA37876	218	Rab2A	GiRab2a	AAG12240	3,4
Ras	EAA42348	227	Rab2B	GiRab2b	BAB58888	1,4
Ras	EAA39611	216	Rab11		AAO49245	1
Ras	EAA39631	274	Rab28 Tb/Tc/Ce			7,9,10
Ras	EAA37050	192		RabA	AAL87243	4,5
Ras	EAA36757	185	RJL	RabB	AAL87240	4,5,8,10
Ras	EAA42675	204		RabD	AAL87240	4,5
Ras	EAA40662	278		RabF	AAK87241	4,5
Ras?	EAA41796	196	Rab?			10
Arf	EAA42967	187		?		10
Arf	EAA41560	197		Arl2		6, 10
Ran	EAA38164	226		?		10
Rho/Ras	EAA40663	218		?		10

1. Iwabe, N Direct submission
2. Murtagh JJ et al., 1992
3 Langford, TD et al., 2002
4. Morrison, HG 2003 Direct Submission
5. Marti, M et al., 2003
6. Marti, M et al., 2003 subject to confirmation
7. El Sayed, N.M. et al., Direct submission
8. Nepomuceno-Silva, JL et al., 2004
9. Berrimen, M. et al., 2005
10. Abodeely, M 2006

Table 4.1. Giardia lamblia Ras-like small GTPases. Of the Fourteen identified Giardia Ras-like sequences, two appear to be Arf-like, one appears to be Ran-like, one appears to be Rho-like and ten appear to more closely related to the Rab family.

Eight of the identified genes encoding Rab proteins have been previously reported: GiRab1, GiRab2 (isoforms A and B), GiRab11, GiRabA/Bt/D/F (107,108). GiRabs 1, 2A, 2B, and 11 are orthologues of the core set of endocytic and exocytic Rabs, which are involved in and are known markers for vesicular trafficking (138), exhibiting >43% amino acid identity to their mammalian counterparts (Figures 4.4, 4.5, 4.6). Classically, Rab1/2 function in the early secretory pathway coordinating membrane traffic between the ER and Golgi (151-153) and localize to ER, IC, cis-Golgi (154). Rab11 has been reported to function in receptor recycling pathways between the *trans*-Golgi (TGN), recycling endosome (RE) and the PM (155-160). In the same study, Marti, M *et al.*, (2003) identified four additional *Giardia* Rab sequences, designated

by convention, GiRabs A/Bt/D/F, which are highly divergent from the core set of Rabs and have unknown function. At the time of this study, we were able to update sequence assignments (Table 4.1) using literature searches and BLAST analysis. We found that GiRabB (accession number EAA36757.1) had also been assigned as GiRjl related to RBJ proteins, which have been proposed as a new family within the Ras-related GTPases (161). In addition, GiRabF (accession number 40662.1) may in fact by a putative Rab28 subfamily member although this subfamily is not highly characterized.

In this study, we also report two additional, highly divergent Rab-like sequences, EAA39631.1 and EAA41796.1. In order to be classified as members of the same family, Kahn *et al.*, (1992) recommends 40% identity between family members. Neither EAA39631.1 nor EAA41796.1 exhibited significant homology (~20% identity at the amino acid level) to the known core domain Rab proteins, and we propose that they be designated GiRabG and GiRabH, respectively.

Phylogenetic analysis allows assignment of orthologies in Giardia lamblia

A nearest neighbor-joining phylogenic tree of the 14 *Giardia* Ras superfamily members along with a reference set of representative Rab sequences from the 4 other Ras superfamily members, Ras, Rho, Ran, and Arf, as outgroup show (Figure 4.2) that 10 of the identified sequences show the greatest sequence homology to the Rab family. A second phylogenetic tree with putative *Giardia* Rabs along with representative sequences from Rab subfamilies focusing on Rab1, 2, 4, 5, 6, 9, and 11 from protists and higher eukaryotes were analyzed (Figure 4.3). Four putative *Giardia* Rab proteins, EAA39486.1, EAA42348.1, EAA37876.1 and EAA39611.1 are assigned as orthologues of defined Rab subfamily members Rab1, 2A, 2B, and 11, respectively, and are referred to as GiRab1, 2A, 2B, and 11. This finding is consistent with previous studies conducted prior to completion of the *Giardia* genome (107,108). *Giardia* sequences EAA37050.1, EAA36757.1, EAA42675.1, and EAA40662.1 had also been previously identified by

Marti, M *et al.*, (2003) (although under different accession numbers, see Table 4.1) and were assigned designations GiRabA, B, D and F, respectively. As identified in this study, these proteins in concurrence with previous studies did fall into the Rab family but with no significant homologies to defined endocytic and exocytic core Rab subfamilies. Nepomuceno *et al.*, (2004) also identified GiRabB/EAA36757.1 and reassigned it to a novel Ras superfamily the RBJ small GTPases and renamed it GiRjl. Another possible reassignment was identified by BLAST searches with GiRabF/EAA40662.1, which showed the highest similarity with the *C. elegans* Rab28 protein suggesting that GiRabF/ EAA40662.1 may be a putative Rab28 orthologue. Rab28 orthologues have also been identified in such organisms as *T. brucei*, *T. cruzi*, and mammals (162-164). In addition to these sequence confirmations, two novel Rab family members were identified in this study, EAA39631.1 and EAA41796.1, which showed no significant homologies to known Rabs subfamilies but by phylogenetic and sequence analysis show the greatest homology with the Rab family (Figure 4.2 and 4.3; Tables 4.2, 4.3, and 4.4). We propose referring to them as GiRabG and GiRabH, respectively. *Giardia* proteins EAA42967.1, EAA41560.1 show sequence homologies to the Arf family of small GTPases (Figures 4.2 and 4.3; Tables 4.1-4.4), while identified *Giardia* proteins EAA38164.1 and EAA40663.1 show sequence homologies to the Ran and Rho/Ras families, respectively. Our focus in this study is the Rab family and how it may help to further characterize *Giardia*'s endocytic system.

Sequence Conservation within the Giardia lamblia Rabs

Structurally, Rabs are highly conserved by sequence and by corefolds through evolution (140). Through sequence homology studies, Rabs were found to share very similar domains. The four main identifiable Rab sequence domains that define this family are the switch regions (G1-G3, G for guanine), the family motifs (F1-F5), the subfamily motifs (SF1-4) and the C terminal hypervariable domain (143). The switch regions I and

II sequence elements bind GTP/GDP and are the only sequence elements that change conformation upon nucleotide binding (144) thereby contributing to effector protein recognition. Alignment of all 14 *Giardia* Ras superfamily members reveals remarkable conservation in the GTP/GDP binding domains (G1-G4) with the consensus motifs (Table 4.2).

GlRab (EEA)	Putative Rab family	G1	G2	G3	G4
		GDSGVGKT	DTAGQE	GNKCD	SAK
39486.1	1	GDSGVGKS	DTAGQE	GSKKD	SSK
42348.1	2	GDSAVGKS	DTAGQE	GNKTD	SAK
37876.1	2	GDTAVGKS	DT GQE	GNKTD	SAK
39611.1	11	GDSAVGKS	DTAGQE	GNKVD	SAS
39631.1	Rab28	GKAYAGKT	DIAGQE	NKID	SAL
37050.1	RabA	GSAG GKT	DTMKGE	ATK D	GL
36757.1	RabB/RJL	GMSQVGKS	DLSGLD	GTKAD	SS
42675.1	RabD	GNARVGKT	DTGGTE	ATKSD	SAA
40662.1	RabF	GDGSVGKS	DIGGQS	GNKSD	SAL
41796.1	Rab	GNAEAGKT	DLGGES	GAKYD	SAE
42967.1	Arf	GLDAAGKT	DIGGQS	ANKQD	VGT
41560.1	Arl2(Arf)	GLD SGKT	DVGGQQ	NKQD	SAM
38164.1	Ran	GDGAIGKT	DTAGQE	GNK D	SAK
40663.1	Rho	GDGSVGKT	DTAGQE	GTKYD	SAR

Table 4.2. **Sequence alignment of the GTP/GDP binding domains (G1-4) of the fourteen identified Giardia Ras superfamily members. These motifs are also referred to as the switch regions. These regions are highly conserved among Rab family members (the consensus sequences are in black type).**

The highest level of conservation is observed within *Giardia*'s core Rab proteins: GiRab1, GiRab2A, GiRab2B, GiRab11. The remaining Ras family members along with the putative Arf, Ran and Ras/Rho *Giardia* proteins show the greatest deviation from the consensus motifs particularly within the G3 and the G4 motifs. Not surprisingly, GiRabB/GiRBJ (EAA36757.1), an apparent orthologue of RJL GTPases characteristically lacks the glutamine residue in the G2 motif that coordinates GTP

hydrolysis and instead has a leucine at the Q61 (Ras numbering) position (161).

The Rab superfamily and subfamily motifs are also highly conserved and not only distinguish the Rab family from the other Ras superfamily members but also define a conserved binding surface that are thought to bind various effector and regulatory proteins to mediate different cellular functions (143). The Rab family motifs (F1-F5) and two of the four subfamily consensus motifs (SF1-SF2) are present in *Giardia*'s canonical Rab protein sequences, GiRab1, 2A, 2B and 11 (Table 4.3).

GlRab (EEA)	Putative Rab family	F1	F2	F3	F4	F5
		IGVDF	KLQIW	RFRSIT	YYRGA	LVYDIT
39486.1	1	IGVDF	KLQIWD	KFRTIT	YYRGA	VVYDVT
42348.1	2	VGVEF	KVQIWD	QFRSIT	YYRGA	LVYDVT
37876.1	2	VGVEY	KFQIWD	SFRSIT	YYRGS	LVYDIT
39611.1	11	IGVEF	RLQ WD	RYRSIT	YYRGA	LVFDVT
39631.1	Rab28	LGVDF	RAQLWD	RYTSLT	YYRNA	VVGDLE
37050.1	RabA	ETVDI	SIRLWD	YMGGVS	AHKSA	VVFDFV
36757.1	RabB/RJL	IGVDY	RINFFD	EYQDIR	FYSDT	LIFDMS
42675.1	RabD	YGVDW	SLHIWD	HYSGMQ	YLRGA	L YDMT
40662.1	RabF	IGVDF	TFNLYD	IGSKML	YISGT	FVYDLT
41796.1	Rab	LGVNF	LLSIWD	EFKNML	V DGS	YIFDLT
42967.1	Arf	PTMGF	ELDVWD	EFRNIW	YYVDK	FVVDAA
41560.1	Arl2(Arf)	PTLGF	AVALWD	TIRTYW	YFSST	WVVDSI
38164.1	Ran	IGVEI	LLNVHD	KFGGLR	YYVDS	LFFDVT
40663.1	Rho	VFDNY	NIGLWD	DYDKLR	SYPGA	FSVVS

Table 4.3. **Sequence alignment of the family motifs (F1-5) of the fourteen identified Giardia Ras superfamily members (the Rab consensus sequences are in black type). As expected, the putative Arf, Ran and Rho orthologues are not conserved within these motifs.**

As was seen in alignments of *T. brucei* Rab protein sequences, the F3 consensus domain exhibited the least conservation of the family motifs (148). Interestingly, SF3 and SF4 consensus motifs were indistinguishable in these sequences (Data not shown.).

The C terminal hypervariable domain, which is the most divergent and unstructured motif, is generally defined by two cysteine residues at the C-terminus which are modified by prenylations (143). They appear to be unique signatures among the different Rab proteins and are postulated to be involved in Rab targeting to

resident membranes (165). GiRab1, GiRab2 (both isoforms), GiRabA, GiRabD and GiRabG possess the distinctive two cysteines at their C terminus consistent with the canonical C-terminal motifs: XXCC, XCXC, CCXX, CCXXX or XCCX (Table 4.4).

GlRab (EEA)	Putative Rab family	SF1	SF2	C-term. Prenylation
		YIFKY	SLLLRFTD	
39486.1	1	YLFKL	ALLLRL D	SKG
42348.1	2	YIFKY	LLLRFVE	GN S
37876.1	2	YLFKY	LLLQFTE	GG G
39611.1	11	HLYKL	ILSRFT	QKKR
39631.1	Rab28	FMFKI	IKRLVH	NKA
37050.1	RabA	MRYKV	TLVHSLAY	SR Y
36757.1	RabB/RJL	VRLKV	LIKYY E	SKAKA
42675.1	RabD	--YKL	SLIVRLTT	KG Y
40662.1	RabF	RIFKV	SI SRFAK	R AVM
41796.1	Rab	LIVKI	SLMVRYVE	YTLIQ
42967.1	Arf	-QARV	TILHQMAY	
41560.1	Arl2(Arf)	NEARV	TIVSSLLG	
38164.1	Ran	ISFKV	TFVTRHIT	
40663.1	Rho	IHIKA		K YIF

Table 4.4. Sequence alignment of the subfamily motifs (SF1-2) and the C-terminal prenylations motif of the fourteen identified Giardia Ras superfamily members (the Rab consensus sequences are in black type; see text for C-terminal prenylations motifs). The Rab SF3 motif (not shown) was not well conserved in Giardia Rab-like sequences.

GiRab11 and GiRabF terminate with one cysteine, while GiRjl and GiRabH have no C-terminal cysteines. The absence of the C-terminal prenylations motifs is not unprecedented although it is more the exception then the rule (143,148).

Identification of Giardia lamblia orthologues of known subfamilies

Additional phylogenetic analyses were performed to explore the relationships between known and putative *Giardia* Rabs with both experimentally characterized and uncharacterized Rab proteins from humans, *S. cerevisiae*, *T. brucei*, *T. vaginalis*, *E. histolytica*. Pair-wise comparisons of aligned subfamily sequences showed that GiRabs

assigned to previously characterized Rab subfamilies exhibited very high sequence homologies. GiRab1, 2A, and 2B showed ~50% amino acid identify to human Rab1 (both A and B isoforms) and Rab2 subfamilies. Not surprisingly, they shared significant sequence homologies to all other representative Rab1 members except to TbRAB1B and the EhRab2 isoforms, although GiRab2A was more similar to EhRab2 isoforms then GiRab2B. GiRab11 also showed significant homology (>40%) to its mammalian, yeast and *Trichomonas* counterparts.

Discussion

With the recent completion of the *Giardia* genome, I conducted BLAST searches to identify Rab orthologues. I report the identification of 14 Ras superfamily-related proteins including 10 Rab proteins all of which had been reported by initial genome sequencing efforts (Iwabe, N., unpublished McArthur *et al.*, 2000 unpublished). While eight of the identified sequences have been previously reported and partially characterized (107,108,161), two appear to be novel Rab proteins.

Langford *et al.*, (2002) isolated GiRab1, 2A and 2B by amplifying gene sequences from genomic DNA with specific primers based on the findings by genome sequencing efforts by McArthur *et al.*, (2000). With immunoelectron microscopy and a *Leishmania* antibodies to LmRab1, Langford *et al.*, (2002) localized GiRab1 to the nuclear envelope, ER and peripheral vesicles and in trophozoites and to the encystation-specific vesicles (ESVs) in encysting cells. However, this sera was not specific to GiRab1 and may have picked up other GiRabs including GiRab2. In their effort to identify putative secretory components in *Giardia*, Marti, M. *et al.*, (2003), identified GiRab1 through a genomic survey of the *Giardia* Genome Database although no characterization was reported. In *Trypanosoma brucei* (*T. brucei*), TbRAB1 is localized to the Golgi in the bloodstream form (BSF) and is reported to function in antigenic variant surface glycoprotein (VSG) secretion, which helps the parasite evade the host immune response (Table 4.5) (146).

g

Organism	Rab orthologue	Protein accession no.	Length (aa)	% ID	% Sim	BLAST P(n)e[c]	Reference
H.sapiens	Rab1A	NP_004152	205	51	65	2e-57	Zahraoui, A., 1989
	Rab1B	CAG38493	201	51	65	2e-56	Ebert, L., 2004 Direct Submission
S.cerevisiae	Ypt1	BAA09201	206	46	63	5e-48	Segev, 1988
T.brucei	TbRAB1A (Trab1)	Tb927.8.890 (XP_823597)	208	48	63	7e-56	Berriman, M., 2005
	TbRAB1B	Tb09.244.2070 (XP_827728)	276	24	39	1e-25	Direct Submission: Lennard, N.J., 2005; Berriman, M., 2005
T.vaginalis	Rab1A	AAZ73762	202	45	65	4e-50	Direct Submission; Xu, X., 2005; Lai, K 2005
E.histolytica	EhRab1A	EAL45948	205	45	65	1e-47	Saito-Nakano, Y., 2001; Loftus, B., 2005
	EhRab1B	EAL43647	185	40	53	9e-35	Saito-Nakano, Y., 2005; Loftus, B., 2005
	EhRab1C**	EAL47665	199	45	64	3e-50	Loftus, B., 2005
G.lamblia	GlRab1	EAA39486 (also AF183936)	212				Direct Submission: Iwabe, N.; Morrisson, H.G.; Langford, T.A., 2002; 2003; Marti, M., 2003

Organism	Rab orthologue	Protein accession no.	Transport step	Reference
H.sapiens	Rab1A	NP_004152	Localization: Pre-Golgi compartments/ ERGIC /VTCs/Intermediate compartment (IC) [1, 2, 3, 6] Function: Anterograde transport ER to Golgi[2]; Retrograde transport [4, 5, 6]	[1]Plutner, 1991 (1B); [2]Tisdale, 1992; [3]Seraste, J, 1995; [4]Palokangas, 1998; [5, 6]Sannerund, R., 2003, 2006
S.cerevisiae	Ypt1	BAA09201	Exocytic pathway: ER to Golgi and intra Golgi	Segev *et al.*, 1988; Rexach and Schekman, 1991; Segev, 1991 Jedd *et al.*, 1995
T.brucei	TbRAB1A (Trab1)	Tb927.8.890 (XP_823597)	Mammalian formBSF: Localized to Golgi; Function: VSG secretion; Maintains Golgi architecture; rescued Ypt1p mutant	Dhir, V., 2004
	TbRAB1B	Tb09.244.2070 (XP_827728)		
T.vaginalis	Rab1A	AAZ73762	No experimental evidence	
E.histolytica	EhRab1A	EAL45948	Did not rescue Ypt1p mutant	Saito-Nakano, Y., 2001
	EhRab1B	EAL43647	No experimental evidence	
	EhRab1C**	EAL47665	No experimental evidence	
G.lamblia	GlRab1	EAA39486	Trophozoites: ER, PVs	Langford, T.A., 2002*
			Encysting cells: ER, NE, periphery of ESVs, PVs	

- Subject to confirmation. ** Found that it was more closesly related to Rab1.
- * Subject to confirmation used a *Saccharomyces cerevisiae* Ypt1p antibody.

Table 4.5. Giardia GiRab1 (EAA39486.1) orthologues from humans (H. sapiens), yeast (S. cerevisiae), trypansomes (T. brucei), trichomonas (T. vaginalis) and Entamoeba (E. histolytica). In the top chart, orthologues are compared to GiRab1 in % identity (ID) and % similarity (Sim) at the amino acid level. In the bottom chart, the known functional characterizations for GiRab1 ortholo•ues are listed.

Rab1 role in exocytic pathways is well defined in humans and in *Saccharomyoces cerevisiae* (*S. cerevisiae*) where it functions in protein transport between the ER and *cis*-Golgi (153,166-168). Interestingly, in mammalian systems, Rab1 localization has been defined to pre-Golgi compartments referred collectively as the intermediate compartment (IC) (also called ERGIC and VTCs) (169) which is believed to mediate traffic between the ER and Golgi (170-173). The IC is thought to arise by homotypic fusion of COPII transport vesicles following budding from ER exit sites (ERES) and is also found studded with COPI which is classically defined as a Golgi coat protein (174,175). Whether the IC is simply a tubular vesicular network comprised of transport vesicles or a distinct endomembrane compartment is a matter of ongoing debate. What is known is that it functions in bi-directional traffic and can behave as either an immobile or dynamic structure, depending on the cell type and metabolic state (176-179). Rab1, along with the coatomer proteins COPI and COPII, appears to help the IC carry out both anterograde and retrograde transport pathways between the ER and Golgi (178-180).

Recent studies investigating endocytosis in *Giardia* may provide additional insight into the role of Rab1 and IC function. *Giardia*'s Rab1 orthologue is ~50% identical to human Rab1 and 48% identical to Ypt1 from *S. cerevisiae* (Figure 4.4). The high conservation in sequence to higher eukaryotic Rab proteins suggests that GiRab1 may have similar exocytic functional role in *Giardia*, especially considering mammalian Rab1 and TbRAB1 were both able to complement Ypt1 mutant (146,181). In *Giardia*, the ER is the main endocytic compartment as shown by the endocytosed fluorescent proteins (Abodeely thesis) and appears as a tubulo-vesicular compartment extending out from the nuclear envelope to the periphery of the cell. Interestingly, in certain cell types the IC also extends out to the periphery of the cell and is comprised of two domains: Globular (near the ERES) and tubular (extending out to the cell periphery) (179). In live cell imaging with GFP-tagged Rab1, the IC appears dynamic, functioning in bi-directional transport. In addition, the IC has been shown to have smooth ER (SER)

characteristics (179,182,183) and can closely associate with the PM (184). Sannerud *et al.*, (2006) hypothesize that there is a Rab1-dependent pathway in these neurons that bypasses the Golgi and instead uses the IC for protein transport although no cargo has been specified. It would be interesting to determine whether the hypothesized Rab1 mediated Golgi bypass pathway in neurons has its origins in the *Giardia* ER and is an ancient remnant pathway.

Similar in localization and function, the Rab2 subfamily of proteins appears to be very similar to the Rab1 subfamily in most organisms. As with Rab1, Rab2 localizes to the IC in humans and functions in both anterograde and retrograde pathways transporting cargo between the ER and Golgi (24,153,185-187). In yeast, there is no Rab2 orthologue, however, in T. brucei, Rab2 has a slightly different localization pattern (Table 4.6)

Organism	Rab orthologue	Protein accession No.	Length (aa)	% ID	% Sim	BLAST P(n)e[c]	Reference
H.sapiens	HsRab2A	NP_002856	212	52/49	70/63	2e-64/2e-59	Tachibana, K., 1992; Zahraoui, A., 1989
	HsRab2B	AAN86142	216	50/47	68/63	3e-63/8e-58	Ni, X., 2002
	HsRab4A	NP_004569	218	43/41	53/53	2e-54/6e-47	Zahraoui, A., 1989
T.brucei	TbRAB2	AAR14147	212	47/48	65/65	4e-58/8e-60	Dhir,V., 2004
E.histolytica	EhRab2A	EAL44537**	212	32/28	50/47	2e-38/5e-37	Saito-Nakano, Y., 2005; Loftus, B., 2005
	EhRab2B	EAL43948	213	41/39	56/54	4e-58/3e-50	
	EhRab2C	EAL51401	231	38/36	53/50	5e-58/4e-50	
G.lamblia	GlRab2A*	EAA37876	214				Lanford, TD, 1999,2002; Direct Submission: Morrisson, H.G., 2003
	GlRab2B*	EAA42348	227				Direct Submissions: Iwabe, N., Morrisson, H.G., 2003

* Subject to confirmation.

** I found that EAL44537 is closer to Rab1 subfamily and highest GI hit was EAA3848 (6 3e-50) which is a Rab1-like small GTPase.

Organism	Rab orthologue	Protein accession no.	Transport step	References
H.sapiens	HsRab2A	NP_002856	Localize to pre-Golgi intermediates/vesicular tubular clusters (VTCs) [1,2]; Exocytic Pathway/Anterograde transport of Cargo from ER to Golgi[1,2,3]; Golgi Structure[4,5]; Retrograde transport: VTCs to ER (PKC, GAPDH,β-COP)[2,3]	[1,2]Tisdale, E.J., 1992, 1996; [3]Lee, 2004; [4]Short, B., 2001; [5]Satoh, 2003
	HsRab2B	AAN86142		
T.brucei	TbRAB2	AAR14147	Mammalian BSF Localization: Partially, NE, ER; minimally Golgi; Function: VSG secretion	Dhir,V., 2004
E.histolytica	EhRab2A	EAL44537	No experimental evidence	
	EhRab2B	EAL43948	No experimental evidence	
	EhRab2C	EAL51401	No experimental evidence	

Table 4.6. Giardia GiRab2 (EAA37876.1 and EAA42348.1) orthologues from humans (H. sapiens), yeast (S. cerevisiae), trypansomes (T. brucei), trichomonas (T. vaginalis) and Entamoeba (E. histolytica). In the top chart, orthologues are compared to GiRab2 in % identity (ID) and % similarity (Sim) at the amino acid level (the first number refers to GiRab2A (EAA37876.1) and the second number to Rab2B (EAA42348.1). In the bottom chart, the known functional characterizations for GiRab2 orthologues are listed.

though it also functions in VSG secretion (146). In addition to localizing to the Golgi as TbRAB1, TbRAB2 partially localizes to the nuclear envelope and ER and minimally to the Golgi. TbRab2 is highly homologous in sequence to both of the *Giardia* Rab2 orthologues exhibiting almost 50% identity (Figure 4.5). It will be interesting to see with antibodies specific to GiRab1 and GiRab2 whether there are also slight differences in localization reflecting slight differences in function at different steps in the endo- and exocytic pathways. Unfortunately, there is no experimental data for EhRab2, which has 3 isoforms in its genome which suggests evolutionary pressure to have different Rab2 isoforms fill different functional needs (141,188). Both *Giardia* Rab2 isoforms (EAA37876.1 and EAA42348.1) share the greatest identity with EhRab2B (Figure 4.5 and Table 4.6).

Giardia has two life stages, the vegetative trophozoite stage and the infectious/ infective cyst stage. As *Giardia* exits its host and travels further down the host intestine, it is stimulated by unknown environmental conditions to initiate cyst formation. Encystation involves a dramatic increase in transcription of CWPs that encode a signal sequence directing the CWP trasnscripts to the ER to access the regulated secretory pathway (10,11,17,26,189). The *Giardia* endomembrane system adapts by forming encystation-specific vesicles (ESVs) that transport the CWPs to the cell periphery where they are secreted for cyst wall formation. Several groups argue that ESVs represent a transient Golgi that may or may not be discernible in the vegetative trophozoite (19,25,106,123). In their effort to identify secretory pathway components, Marti *et al.*, (2003) identified 8 Rab proteins including Rab11. Extensively characterized in mammals and yeast, Rab11 functions primarily in the endocytic processes and especially in receptor recycling pathways from the recycling endosome (RE) to the plasma membrane (Table 4.7) (155,156,160,190-192). By generating antibodies to recombinant GiRab11, they localized GiRab11 to the peripheral region of the cell in vegetative trophozoites. However, it would be interesting to determine whether GiRab11 localizes to the PVs or to

the peripheral TVN or some other compartment by immuno-EM using a gold conjugated antibody to GiRab11. In encysting cells, GiRab11 partially co-localized with CWP2 to ESVs by IFA, however the role of GiRab11 in ESV formation or maturation remains to be defined.

As an enteric protozoan, *E. histolytica* also has trophozoite and infective cyst stages. Interestingly, *E. histolytica* encodes for four Rab11 isoforms in its genome. The fact that *E. histolytica* in its amoeboid life stage phagocytoses nutrients from its environment might account for the multiple EhRab11 genes in its genome. Thus far, EhRab11A, which shows the greatest homology to GiRab11 (Figure 4.6; Table 4.7) (145), is the only isoform to have been partially characterized, localizing to late endosomes (193). Coincidently, when stimulated to encyst, EhRab11 also translocates to the cell periphery thus possibly having a similar function in encystation (193).

T. brucei has one Rab11 orthologue, TbRAB11, (previously Tb927.8.4330) which shows 37% sequence identity to GiRab11 (Figure 4.6; Table 4.7) (162,194). TbRAB11 has been localized to endosomal structures including a putative RE structure and functions as other Rab11 orthologues in recycling pathways to the plasma membrane (194-196).

In this genome survey, we report the identification of two novel Rab proteins in the *Giardia* genome, EAA39631.1 and EAA41796.1 that we propose naming RabG and RabH, respectively. Though they were first identified in genome sequencing efforts, no further sequence analysis was conducted. EAA39631.1 and EAA41796.1 show no homology to any of the well-defined core Rab subfamilies (Figure 4.3) though by sequence analysis they do appear to fall into the Rab family with the other divergent *Giardia* Rab sequences (Figure 4.2; Tables 4.2, 4.3 and 4.4). However, in a second phylogenetic analysis as seen in Figure 4.3, EAA39631.1 is grouped with the Arf-like *Giardia* Rab proteins. By sequence alignments EAA39631.1 shows higher similarity in Rab consensus motifs, even having the canonical double cysteine signature at its

C terminus (Tables 4.2, 4.3 and 4.4). In contrast EAA41796, shows more sequence divergence then other GiRab proteins, though by phylogenetic analysis EAA41796 segregates with other divergent Rabs into the Rab family with the closest similarity to GiRabD and GiRabF (Figures 4.2 and 4.3).

GiRabF, also known as *Giardia* Rab protein EAA40662.1, appears to be orthologous to Rab28, which is distantly related to other Rab genes and previously identified in mammals (164), *T. brucei* (162), *T. cruzi* (163) and *C. elegans* {The *C. elegans* consortium, Direct submission}. In rats, Rab28 was identified in rat lipocytes and brain cells with 2 other isoforms that differ in the C-terminal end as a result of alternative splicing events. Unfortunately, there is no additional experimental or functional information on Rab28.

GiRabB, published as GiRjl (accession number EAA36757.1), is a part of a unique family of small GTPases that emphasizes *Giardia*'s place in evolution. The RJL class of proteins has its roots in RabJ proteins, which have been proposed to be a new family of Ras-related GTP-binding proteins (161). RabJ proteins, also referred to as RBJ proteins, possess a conserved C-terminal DNAJ domain, which is reported to interact with Hsc70 chaperones via the "J" domain (197). Strikingly and unlike higher eukaryotic orthologues in multicellular organisms, the *T. cruzi*, *T. brucei* and *L. major* orthologues, TcRjl, TbRjl, LmRjl, all lack not only the "J" domain, but also the C-terminal targeting signal characteristic of other Rab family members (198). In humans, there is an alternatively spliced variant, which like GiRjl, is also lacks the C-terminal prenylation motif and is also only similar in the GTP binding domain (which carries a Q $\rightarrow$ L substitution in the G2 domain) (Tables 4.2 and 4.4). This substitution is also seen in Ras proto-oncogenes and contributes to tumor formation (199). At the time of this genome survey, no additional functional data was published describing protozoan RJL proteins.

Emerging before the divergence of plants and animals, *Giardia* and its endomembrane system represent the foundation of eukaryotic biology. The

Giardia endomembrane system though simple compared to yeast and mammalian cells has evolved to carry out many of the same fundamental cellular processes, including constitutive and regulated secretion and endocytosis (14). *Giardia*'s endomembrane system is able to maintain these functions having much of the same basic machinery functioning in higher eukaryotic cells, such as adaptins, clathrin, and Rabs. *Giardia*'s genome encodes three of the core set of Rabs involved in endo- and exocytosis, Rab1, 2 (two isoforms) and Rab11. Interestingly orthologues of Rab4, 5, 6, 7 and 9 were not identified in this or previous genome surveys (Figure 4.7).

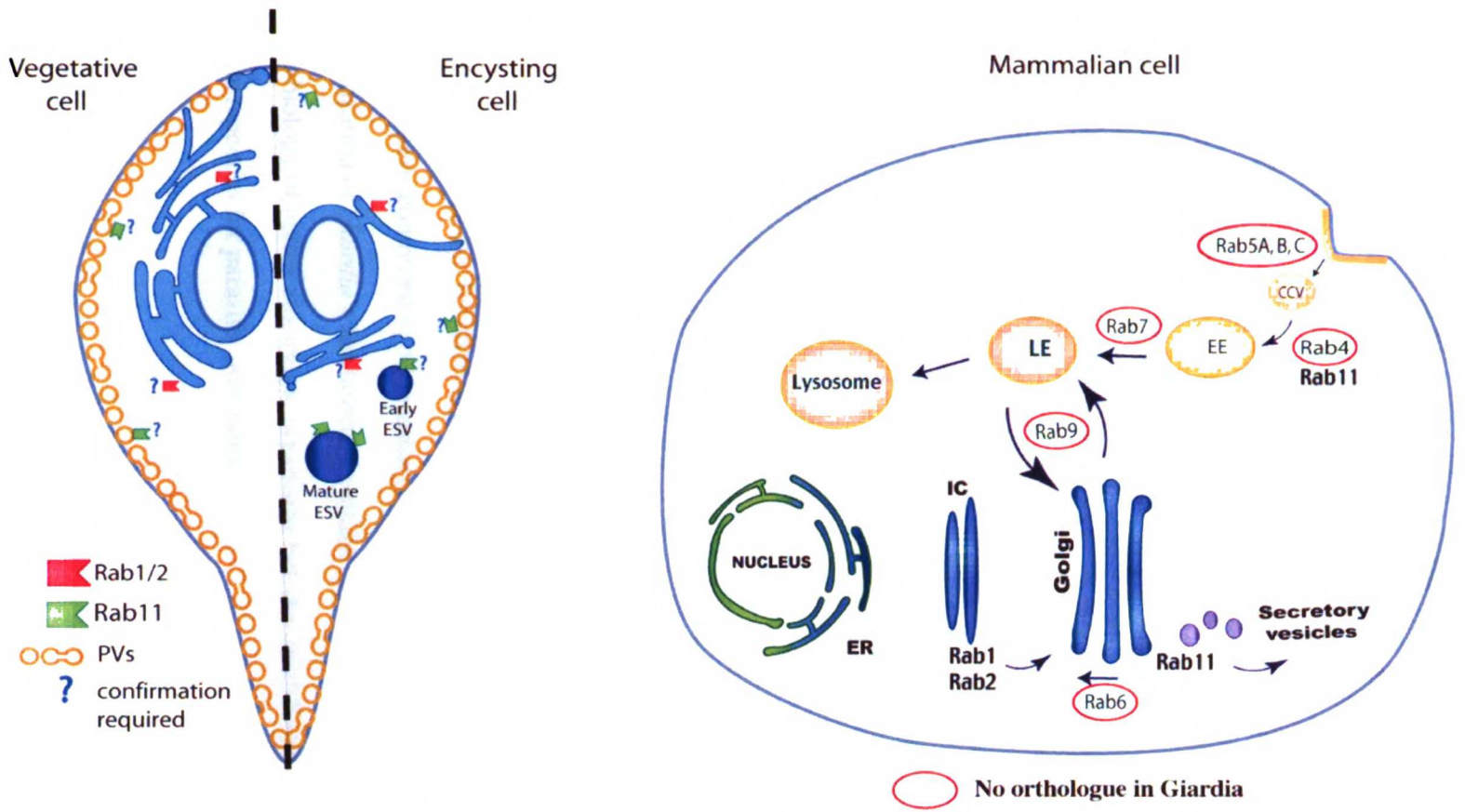

Figure 4.7. Rab localization in Giardia and the mammalian cell. The Giardia genome encodes four of the core endo- and exocytic Rab proteins, Rab1, Rab2 (two isoforms) and Rab11. Though further characterization in required (?), GiRab1 and both isoforms of GiRab2 are postulated to function at the perinuclear region and TVN in vegetative (left of dashed line) and encysting cells (right of dashed line). Preliminary results localize GiRab11 to the PVs and to ESVs. Giardia does not have orthologues for the other canonical core endo- and exocytic Rabs: Rab4, 5 (isoforms A,B,C), 6, 7and 9 (in mammalian cell, circled in red).

The canonical endocytic Rabs, 5, 6 and 7, function in the sequential endocytic transport steps: clathrin-coated vesicle assembly at the plasma membrane and endosome fusion, intra-Golgi and Golgi to ER transport, and early endosome to late endosome and early endosome to lysosome transport, respectively. Rab4 functions in receptor recycling between the early endosomes and plasma membrane, while Rab9 is involved in protein transport from the late endosome to the *trans*-Golgi. Since *Giardia* does not have either a classical discernible Golgi (The Golgi structural protein, Golgin, has not been identified in the completed *Giardia* genome.) or endosomes, it may not be surprising that we do not find Rab4, Rab5, Rab6 and Rab9. *Giardia*'s peripheral vesicles (PVs) were thought of as lysosome-like compartment. However, representative lysosomal enzymes, cathepsin B-like cysteine proteases, very minimally localize to the PVs in *Giardia* (Abodeely thesis). In mammalian systems, Rab9 recycles the mannose 6-phosphate receptor to the trans-Golgi from the late endosome (200). The mannose 6-phosphate (M6P) receptor is responsible for lysosomal protease trafficking to the lysosome in an M6P-dependent manner. Since *Giardia* has neither phosphotransferases (required for M6P biosynthesis) nor the M6P receptor, it is not surprising that we did not find Rab9 in the *Giardia* genome. Interestingly, several studies have provided evidence for an M6P-independent protein trafficking pathway in higher eukaryotic systems (61,201). *Giardia* may encode other small GTPases that function in place of these or perhaps *Giardia* has different specialized needs compared to other eukaryotic organisms. Regardless, through detailed characterization of *Giardia*'s fundamental cellular processes we will not only gain insight into the biology of higher eukaryotic organisms but also be able to identify leads for future therapeutics for parasitic infections.

Chapter Five

*Gl*CP2 is sorted to encystation-specific vesicles (ESVs) with the onset of encystation

Introduction

During encystation, *Giardia* increases transcription of the cyst wall genes (CWP1, 2 and 3), which encode a signal sequence that directs the transcripts to the ER and secretory pathway for packaging into encystation-specific vesicles (ESVs) (116). The ESVs carry the newly processed CWPs to the cell periphery where they are released for cyst wall synthesis. The ESVs are considered to be separate endomembrane compartment with their biogenesis initiated when the *Giardia* cell is stimulated to encyst. They appear to bud from the ER-like TVN (18,25). CWP2 is known to be endoproteolytically processed by a cysteine protease but it is an ongoing debate as to whether the activity is a cathepsin C-like protease (104) or another endoprotease. *Gl*CP2 is the most abundantly expressed cysteine protease in both vegetative and encysting trophozoites {Dubois, K personal communication}, therefore, I investigated whether *Gl*CP2 may have a role in encystation by determining *Gl*CP2 subcellular localization in encysting trophozoites by deletion analysis, IFA and immuno-EM. I also investigated whether *Gl*CP2 as cargo partners with other proteins for vesicle targeting during the encysting process by affinity chromatography and mass spec analysis.

Results

Subcellular localization

In this study, I first sought to determine *Gl*CP2 subcellular localization in encysting trophozoites. Full-length *Gl*CP2 and *Gl*CP2sspro14 (The latter construct consists of the *Gl*CP2 signal sequence, **pro**domain and **14**a.a. of mature/catalytic domain to preserve the endogenous *in vivo* processing site located at the C-terminus of the prodomain and the N-terminus of the catalytic domain.) were cloned into the shuttle plasmid vector, pGFP.pac (Ted Nash, NIH and Lei, Li UCSF) with GFP fused in frame to the C-terminus of *Gl*CP2 and *Gl*CP2sspro14. The *Gl*CP2-GFP fusion constructs were transfected into vegetative *Giardia* by electroporation. Once the *Gl*CP2-GFP

fusion proteins were expressed at detectable levels by confocal microscopy, the *Giardia* transfectants were stimulated to encyst. During vegetative growth, the full-length *Gl*CP2-GFP and the *Gl*CP2sspro14-GFP fusion proteins co-localized with PDI2 to the TVN by confocal microscopy (Figure 5.1, panels a-c)

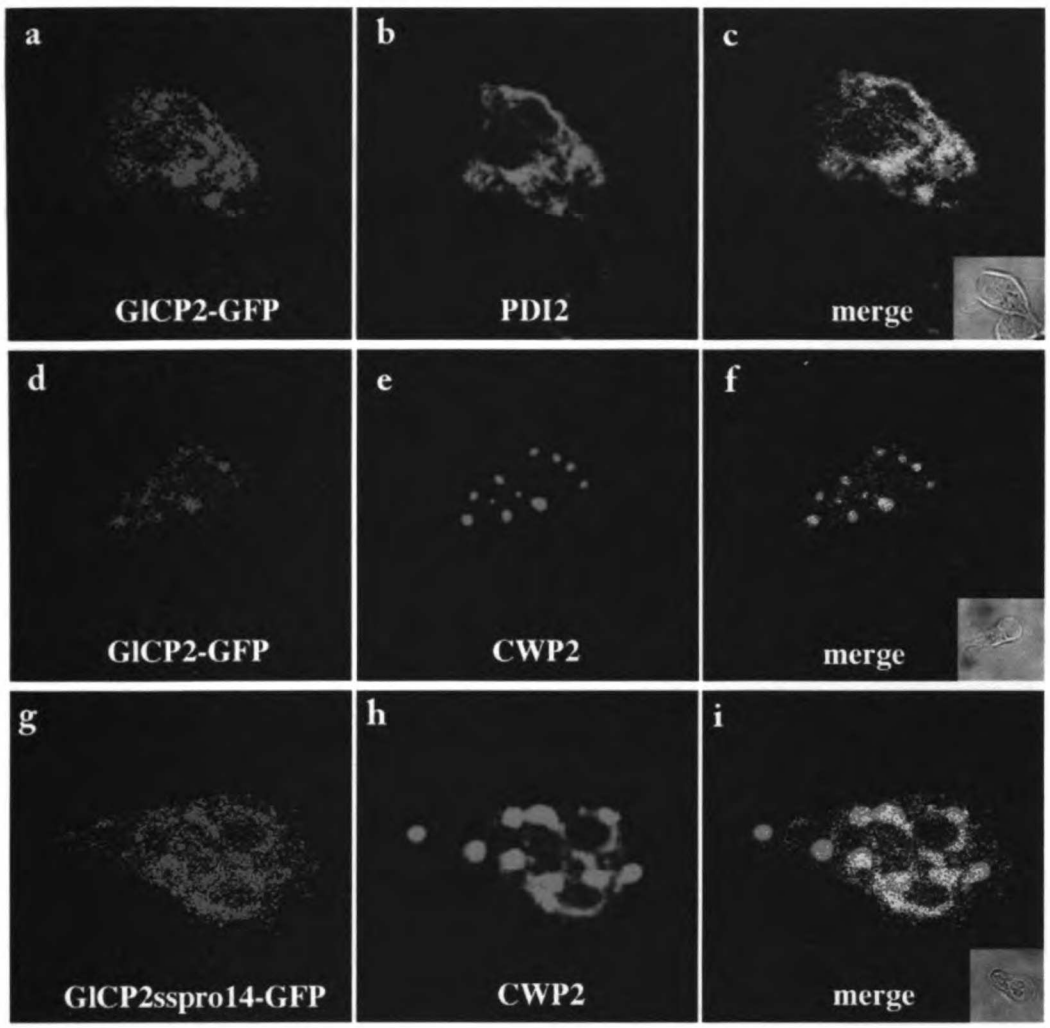

Figure 5.1. Subcellular localization of GlCP2-GFP fusion proteins. In vegetative cells GlCP2-GFP (panel a) co-localized with PDI2 (panel b) in the ER-like TVN (merge is yellow, panel c). The same localization pattern was observed for GlCP2sspro14-GFP (Data not shown.). In encysting cells, GlCP2-GFP and GlCP2sspro14-GFP (panels d and g) co-localized with CWP2 (panels e and h) in the ESVs (merge is yellow, panels f and i).

However during encystation, both constructs also co-localized with CWP2 to ESVs by confocal microscopy (Figure 5.1, panels d-i). Ultrastructural analyses confirmed the subcellular localization patterns. In previous work using vegetative trophozoites, EM ultra-thin sections from transfectants harboring the empty pGFP.pac vector exhibited uniform GFP distribution throughout the entire cell (Data not shown.) while full-length *Gl*CP2-GFP and the *Gl*CP2 sspro14-GFP fusion proteins showed subcellular compartment localization in the nuclear envelope, ER-like TVN and, occasionally, a PV (Figure 5.2).

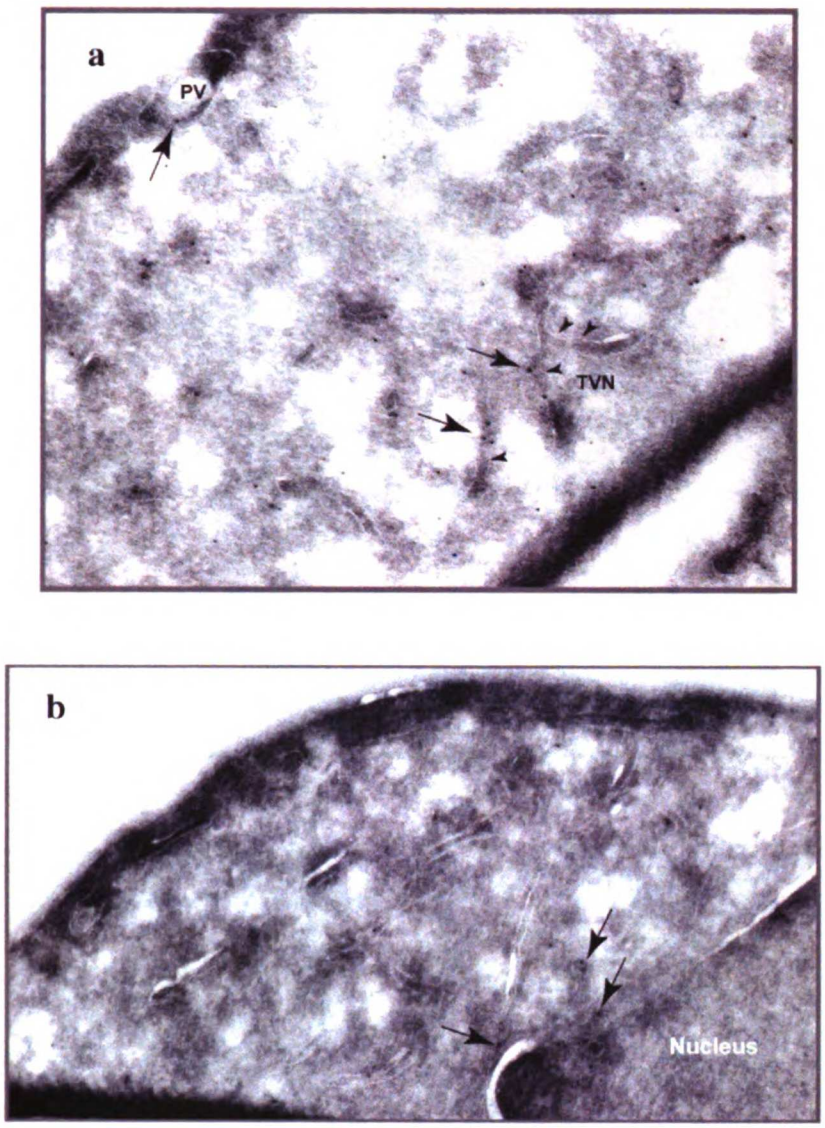

Figure 5.2. Subcellular localization of GlCP2sspro14-GFP fusion protein in a vegetative trophozoite by immuno-EM. In panel a, GlCP2sspro14-GFP (small arrows, 1nm gold) is observed in the ER-like TVN (small arrowheads), branching throughout the cytoplasm. GlCP2sspro14-GFP is occasionally observed in a PV. Panel b, shows GlCP2sspro14-GFP fusion protein localized to the perinuclear region of the cell. GlCP2-GFP had an identical subcellular localization pattern (Data no shown.).

Co-localization studies in encysting cells using Immuno-EM also confirmed the subcellular co-localization of CWP2 using a 10nm gold-conjugated secondary antibody and *Gl*CP2-GFP fusion proteins using a 1nm gold-conjugated monoclonal antibody to GFP to ESVs (Figure 5.3). These observations suggest a putative role for *Gl*CP2 during encystation and, possibly in CWP-processing.

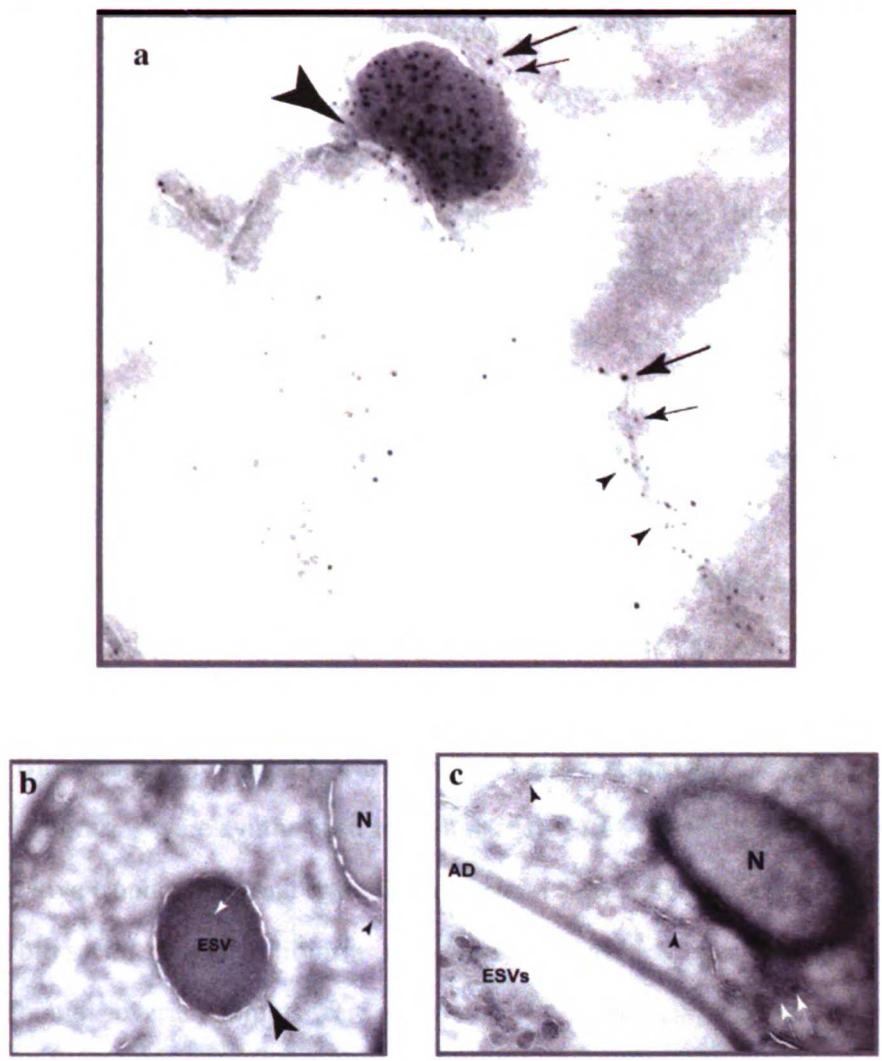

Figure 5.3. GlCP2-GFP fusion protein co-localized with CWP2 to ESVs in encysting cells by immuno-EM. In panel a, GlCP2 (small arrows, 1nm gold) along with CWP2 (large arrow, 10nm gold) are transported through the TVN (small arrowheads) and delivered to the budding ESV (large arrowhead). In panels b and c, CWP2 (white arrow, 1nm gold) is localized to the TVN and perinuclear region (small arrow heads) and to budding ESVs (large arrow head). In panel c, ESVs migrated to the cell periphery in an adjacent encysting cell (lower left).

I had a *Gl*CP2 peptide antibody generated in rabbits by SynPep and Covance. The peptide corresponded to a *Gl*CP2-specific sequence in the mature/catalytic domain that was not found in *Gl*CP3, since they share 80% similarity at the amino acid level. However, I did not observe specific *Gl*CP2 staining with *Giardia* lysates by Western blot analysis or by confocal microscopy. The lab is still pursuing efforts to express *Gl*CP2 at levels high enough for antibody production using a variety of approaches.

GlCP2 Trafficking partners

In higher eukaryotic systems, cysteine proteases have been shown to have endosomal/lysosomal trafficking partners that are independent from the M6P pathway. In plants, yeast and trypanosomes, amino acid sorting signals has been identified in the pro region of a protease (202,203). Since my preliminary studies suggested that the *Gl*CP2 prodomain is sufficient for proper targeting to the TVN in vegetative cells and to ESVs in encysting cells, I sought to identify putative *Gl*CP2 trafficking partners.

In initial studies to identify proteins involved in *Gl*CP2 trafficking, I performed yeast two-hybrid screens using the prodomain of *Gl*CP2sspro14 as bait. Since there are no commercially available *Giardia* cDNA libraries, I generated *Giardia* cDNA libraries using BD Biosciences Clontech Matchmaker™ Library Construction & Screening kits. Four cDNA libraries were synthesized including two cDNA libraries using mRNA from vegetative trophozoites and two cDNA libraries with mRNA from encysting cells. In both sets, I generated libraries using first oligo dT primers and then random primers. Though several attempts were made using this approach, I did not identify any candidates.

In a second approach to identify putative *Gl*CP2 interacting proteins, I used a hexa His-tagged *Gl*CP2 propeptide as bait in affinity chromatography experiments. This methodology employed chemical cross linkers and cell lysates from both vegetative and encysting trophozoites. In previous efforts, we tried unsuccessfully

to express significant amounts of both the full-length and sspro14 *Gl*CP2 proteins in bacteria and yeast systems to use as bait in the affinity chromatography studies (Abodeely, Dubois and Sajid unpublished data). As an alternative, we commissioned Synpep to synthesize the largest possible portion of the *Gl*CP2 pro domain. Due to technical limitations, Synpep synthesized 30 of the 52 propeptide amino acids and a hexa-His tag. The 30a.a. *Gl*CP2 propeptide included an N-terminal conserved 10 amino acid motif, WKAGIPKRF that has been implicated in M6P-independent protease trafficking in *Trypanosoma cruzi* and mammals (Figure 5.4) (56).

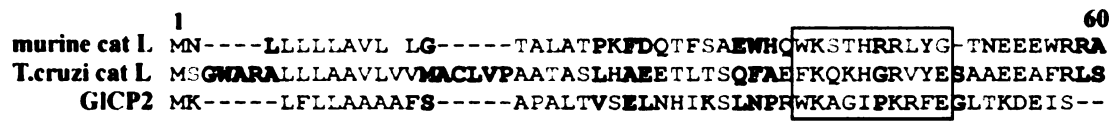

Figure 5.4. Pro region alignment. A conserved trafficking motif (boxed region) was implicated in a M6P-independent protease trafficking pathway in mice and *T.cruzi*. The trafficking motif is located in the proregions of murine cathepsin L and *T. cruzi* cathepsin L (cruzain). The *Giardia* cathepsin B-like protease, GlCP2, exhibits some homology in this region.

The methodology for the affinity chromatography approach was as follows: we solubilized lysate from either vegetative or encysting cells using the detergents 0.5% Triton X100 in 25mM Tris-Hcl pH7.2 in the presence of the protease inhibitors, 100mM PMSF and 10μM E64. Following incubation for 3hrs, we dialyzed out the Triton X100 from the two sets of solubilized lysate. In a two-step process, we bound the *Gl*CP2 propeptide to putative trafficking partners in *Giardia*'s two different life stages. First, we incubated *Gl*CP2 propeptide with either the lysate from vegetative or encysting cells and then followed with a second incubation in the presence of sulfo-EGS, a membrane impermeable chemical cross-linker, in serial dilutions as follows: 0.5, 5.0, 10, 50,

100mM. The protein mixtures containing the *Giardia* proteins and the His-tagged *Gl*CP2 propeptide were then denatured in 8.0M urea in 100mM Tris-Hcl, pH8.0 and applied to a nickel-NTA column (Qiagen). Unbound proteins were removed in a series of washes in 8.0M urea. The purified samples, which were bound to the nickel-NTA, were solubilized in sample loading buffer with (5.0% SDS with 50mM DTT) and resolved using a 10-20% gradient Tris-glycine gel under sterile conditions.

In the gel-containing samples prepared with the vegetative trophozoite lysate, 10 bands were excised at various concentrations of cross-linker (These samples were not present in the control lane containing cell lysate with cross-linker incubated with the Nickel NTA beads). However, the 10 bands were only visible by silver staining. By LCMS mass spectrometry, we identified the following proteins: tubulin beta chain, arginine deiminase, ornithine carbamyltransferase, glyceraldehyde-3-phosphate dehydrogenase 1, putative fructose-1, 6-bisphosphate aldolase, ribosomal protein L5 and 14-3-3 protein (Figure 5.5).

Figure 5.5 Mass spectrophotometry hits from vegetative lysates.

Species Protein Name	Acc #	# Hits	Reference PUBMED	Notes
Ornithine carbamoyltransferase	O76458	54	Direct submission	In plants and microbes OTC is involved in arginine biosynthesis. In mammals, it is located in the mitochondria and is part of the urea cycle.
Carbamate kinase	O97438/ Q7QY52	9	10347186/ DS	carbamate kinase (CK) and ornithine carbamoyltransferase may interact involved in synthesis of carbamoyl phosphate (CP) a precursor to pyrimidines and arginine
Glyceraldehyde-3-phosphate dehydrogenase 1	P53429	6	Direct submission	Carbohydrate degradation; glycolysis
Tubulin	P05394	4	3267222	Tubulin is the major constituent of microtubules.
Thioredoxin reductase	Q7R527	4	N/A	Posttranslational modification, protein turnover, chaperones
14-3-3 protein	Q2QBT8/ EAA42214/ AAZ91664	1	16368691	Family of highly conserved protein involved in signal transduction for cellular process including cell cycle, differentiation and apoptosis

These results are consistent with abundant cytoplasmic proteins not associated with the

ER or endomembrane compartments.

In samples of bound proteins using encysting trophozoite lysate, I observed more abundant protein detectable by staining with Coomassie. The gel bands from the entire lane containing the sample incubated with 10mM of chemical cross-linker were excised and prepared for LCMS mass spectrometry analysis. Multiple protein candidates were identified with the top hits summarized in Figure 5.6.

Figure 5.6. Mass spectrophotometry hits from encysting lysates.

Species Protein Name	Acc #	# Hits	Reference PUBMED
Cytosolic-type hsp90	Q5KTX3	11	15496553
Vacuolar sorting protein 35-like	Q6Y0Y2	9	14667372
14-3-3 protein	*Q2QBT8 AAZ91664_EAA42214	8	16368691
Dynamin-like protein	Q8T6L2	7	12711599
Protein disulfide isomerase-2 precursor (1hit PDI4)	O97452	6	10514458
Vacuolar ATPase catalytic subunit A	P92128	6	
Guanine nucleotide-binding protein Rab1A	Q9GU79	4	12243734
Rab-like protein A	*Q966X6	4	N/A
Cytoplasmic 70 kDa heat shock protein	Q24966	4	8159675
Putative adaptor protein complex large chain BetaB	Q8MZS0	3	12711599
GTP-binding nuclear protein Ran	P38543	3	8006038
Chaperonin subunit epsilon CCTepsilon	Q9GU01	3	11018153
Chaperone-t-complex eta subunit	Q8ISL9	3	N/A
Putative adaptor protein complex med subunit (AP-2)	Q8T4M7	1	12711599
Vacuolar protein sorting 26-like	Q6Y0Y3	1	14667372

* The provided accession number didn't provide a link to a sequence.

Both Dynamin-like protein and PDI2 had been previously identified as ESV-associated proteins (33). The other identified proteins such as cytosolic Hsp90, vacuolar sorting protein 35-like, vacuolar ATPase catalytic subunit A and AP-2 subunits are interesting putative *Gl*CP2- and ESV-associated proteins, which may provide insights into the ESV maturation process and the role of *Gl*CP2 and requires further investigation (Figure 5.7).

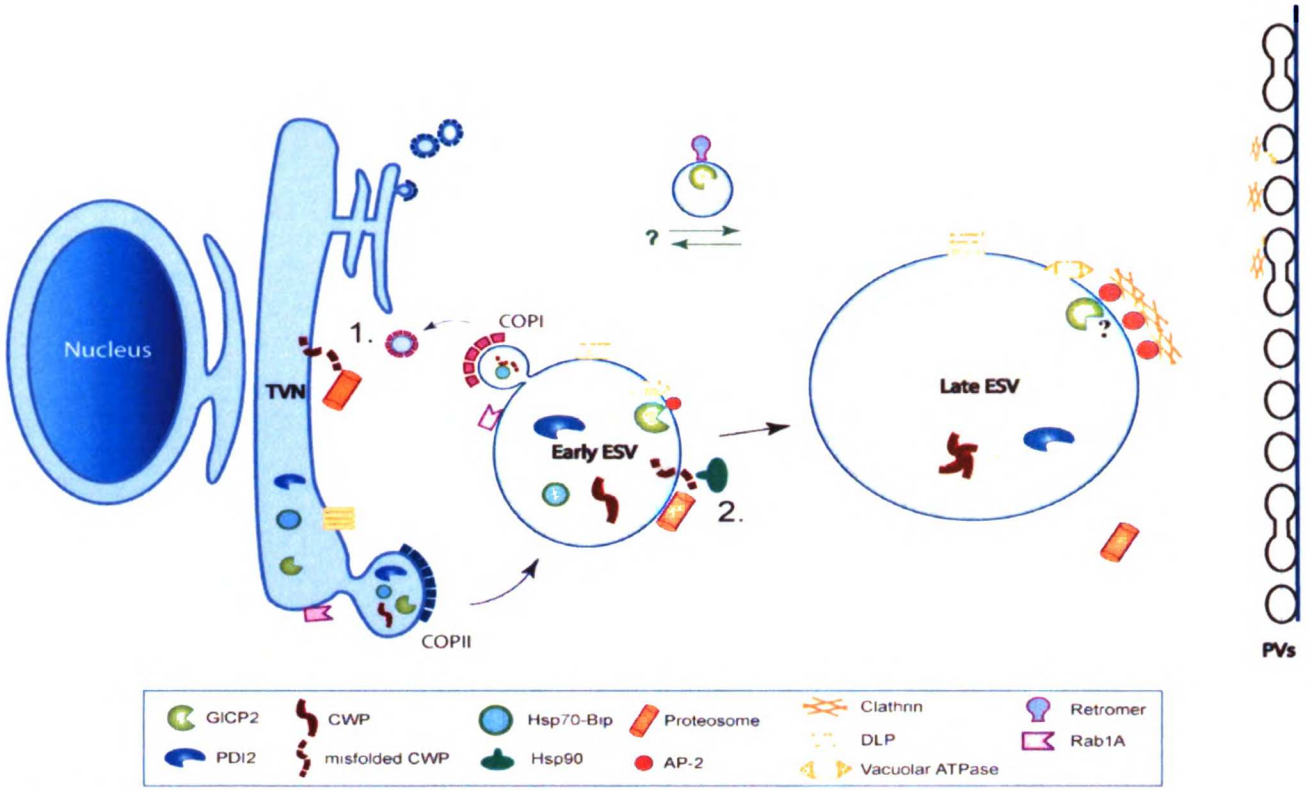

Figure 5.7. Proposed model for GlCP2 trafficking and function in encysting cells. GlCP2 is delivered to the endomembrane system by an N-terminal signal sequence. At the TVN, GlCP2 is packaged into budding COPII-coated ESVs along with the CWPs, PDI2 and Hsp70-Bip. Within the COPI-associated early ESVs , CWP2 is processed by GlCP2 and heterodimerized with CWP1. CWP complex foramation is mediated by PDI2. To ensure quality control, misfolded CWPs may be returned to the TVN in COPI vesicles through interactions with Hsp70-Bip (with KDEL) and, subsequently, retrotranslocated to the cytosol for proteaseome-mediated degradation (1.). In a second quality control sceneraio, misfolded proteins exit the early ESVs by interaction with Hsp90 and GlCP2 for degradation by ESV-associated proteasomes (2.). Mature ESVs contain complexed CWPs, GlCP2, PDI2 and become clathrin-coated as they migrate to the cell periphery. Recruitment of the clathrin coat may be mediated through interactions between GlCP2, AP-2 and an unknown effector protein(s). Mature ESVs are no longer associated with the proteasome suggenting quality control occurs in the earlier stages of encystation. GlCP2 maybe recycled back to early ESVs or to the TVN through interactions with the retromer complex (the Vsp 35-like and 26-like subunits). In contrast, retromer may also function in anterograde transport of GlCP2 to ESVs. Vacuolar ATPase may function to maintain the appropriate pH within the ESVs to ensure the proper environment for CWP complex formation. Rab1A may contribute to vesicle formaion at the TVN and early ESV, while Dynamin-like protein may function to maintain ESV morphology.

GlCP2 trafficking motifs

Since the *Gl*CP2sspro14 construct was sufficient for the correct targeting of *Gl*CP2 in vegetative and encysting cells, I sought to identify the putative prodomain targeting sequence(s). In collaboration with the Kuntz laboratory (UCSF), we performed homology modeling of *Gl*CP2 using the prodomains of mammalian cathepsin B and cathepsin L as templates to help plan rational deletions in the pro region and full-length *Gl*CP2-GFP chimera protein to identify the precise amino acid trafficking motif. To accomplish this, the promature *Gl*CP2 sequence was aligned against the promature regions of human cathepsin B, L and cathepsin L (cruzain) of *T.cruzi*, whose prodomains have been implicated in protease trafficking and whose structures have been solved (204) (205). These prodomain alignments were used to model the molecular structure of the *Gl*CP2 prodomain. This analysis revealed the presence of a solvent accessible conserved region that corresponded to a *Giardia*'s conserved 10 amino acid motif, WKAGIPKRF, which has been implicated in M6P-independent protease trafficking (56) (Figures 5.4, 5.8). A series of deletion constructs were designed in both *Gl*CP2-GFP and in the *Gl*CP2sspro14-GFP chimera proteins in accordance with the putative conserved motif (Figure 5.9).

Figure 5.8. Homology modeling of the full-length GlCP2 (white outline) and the proregion of human cathepsin L (thicker outline, larger white arrow heads) which includes the conserved trafficking loop (yellow, small white arrow head). Prodomain alignments were used to model the molecular structure of GlCP2 pro region (white arrow) which exhibits sequence homology to the cathepsin L pro region traffick motif. The GlCP2 proregion is shown here as solvent-accessible and, therefore it may be able to interact with trafficking or effector partners.

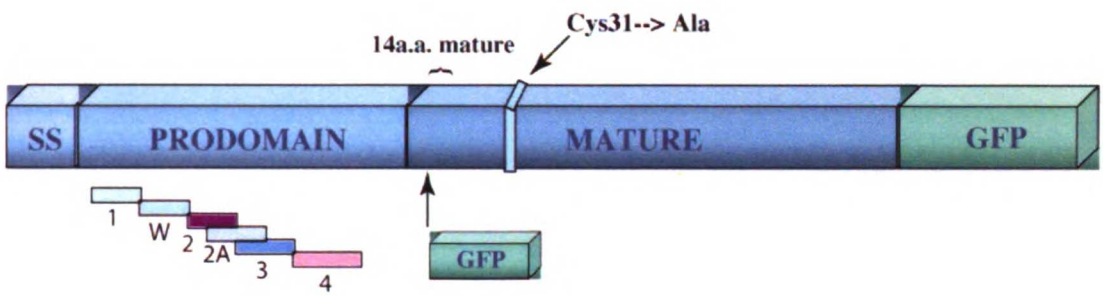

Figure 5.9. Schematic of full-length GlCP2-GFP trafficking constructs. Prodomain deletions 1, W, 2, 2A, 3 and 4 (PD) were approximately 9-10a.a. in length spanning the proregion, including the putative conserved region, PDW, (light blue box). These mutations were constructed in both the full-length GlCP2-GFP and the GlCP2sspro14-GFP fusion proteins. The GlCP2sspro14 included the signal sequence, proregion and 14a.a. of the mature domain to preserve the pro-mature cleavage site. In addition to the deletion mutants, an inactive GlCP2-GFP fusion protein was constructed by replacing the active cysteine (Cys31, GlCP2 numbering) with an alanine.

The deletion mutants were transfected into *Giardia* and visualized using confocal microscopy in vegetative trophozoites and encysting cells. Surprisingly, the localization

patterns were not affected by the deletions in either trophozoites or encysting cells (Figure 5.10). In addition, I also constructed an inactive *Gl*CP2-GFP fusion protein by replacing the active cysteine (Cys31) with an alanine residue. The inactive *Gl*CP2 was trafficked properly in both life stages (Figure 5.10). These results suggest that proper trafficking does not require the conserved motif in the prodomain, but does require, as discussed below, endoproteolytic processing of the prodomain at the pro-cat junction and access to the ER and secretory pathway by way of the signal sequence.

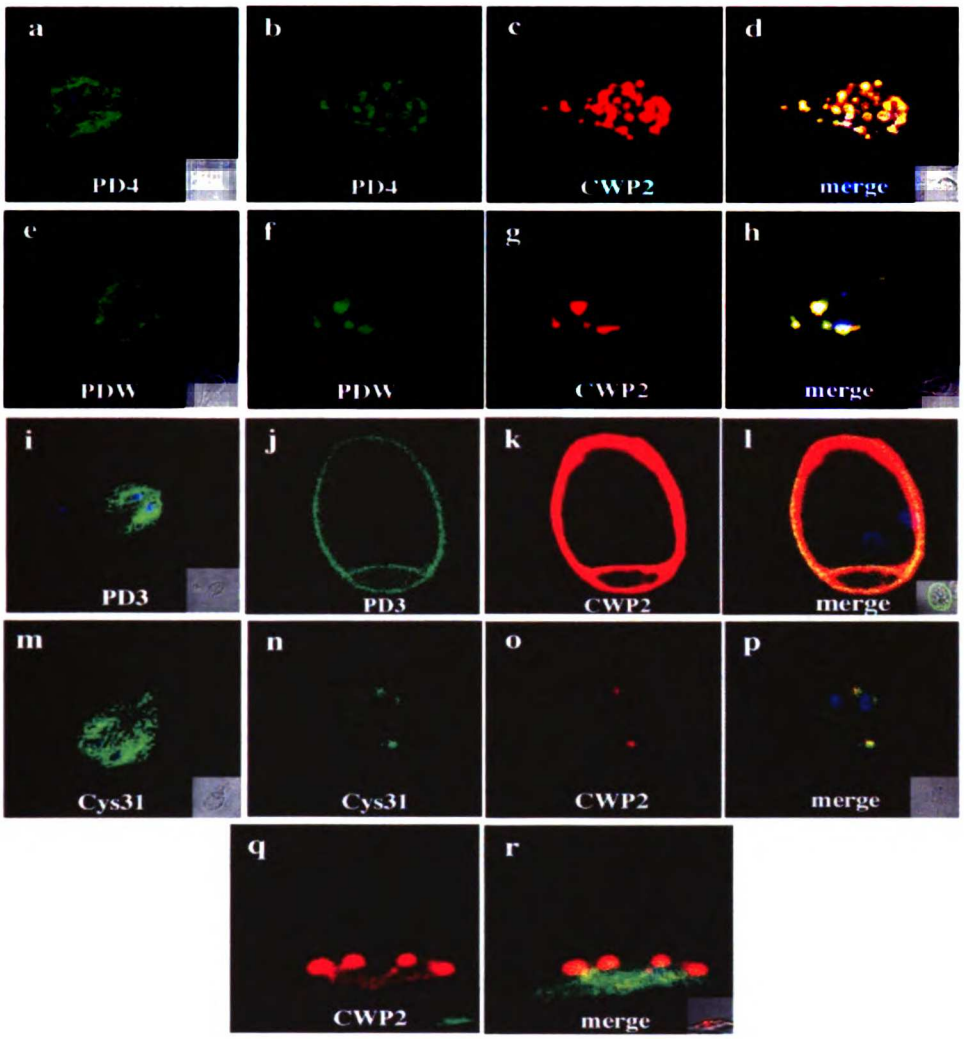

Figure 5.10. The GlCP2-GFP prodomain deletions (PD): 1, 2, 2A, 3, 4 and W (putative conserved motif) as well as inactive GlCP2-GFP fusion proteins exhibited identical subcellular localizaion patterns in trophozoites (panels a, e, i and m) and in encysting cells (b, f and n). The GlCP2-GFP PDs and inactive GlCP2-GFP co-localized with CWP2 to ESVs (panels d, h and p). The difference in ESV numbers and localization reflect different stages during the encystation process. Panels j-l show the PD3 mutant co-localized with CWP2 at eary cyst formation. In panels q and r, PD3 is observed at the encysting phase localized with CWP2 to budding ESVs (from the TVN) in a side view of an encysting trophozoite.

*Gl*CP2, which is an orthologue of mammalian lysosomal enzymes, is only minimally localized to the acidic peripheral vesicles (PVs) visualized by immuno-EM (Figure 5.2). This finding was at first surprising since the PVs have been thought to be the lysosome equivalent in *Giardia*. However as previously noted, in the vegetative trophozoite, the *Gl*CP2-GFP fusion protein co-localized with the ER marker, PDI2, in the ER-like TVN (Figure 5.1, panels a-c). In addition, both fusion constructs localized in the nuclear envelope, but not inside the nucleus (Figure 5.1 and 5.2). There was no co-localization with clathrin, which is believed to partially coat the PVs although not uniformly (Figure 3.4C) (Adrian Hehl, direct communication.). There was minimal co-localization with an antibody to COPI β heavy chain (data not shown). COPIβ localized to an endomembrane tubulo-vesicular system immediately beneath the peripheral clathrin-coated compartments (Adrian Hehl, direct communication).

I also generated the following *Gl*CP2-GFP constructs, *Gl*CP2 signal sequence alone and the *Gl*CP2 signal sequence with the pro region not including the pro-cat processing site. Transfection with both of the aforementioned fusion constructs resulted in cell lysis upon increased expression. These results suggest first that proper subcellular targeting may require not only the signal sequence alone, but also the prodomain. Second, there appears to be a requirement for prodomain processing as was reported for *T. cruzi*. Huete-Perez *et al.*, (1999) observed a disruption in successful targeting of the *T. cruzi* cathepsin L-like fusion protein when the pro-cat processing site was mutated. In the control experiment GFP alone without a signal sequence had diffuse cytoplasmic localization (Figure FI), suggesting that without the signal sequence GFP is denied access to the ER and thus the endomembrane system. However, since GFP expression could not be detected at this early stage in the selection process, it is unclear why these fusion proteins are toxic to the cells. One possibility may be excessive *Gl*CP2-GFP fusion protein accumulation within the TVN or an intermediate vesicle population that is

lethal to the cell. Engel *et al.*, (1999) reported that administration of a cysteine protease inhibitor to *T. cruzi* results in an accumulation of unprocessed proenzymes in the late Golgi resulting in cell death. Selzer *et al.*, (1999) made a similar observation when *Leishmania* were grown in the presence of a cysteine protease inhibitor that resulted in accumulation of inactive cathepsin B-like protease in the flagellar pocket.

Discussion

Upon induction to encyst, the *Giardia* trophozoite is stimulated to initiate encystation-specific gene transcription. A key family of regulated gene products is the cyst wall proteins (CWPs), which are targeted to the TVN and are packaged into vesicles, which bud from the TVN. The vesicles increase in size and associate with different endomembrane markers as they migrate to the cell periphery. ESV maturation is a 15-24h process that results in secretion of an extracellular fibrillar matrix and cyst wall formation. Previous work has provided insights into ESV and cargo maturation processes by using either an *in silico* approach or a combination of subcellular fractionation followed by two-dimensional gel electrophoresis to identify associated proteins (25,33,107). By investigating ESV association with different endocytic markers, ESVs initially resemble an ER/Golgi compartment and later take on the characteristics of a late endosomal/lysosomal compartment. ESV maturation is concomitant with progression through the endomembrane system.

Early ESVs

Early ESVs bud from the TVN compartment to begin the migratory process to the cell periphery at approximately 5-8h post-induction (11,14,206). Before being packaged into ESVs, CWPs partially co-localize with the small GTPase sar1p at specific "ER exit" sites at the TVN; this step is essential for ESV biogenesis (Stefanic and Hehl, unpublished results). Since sar1p recruits COPII coatomer formation to the cytoplasmic side of the ER membrane in higher eukaryotes, sar1p is used as an endocytic marker for

COPII coatomer in *Giardia* (25). Interestingly, β-COPI, a subunit of COPI coatomer associates with nascent ESVs along with CWP-negative structures. In yeast and mammalian systems, COPII vesicles mediate anterograde transport from the ER to the *cis*-Golgi while COPI vesicles mediates retrograde transport from the *cis*-Golgi to the ER (23,24). Whether ESVs develop by simply budding from the TVN (35) or by homotypic fusion of COPI vesicles (25) continues to be debated.

In addition to coatomer, the cytoplasmic side of early ESV membranes were found to be associated with GiYipl and GiDLP. In yeast cells, Yip1, a transmembrane protein, directly binds Ypt1p and Ypt31p, the respective Rab1 and Rab11 mammalian orthologues, at the Golgi network. When Yip1 is depleted in *S. cerevisiae*, the ER membrane expands and there are aberrations in secretion and glycosylation of the enzyme invertase (207). *Giardia* Yip1 is also partially localized to the TVN. DLP (dynamin-like protein) is a large GTPase that functions in clathrin-coated vesicle formation primarily at the plasma membrane although it has been observed at the ER, Golgi and endosomal compartments in mammalian cells (208). In addition, recent studies report that DLP also functions in maintaining ER and mitochondrial morphology (208). *P. falciparum* genome encodes for two DLP proteins. One of the DLP proteins, Pfdyn1, is expressed during the erythrocyte stage and partially co-localizes with the ER-resident protein PfGrp78 at the ER. Pfdyn1 may be involved in protein secretion or responsible for the proper targeting of endocytosed material (209). *Giardia* DLP is observed at several subcellular compartments including the TVN, unknown cytoplasmic structures and at the PVs. In contrast to GiYipl and GiDLP, Gisar1p and the *Giardia* syntaxin proteins selectively localize to the TVN and not to ESVs or any other endomembrane compartment further demonstrating that ESV maturation is a regulated process.

Within the early ESV the newly translated CWPs are post-translationally modified as follows (i) disulfide bond formation and reshuffling by protein disulfide isomerases (PDI) (28) (ii) cleavage of the 13 kDa carboxy-terminal extension of CWP2 mediated

by cysteine protease activity (104) and (iii) phosphorylation by an unknown kinase (27). If either disulfide bond formation or CWP2 cleavage is inhibited, the ESV spherical morphology is altered to a tubular or disintegrated form, thereby abolishing cyst wall formation (28,32). Not surprisingly, PDI2 along with Hsp70-Bip were identified in the TVN by confocal laser scanning microscopy (CLSM) and subcellular fractionation (30,33). PDI2, which functions within the ER of higher eukaryotes, localized to both the TVN and ESVs in encysting *Giardia*. Similarly, *Giardia* Hsp70-Bip was observed to cycle between the ER and ESVs. GiHsp70-Bip cycling is dependent on a conserved C-terminal KDEL retrieval sequence. One of the most intriguing features of the early encystation process is the re-localization of the proteasomal complex subunits, alpha structural subunit of the 20S proteasomal complex and the cim5 homologue of the19S cap, from cytoplasmic structures to the cytosolic side of early ESV membranes during the early stages of encystation. Stefanic *et al.*, (2006) propose that the proteasomal subunits and Hsp70-Bip function in a type of ER quality control pathway ensuring the integrity of the CWP complexes essential for cyst wall biosynthesis.

Mature ESVs

As the ESVs mature, approximately 10-24h post-induction, ESVs undergo a reorganization of associated proteins. Throughout the maturation process, ESV cargo continues to include CWPs, PDI2, and HSP70 and retain their cytoplasmic association with GiDLP. However, *Giardia* Clathrin (GiCLH) replaces GiYip1and Giβ-COPI on the ESV membrane surface. In addition, GiCLH and GiDLP show partial PV localization. Rab11 also partially localizes to both ESVs and PVs in encysting cells. The precise subcellular localization pattern of Rab11 and its role in ESV maturation requires further investigation. Interestingly, the proteasomal proteins, which localize to the membranes of early ESVs, disassociate from mature ESV membranes and re-localize to the cytosol in the late stages of encystation. Since the proteasome only associates with early ESVs, this suggests that proteasomal activity serves a specific, developmental function.

Touz *et al.*, (2002) demonstrated that CWP2 processing was dependent on a cysteine protease activity and proposed a cathepsin C protease they named ESCP (encystation-specific cysteine protease). ESCP contains a transmembrane region at the C-terminus as well as a tyrosine-based motif YXXØ consensus, YRPI, that interacts with the adaptor protein, AP1. In higher eukaryotes, the AP1 medium subunit (μ) mediates cargo interactions through a conserved C-terminal peptide motif. Touz *et al.*, (2002) proposed that the ESCP signal peptide grants ESCP access to the TVN and secretory pathway where it is trafficked first to the PM and then endocytosed into the PVs. In the late stages of encystation, ESCP is trafficked from the PVs to mature ESVs. Though a HA-tagged ESCP is observed in both PVs and in mature ESVs only, the trafficking route could not be reproduced.

GlCP2 and putative interacting partners in a revised model

GlCP2 function

In vegetative trophozoites, *Gl*CP2 functions in the degradation of endocytosed proteins within the TVN. Proper *Gl*CP2 trafficking to the TVN simply requires access to the endomembrane system, which is mediated by the N-terminal signal sequence. During encystation, *Gl*CP2 is packaged into developing ESVs, which are seen budding from the TVN. *Gl*CP2sspro14-GFP and *Gl*CP2-GFP along with a series of deletion mutants co-localize with CWP2 in ESVs by CLSM and immuno-EM (Figures 5.1, 5.3, 5.10). In contrast, ESCP, which has been implicated in CWP2 processing, is only observed in mature ESVs. By quantitative RT-PCR, *Gl*CP2 is expressed at significantly higher levels during encystation compared to each of the 22 other cysteine proteases encoded in the *Giardia* genome, including ESCP (Dubois, personal communication). The CWP2 processing step is essential to cyst wall formation and dependent on a cysteine protease endoproteolytic activity (104). The cathepsin C-like protease, ESCP, was isolated from cell lysates using an inhibitor that is able to more efficiently bind other proteases

including cathepsin Bs. In addition, cathepsin C proteases are known to exclusively function as exopeptidases (Turk, personal communication). By sequence homology, *Gl*CP2, a cathepsin B protease, is predicted to function as an endopeptidase (58). These findings suggest that a contaminant may be responsible for the CWP-processing observed by Touz *et al.*, (2002). I propose that *Gl*CP2 may be the CWP2 processing enzyme. Ongoing experiments include expressing active recombinant *Gl*CP2 and CWP2 to determine whether it is the CWP2 processing enzyme or one of the processing enzymes. In addition, it would be interesting to determine the precise *Gl*CP2-CWP2 processing site by N-terminal sequencing and compare *Giardia* cathepsin B substrate specificities with other known cathepsin B proteases for insights into structure function relationships.

GlCP2 interacting proteins

By using affinity chromatography with the *Gl*CP2 proregion as bait, several *Gl*CP2 interacting proteins were identified from encysting cell lysates summarized in Figure 14. Among the proteins identified, several candidates were previously identified as ESV-associated proteins including PDI2 (28), Hsp70-Bip (33), DLP (33), Rab1A (108) and a14-3-3 protein (210). Rab1A localized to the ER/TVN and to the PV membranes in vegetative cells. In late encysting cells (the authors did not investigate early encysting cells), Rab1A was observed at the periphery of ESVs (108). However, Rab1A subcellular localization requires further investigation, since the antisera used was generated against the *Leishmania* Ypt1p homologue and also cross-reacted with Rab2. *Giardia* encodes a single gene copy of 14-3-3 that is constitutively expressed during both life stages. In higher eukaryotes, 14-3-3 proteins function in a diverse array of processes such as apoptosis, cell differentiation, cell-cycle regulation and other signaling pathways through direct interactions with enzymes, transcription factors and structural proteins (211-213). In the protist, *P. falciparum*, Pf14-3-3 is expressed only in the young trophozoite during the erythrocyte stage and may mediate developmental processes (214). The *Giardia* 14-3-3 protein is highly polyglycylated during vegetative growth. However, as

Giardia proceeds through encystation, the *Giardia*14-3-3 undergoes dramatic reduction in polyglycylation, which is proposed to mediate translocation to the nucleus (210). The nuclear subcellular staining should be confirmed by co-localizing *Giardia* 14-3-3 with an ER marker such as PDI2 in a z-series sequence.

Though vacuolar ATPases have not been previously observed as ESV-associated, the vacuolar ATPase catalytic subunit A was identified as a putative *Gl*CP2 interacting protein. Vacuolar ATPases are enzyme complexes that belong to a family of ion pumps that couple the energy of ATP hydrolysis to ion transport across the plasma membrane and intracellular membranes of such organelles as endosomes, lysosomes and clathrin-coated vesicles (215,216). They function in the acidification of compartments that are required for the degradation of macromolecules, ligand-receptor dissociation and receptor recycling following receptor-mediated endocytosis. Inhibition of vacuolar ATPases affects retrograde transport from the Golgi to the ER (180,217). This affect appears to be mediated through binding of proteins associated with vesicle formation. Aniento *et al.*, (1996) reported that early endosomal membranes could not associate with the coat protein COPI in the presence of the vacuolar ATPase inhibitor bafilomycin, Baf A1. In addition, Palokangas *et al.*, (1998) observed a decrease in COPI vesicles that were recycling p58 (an abundant membrane protein) (218) to the ER. Baf A1 also inhibits delivery of endocytosed material from endosomes to lysosomes thereby suggesting a role for vacuolar ATPases in this trafficking step as well. The affects on intracellular trafficking by vacuolar ATPases inhibitors suggest that the luminal pH of endosomal compartments regulates the functional properties and binding capacities of intracellular membranes. Perhaps, a similar vacuolar ATPase resides within the ESV membrane and functions to maintain the luminal pH of the ESV in order to process CWPs and mediate COPI coatomer binding. This may be particularly true for early ESVs, which have found to be associated with COPI. It has been argued that induction of encystation and the subsequent, rapid increase in CWP translation and packaging into ESVs could lead

to a greater incidence of accumulation of misfolded proteins. It has been proposed that Hsp70-Bip binds misfolded proteins in the ESV lumen and together they are recycled in COPI-coated vesicles to the TVN. Within the TVN, Hsp70-Bip delivers the misfolded proteins to sec61 pore complex for retro-translocation to the cytosol for proteasomal degradation.

However, the aforementioned model does not explain why proteasomal subunits were found to associate with early ESVs. A second explanation might be that Hsp70-Bip binds and retro-translocates misfolded proteins through the sec61 pore complex embedded within the ESV membrane for degradation by ESV-associated proteasomes on the cytoplasmic side of the membrane. Though the *Giardia* genome codes for a sec61 protein, the pore complex was not localized to the endomembrane system. In yeast and mammalian cells, the proteasome has been observed at the ER (219,220). I also identified Hsp90 function in protein folding and in signaling pathways usually as part of a complex with other co-chaperonins (221,222). In recent studies, a role for Hsp90 growth factor and protein toxin trafficking has been defined. Hsp90 has been shown to mediate fibroblast growth factor 1 and 2 (FGF-1, -2) translocation from endosomes to the cytosol and nucleus. Pathogens have exploited this pathway. Diphtheria toxin and *C. botulinum* C2 toxin use the Hsp90 translocation mechanism to exit the acidic endosomes and gain entry to the host cytosol (223,224). Interestingly, translocation of the toxin catalytic subunits is also reliant on endosome acidification maintained by vacuolar ATPase (225,226). Wesche *et al.*, (2006) proposed a model in which Hsp90 is directly involved in the translocation mechanism by "pulling" the partially unfolded proteins through the membrane into the cytosol. During encystations, perhaps the *Giardia* Hsp90 contributes to ESV cargo quality control by facilitating translocation of misfolded protein to the ESV-associated proteasomes.

Dacks *et al.*, (2003) identified two retromer components, Vps26p and Vps35p, in the *Giardia* genome and claimed that this finding demonstrated that *Giardia* does, in

fact, contain "Golgi bodies". In higher eukaryotes, the retromer complex mediates cargo protein recruitment and packaging into retrograde vesicles for transport to the *trans*-Golgi from the late endosomes in mammalian cells and the prevacuolar compartment in fungi and plants. In yeast, the retromer complex consists of 5 subunits (Vps5, 17, 26, 29 and 35) and is localized on endosomes at a steady state where it functions in Vps10p (carboxypeptidase Y receptor) retrieval to the *trans*-Golgi (227). In humans, Vps17 was not identified, however orthologues to the other subunits have been identified and are essential to cation-independent mannose 6-phosphate receptor (CI-MPR) retrieval to the *trans*-Golgi (228,229). Interestingly, *E. histolytica* does not have orthologues to either CI-MPR or Vps10p, however, *E. histolytica* does encode for three of the five retromer components: Vps26, Vps29 and Vps35 (230). *E. histolytica* secretes cysteine proteases (CPs) to facilitate tissue invasion, host protein degradation and colonization (89). CP transport in *E. histolytica* is regulated by the retromer complex (231). When *E. histolytica* physically contacts an erythrocyte, the retromer complex and the GTP-bound Rab7A translocate from the cytoplasm to the prephagosomal vacuole (preparatory vacuole of digestive enzymes) through a direct interaction between the activated Rab7A and Vps26 retromer subunit (231). The Vps35 subunit of retromer interacts with the cytosolic tails of cargo proteins such as CI-MPR and Vps10p (227-229). In humans and yeast, these cargo receptors mediate trafficking of the soluble hydrolases, lysosomal enzymes and carboxypeptidase Y, respectively. In this study, I identified the *Giardia* orthologue of Vps35 using the soluble hydolase, *Gl*CP2 prodomain, as bait implicating a putative role for retromer in *Giardia*. Future directions should include determining whether or not retromer regulates *Gl*CP2 intracellular trafficking. Since the *Giardia* genome encodes an orthologue to Vps26, it could be determined whether it interacts with a small GTPase similar to the endomembrane system of *E. histolytica*. A dominant negative specific to that small GTPase could be transfected into *Giardia* and any subsequent alterations in the subcellular localization of *Gl*CP2 would suggest

that retromer is involved in proper *Gl*CP2 trafficking. It would also be important to determine whether or not this is a direct interaction or mediated by a receptor as in higher eukaryotes.

ESCP, which is membrane associated is trafficked by the adaptor protein 1 (AP-1) to the PVs and subsequently to mature/late ESVs. This AP-1 interaction is dependent on a C-terminal tyrosine-based motif, YRPI. Adaptor proteins or complexes regulate post-Golgi trafficking by recognition of tyrosine-based (YXXØ) or dileucine-based (LL) motifs in the cytoplasmic tail of transmembrane proteins (232,233). This interaction is coupled to clathrin binding which induces the formation of the clathrin-coated vesicles (CCVs) (234,235). There are four cytosolic adaptor complexes (AP-1, -2, -3, -4) consisting of 4 subunits: two large (λ/α/δ/ε and β1-4), one medium (μ1-4) and one small (σ 1-4). The large subunit binds to the target membrane, whereas the large subunit Beta directly recruits clathrin (236). The AP complexes recognize and bind cargo through interaction with its μ subunit (233). Variant surface protein (VSP), which does not contain a tyrosine-based sorting motif, is constitutively trafficked to the plasma membrane and disruption of APμ1 does not affect VSP trafficking (120). However, targeted disruption of APμ1 does disrupt targeting of the soluble PV enzyme, acid phosphatase, though the mechanism remains to be identified. *Gl*CP2 contains a putative tyrosine-based sorting motif, YAGF, residing in its cytoplasmic tail. This is somewhat surprising, since *Gl*CP2 does not have a transmembrane domain. The YAGF motif would require confirmation that it is a sorting motif by deletion analysis. Interestingly, I did identify putative AP subunits, β and μ. The β subunit could not be identified as either the β subunit of AP-1 or AP-2 by phylogenetic analysis using MacVector (To date, *Giardia* encodes only the AP-1 and AP-2 complexes in its genome.). However, the μ subunit, which had been previously cloned, is a putative AP-2 subunit (120). Touz *et al.*, (2004) reported that disruption of μ2 did not disrupt ESCP trafficking. However, this work was performed with dsRNA disruption and has not been reproduced. AP-

1 initiates clathrin assembly at the *trans*-Golgi (TGN) and is involved in recycling of the mannose 6-phosphate receptor from endosomes to the TGN. In contrast, AP-2 is involved in receptor-mediated endocytosis and is recruited from the cytosol to the PM. Though mature ESVs are clathrin-coated, it is not clear what role AP-2 might have during encystation. The medium subunit, μ2, was identified considering that only the proregion of *Gl*CP2 was affixed to the column, and not the mature domain containing the C-terminal sorting signal. One possibility is that a multi-protein complex interacts with *Gl*CP2 via the prodomain to mediate clathrin-coat assembly. At least one transmembrane protein, vacuolar ATPase, is in this complex and could mediate intra and extra-vesicle partners.

In summary, follow up experiments should include determining the subcellular localization for each of these proteins either by generating anti-sera or by transfection of HA-tagged recombinant fusion proteins.

Chapter Six

Materials and Methods

Cell Culture and Transfection

WB isolate *Giardia lamblia* trophozoites from the American Type Culture Collection (ATCC) were maintained in a modified TYI-S-33 medium supplemented with 10% FBS (Omega Scientific, Inc.), penicillin-streptomycin (UCSF CCF), vitamins (Gibco/Invitrogen) and Fungizone (UCSF). The pGFP.pac vector (Gift from Theodore Nash, NIH; modified by Lei Li, CC Wang laboratory, UCSF by substituting the *Giardia* tubulin gene promotor for the *Giardia* Giardin gene promoter) was used to transiently and episomally express C-terminal GFP fusion proteins in *Giardia* trophozoites. The transfection protocol used by Singer *et al.*, (1998) was followed with modifications as follows: 1-2x10^6 trophozoites were incubated on ice for 20 minutes with 50μg of circular plasmid DNA and then electroporated (GenePulser XCell, Bio-Rad) at 0.45kv, 950μF. Transfectants were selected in a dose-dependent manner using puromycin dihydrochloride (Sigma Inc.) increased in 5-20μg/ml increments to a final concentration of 80 to 120μg/ml. Accession numbers: *Gl*CP1 (AJ302011), *Gl*CP2 (AJ AJ302012) and *Gl*CP3 (AJ302013).

Microscopy

A confocal microscope (LSM510 META; Carl Zeiss MicroImaging, Inc.) equipped with multiline (458, 477, 488, and 514 nm) Ar, 543 nm HeNe, and 633 nm HeNe visible lasers and a Chameleon two-photon laser module (Coherent, Inc.) with a "Plan-Apochromat" 63x/1.40 Oil DIC oil immersion lens (Carl Zeiss MicroImaging, Inc.) was used for fluorescence and live cell imaging experiments. Microscopy was done at room temperature. The cells were pulsed with sufficient oxygen at 37°C for 1 to 3 hours and fixed in 3% paraformaldehyde (Electron Microscopy Sciences) for 40 minutes at room temperature and mounted with ProLong Gold mounting media (+ or – DAPI) (Molecular Probes). Live imaging was done in PBS. In the time frame of these experiments, *Giardia* were viable and active in PBS. No difference was noted in

comparisons to control imaging in *Giardia* media, but PBS was preferred as background fluorescence was minimal. LSM Image Browser software (Carl Zeiss MicroImaging, Inc.) was used for confocal image acquisition and analysis. Adobe Photoshop CS (Adobe Systems, Inc.) was used for subsequent processing.

Ultrastructural Tomography

For tomography studies, a Tecnai T20 electron microscope (FEI Company) equipped with a bottom mounted four-quadrant 4K x 4K Gatan UltraScann CCD (Gatan Inc.) was run at 200 kV and images were collected every 2 degrees from –60 to +60 degrees. The cameral was set at binning 2 (2K x 2K) resolution and images were collected at 21,500X magnification. Samples were 250nm thick. Images were processed, analyzed and visualized using PRIISM software (237). Data were analyzed further using Openlab software (Improvision Ltd., England). To obtain a pseudo 3D view, the transparent background of 3 selected consecutive 0.25μm images was set to 75, 50, 35, and 0% opacity, respectively, prior to image merging.

Antibodies and Reagent

Anti-*Giardia* clathrin heavy chain polyclonal and anti-*Giardia* PDI2 polyclonal (107) were used at 1:500 and 1:3500, respectively. Anti-KDEL monoclonal antibody (Stressgen Bioreagents) and anti-spinach HSC70 monoclonal (Stressgen Bioreagents) were used at the recommended dilutions. Although the HSC70 monoclonal antibody was raised against the spinach HSC70, the spinach HSC70 protein sequence is identical to the *Giardia* HSC70 protein sequence (http://gmod.mbl.edu). Rhodamine-labeled anti-mouse IgG (γ) (KPL Inc.) and fluorescein-labeled anti-mouse IgG (γ) (KPL Inc.) were used at 1:10. For endocytosis studies, fluorescent proteins (3.75μg/ml casein; 5.0μg/ml albumin) or 0.04μm biotin-conjugated Fluospheres (2.8 x 10^{14} particles/ml; 1.0 μl/ml final) (excitation/emission:505nm/515nm) (Molecular Probes) were incubated with

trophozoites for 30 minutes at 37°C in media or PBS. Sodium azide and cytochalasin D were used at 20mM and 10μM, respectively. Cells were fixed and visualized. Lucifer Yellow lithium salt (excitation/emission:428nm/536nm; Molecular Probes) was used to visualize PVs. Trophozoites were incubated in 1ml of PBS and Lucifer yellow to a final concentration of 1mg/ml in PBS for 15 minutes at 37°C. Following incubation, cells were then fixed and visualized.

Immunofluorescence Localization of Organelle Markers

Trophozoites were stained as previously described (107) with modifications. All experiments were carried out at room temperature, unless otherwise stated. Cells were harvested following a 15 minute incubation on ice and a 15-20 minute spin at 411x*g* to pellet the cells. Cells were washed with cold PBS (Ca^{2+} and Mg^{2+} free) before fixing for 40 minutes with fresh 3% paraformaldehyde (EMS). Following a 5 minute incubation in 0.1M glycine in PBS, the cells were permeabilized in 0.1%Triton X-100 in PBS for 30 minutes and blocked with 2% BSA in PBS. Trophozoites were incubated with primary and secondary antibodies (diluted in 2% BSA/0.1% Triton X-100 in PBS) for 1 hour each.

Protease Activity Assays

Protease activity from *Giardia* lysates was isolated by anion exchange chromatography using a MonoQ column (GE Healthcare). The fluorogenic substrates Z-FR-AMC (N-carbobenzoxy-phenylalanyl-arginyl-7-amido-4-methylcoumarin) and Z-RR-AMC (N-carbobenzoxy-arginyl-arginyl-7-amido-4-methylcoumarin; excitation/ emission:360nm/470nm) were incubated with *Giardia* lysates in citrate/dibasic sodium phosphate buffers (pH 4.0-8.0) containing 4mM DTT, 5mM Pefabloc, and 50mM EDTA. Subsequent protease activity was measured by monitoring the increase in relative fluorescence units (RFU) over time.

The fluorescent substrates Z-FR-MNA (N-carbobenzoxy-phenylalanyl-arginyl-

4-methoxy-β-naphthylamide) and Z-RR-MNA (N-carbobenzoxy-arginyl-arginyl-4-methoxy-β-naphthylamide) (Bachem) were used in an adapted *in vivo* protease assay ((238). Trophozoites were washed once with PBS (Ca^{2+} and Mg^{2+} free), then incubated in PBS with 70μM Z-FR-MNA and two volumes of coupling reagent (5-nitro-2-salicylaldehyde; 2M cacodylate buffer (excitation/emission:395nm/575) for 30 minutes at 37°C. For Z-RR-MNA, trophozoites were washed in 100mM cacodylate buffer pH6.8 and 5% sucrose and incubated with Z-RR-MNA at a final concentration of 500μM in 100mM cacodylate buffer pH 6.8 for 1 hour at 37°C followed by a 20 minute incubation at 37°C with coupling reagent. The cells were fixed and visualized.

Giardia lysate was incubated for 30 minutes with 50μg casein-resorufin (Molecular Probes) in 200μl citrate/dibasic sodium phosphate buffers containing 5mM Pefabloc and 50mM EDTA. 960μl 5% (w/v) TCA was added, samples were incubated 10 minutes, and were centrifuged at 16K*xg* to pellet precipitant. 400μl supernatant was added to 600μl 0.5M Tris, pH 8.8. Hydrolysis was quantified by measuring fluorescence of resorufin-containing peptides (excitation/emission:574/584).

1.0 X 10^6 *Giardia* trophozoites were incubated with 20μg casein-FITC for 30 minutes in vegetative media and chased with fresh media. Cells were incubated at 37°C for 1 hour, 5 hours, and 16 hours. Cells were also incubated for 16 hours in the presence of three known cell permeable cysteine protease inhibitors (10μM, DMSO<1%): E64d, K11777 (K777), and WRR477. Cells were lysed and proteins fractionated by SDS-PAGE. In-gel casein-FITC was detected using a Typhoon 8600 Variable Mode Imager (Amersham).

Localization of Endocytosed Albumin-Gold by Electron Microscopy

A trophozoite monolayer was washed and incubated with ultrasmall gold (≤5nm) conjugated albumin (Electron Microscopy Sciences) or albumin-conjugated 10nm gold (Ted Pella, Inc. and without sodium azide from British Biocell) at dilutions ranging from

1:10 to 1:100 in PBS at pH 7.0 for 30 minutes at 37°C. Cells tolerated these conditions for up to 4 hours with no evidence of deterioration by microscopy. Cells were fixed (3% glutaraldehyde/1% paraformaldehyde, 0.1M cacodylate buffer, pH 7.4) and processed for LR White (EM Science) embedding. Sections were silver enhanced (HQ Silver Enhancement Kit, Nanoprobes) for 25 minutes at 4°C.

Localization of Glucose-6-Phosphatase Activity by Electron Microscopy

A trophozoite monolayer was fixed for 30 minutes. Glucose-6-phosphatase reaction was performed as previously described (Lewis and Knight, 1982). Cells were washed with 0.1M Tris/maleate, 3mM lead nitrate, 4mM disodium glucose-6-phosphate and 5% sucrose, pH 6.5 at 37°C for 60 minutes. Cells were post-fixed with the aforementioned fixative and osmium tetroxide and embedded in epon. Blocks were sectioned with a Leica ultracut UCT ultramicrotome. Sections were viewed with FEI Tecnai 10 electron microscope (FEI Company).

Endocytosis visualized by Live Cell Imaging

Trophozoites were allowed to adhere to chambered coverglass (Lab-Tec) in vegetative growth media. Media was replaced with 400μl PBS at 37°C. Filming began as 5×10^9 to 5×10^{10} biotin-conjugated Fluospheres (excitation/emission:505nm/515nm) 0.04μm (Molecular Probes) or 250ng of DQRed BSA (excitation/emission:590nm/620nm) (Molecular Probes) were added to the chamber of adhered trophozoites containing 400ul PBS.

Database Mining

Extensive BLAST searches using the NCBI protein database and specific eukaryotic sequencing projects including the *Giardia lamblia* database (http://gmod.mbl.

edu) identified 14 full-length *Giardia* protein sequences with significant homology to the Ras superfamily of small GTPases including 10 Rab family members. Two strategies were used to identify and confirm the putative *Giardia* Rab orthologues. First, the *Giardia* genome both accessible at NCBI and through the *Giardia* sequencing project was searched with Rab consensus sequences using Rab family and subfamily defining sequence motifs and using Rab proteins from various organisms as query subjects. The highest scoring hits were then consolidated. Specifically, using MacVector and Clustal W, duplicates were identified by sequence analysis and were either discarded or consolidated under one protein accession number. These sequences were used to reverse BLAST the *Giardia* sequence to obtain sequences with the highest homology to the original *Giardia* protein query; this sequence was considered an orthologue. The *Giardia* sequences were consolidated under the designation prefix-signature EAA.

Phylogenetic Analysis

All putative *Giardia* Ras superfamily sequences were aligned and analyzed with MacVector first with representatives of each of the five known Ras superfamily members including Ras, Rho, Arf, Ran and Rab and then with Rab subfamily representatives from humans, *Saccharomyoces cerevisiae*, *Trypanosoma brucei*, *Trichomonas vaginalis* and *Entamoeba histolytica*. Phylogenetic trees were generated using MacVector (Accelrys Software Inc.) using neighbor-joining and bootstrapping algorithms. Some very divergent Rab sequences may be due to sequence similarity being sub-threshold.

References

1. Adam, R. D. (1991) *Microbiol Rev* **55**, 706-732
2. Adam, R. D. (2001) in *Clinical Microbiology Review* Vol. 14, pp. 447-475
3. Thompson, R. C. (2000) *Int J Parasitol* **30**, 1259-1267
4. Quick, R., Paugh, K., Addiss, D., Kobayashi, J., and Baron, R. (1992) *J Infect Dis* **166**, 673-676
5. Adam, R. D. (2000) *Int J Parasitol* **30**, 475-484
6. Sogin, M. L., Gunderson, J. H., Elwood, H. J., Alonso, R. A., and Peattie, D. A. (1989) *Science* **243**, 75-77
7. Hashimoto, T., Nakamura, Y., Nakamura, F., Shirakura, T., Adachi, J., Goto, N., Okamoto, K., and Hasegawa, M. (1994) *Mol Biol Evol* **11**, 65-71
8. Hashimoto, T., Nakamura, Y., Kamaishi, T., Nakamura, F., Adachi, J., Okamoto, K., and Hasegawa, M. (1995) *Mol Biol Evol* **12**, 782-793
9. Manning, P., Erlandsen, S. L., and Jarroll, E. L. (1992) *J Protozool* **39**, 290-296
10. Mowatt, M. R., Lujan, H. D., Cotten, D. B., Bowers, B., Yee, J., Nash, T. E., and Stibbs, H. H. (1995) *Mol Microbiol* **15**, 955-963
11. Lujan, H. D., Mowatt, M. R., Conrad, J. T., Bowers, B., and Nash, T. E. (1995) *J Biol Chem* **270**, 29307-29313
12. Kirk-Mason, K. E., Turner, M. J., and Chakraborty, P. R. (1989) *Mol Biochem Parasitol* **36**, 87-99
13. Yu, D. C., Wang, A. L., Botka, C. W., and Wang, C. C. (1998) *Mol Biochem Parasitol* **96**, 151-165
14. Hehl, A. B., and Marti, M. (2004) *Mol Microbiol* **53**, 19-28
15. Gillin, F. D., Reiner, D. S., and McCaffery, J. M. (1996) *Annu Rev Microbiol* **50**, 679-705
16. Erlandsen, S. L., Macechko, P. T., van Keulen, H., and Jarroll, E. L. (1996) *J Eukaryot Microbiol* **43**, 416-429
17. Hehl, A. B., Marti, M., and Kohler, P. (2000) *Mol Biol Cell* **11**, 1789-1800
18. Reiner, D. S., McCaffery, M., and Gillin, F. D. (1990) *Eur J Cell Biol* **53**, 142-153
19. McCaffery, J. M., and Gillin, F. D. (1994) *Exp Parasitol* **79**, 220-235
20. Faubert, G., Reiner, D. S., and Gillin, F. D. (1991) *Exp Parasitol* **72**, 345-354
21. Lujan, H. D., Mowatt, M. R., and Nash, T. E. (1997) *Microbiol Mol Biol Rev* **61**, 294-304
22. Jarroll, E. L., Macechko, P. T., Steimle, P. A., Bulik, D., Karr, C. D., van Keulen, H., Paget, T. A., Gerwig, G., Kamerling, J., Vliegenthart, J., and Erlandsen, S. (2001) *J Eukaryot Microbiol* **48**, 22-26
23. Barlowe, C. (2000) *Traffic* **1**, 371-377
24. Lee, M. C., Miller, E. A., Goldberg, J., Orci, L., and Schekman, R. (2004) *Annu Rev Cell Dev Biol* **20**, 87-123
25. Marti, M., Li, Y., Schraner, E. M., Wild, P., Kohler, P., and Hehl, A. B. (2003) *Mol Biol Cell* **14**, 1433-1447
26. Lujan, H. D., Marotta, A., Mowatt, M. R., Sciaky, N., Lippincott-Schwartz, J., and Nash, T. E. (1995) *J Biol Chem* **270**, 4612-4618
27. Slavin, I., Saura, A., Carranza, P. G., Touz, M. C., Nores, M. J., and Lujan, H. D. (2002) *Mol Biochem Parasitol* **122**, 95-98
28. Davids, B. J., Mehta, K., Fesus, L., McCaffery, J. M., and Gillin, F. D. (2004) *Mol*

Biochem Parasitol **136**, 173-180
29. Knodler, L. A., Noiva, R., Mehta, K., McCaffery, J. M., Aley, S. B., Svard, S. G., Nystul, T. G., Reiner, D. S., Silberman, J. D., and Gillin, F. D. (1999) *J Biol Chem* **274**, 29805-29811
30. Gupta, R. S., Aitken, K., Falah, M., and Singh, B. (1994) *Proc Natl Acad Sci U S A* **91**, 2895-2899
31. Emmerlich, V., Scholze, H., Gillin, F. D., and Bakker-Grunwald, T. (2001) *Parasitol Res* **87**, 112-115
32. Reiner, D. S., McCaffery, J. M., and Gillin, F. D. (2001) *Cell Microbiol* **3**, 459-472
33. Stefanic, S., Palm, D., Svard, S. G., and Hehl, A. B. (2006) *J Biol Chem* **281**, 7595-7604
34. Bukau, B., Weissman, J., and Horwich, A. (2006) *Cell* **125**, 443-451
35. Lanfredi-Rangel, A., Attias, M., Reiner, D. S., Gillin, F. D., and De Souza, W. (2003) *J Struct Biol* **143**, 153-163
36. Cavalier-Smith, T. (1983) *Endocytobiology II* (Schwemmler, W. S., H.E.A., Ed.), de Gruyter, Berlin
37. Tovar, J., Fischer, A., and Clark, C. G. (1999) *Mol Microbiol* **32**, 1013-1021
38. Williams, B. A., Hirt, R. P., Lucocq, J. M., and Embley, T. M. (2002) *Nature* **418**, 865-869
39. Tovar, J., Leon-Avila, G., Sanchez, L. B., Sutak, R., Tachezy, J., van der Giezen, M., Hernandez, M., Muller, M., and Lucocq, J. M. (2003) *Nature* **426**, 172-176
40. Dyall, S. D., Brown, M. T., and Johnson, P. J. (2004) *Science* **304**, 253-257
41. Sutak, R., Dolezal, P., Fiumera, H. L., Hrdy, I., Dancis, A., Delgadillo-Correa, M., Johnson, P. J., Muller, M., and Tachezy, J. (2004) *Proc Natl Acad Sci U S A* **101**, 10368-10373
42. Pilon-Smits, E. A., Garifullina, G. F., Abdel-Ghany, S., Kato, S., Mihara, H., Hale, K. L., Burkhead, J. L., Esaki, N., Kurihara, T., and Pilon, M. (2002) *Plant Physiol* **130**, 1309-1318
43. Biagini, G. A., Suller, M. T., Finlay, B. J., and Lloyd, D. (1997) *J Eukaryot Microbiol* **44**, 447-453
44. Andersson, S. G., and Kurland, C. G. (1999) *Curr Opin Microbiol* **2**, 535-541
45. Dyall, S. D., and Johnson, P. J. (2000) *Curr Opin Microbiol* **3**, 404-411
46. Embley, T. M., van der Giezen, M., Horner, D. S., Dyal, P. L., and Foster, P. (2003) *Philos Trans R Soc Lond B Biol Sci* **358**, 191-201; discussion 201-192
47. Embley, T. M., van der Giezen, M., Horner, D. S., Dyal, P. L., Bell, S., and Foster, P. G. (2003) *IUBMB Life* **55**, 387-395
48. Lill, R., and Kispal, G. (2000) *Trends Biochem Sci* **25**, 352-356
49. Muller, M. (2003) *Moleculer Medical Parasitology* (Marr, J., Ed.), Academic, London
50. Lloyd, D., and Harris, J. C. (2002) *Trends Microbiol* **10**, 122-127
51. Lloyd, D., Ralphs, J. R., and Harris, J. C. (2002) *Trends Parasitol* **18**, 155-156
52. Roger, A. J., Svard, S. G., Tovar, J., Clark, C. G., Smith, M. W., Gillin, F. D., and Sogin, M. L. (1998) *Proc Natl Acad Sci U S A* **95**, 229-234
53. Hashimoto, T., Sanchez, L. B., Shirakura, T., Muller, M., and Hasegawa, M.

(1998) *Proc Natl Acad Sci U S A* **95**, 6860-6865
54. Gray, M. W., Burger, G., and Lang, B. F. (1999) *Science* **283**, 1476-1481
55. Drenth, J., Jansonius, J. N., Koekoek, R., Swen, H. M., and Wolthers, B. G. (1968) *Nature* **218**, 929-932
56. Sajid, M., and McKerrow, J. H. (2002) *Mol Biochem Parasitol* **120**, 1-21
57. Barrett, A., Rawlings, ND and Woessner, JF. (1998) *Handbook of Proteolytic Enzymes*, Academic Press, London, UK
58. Barrett, A., Rawlings, ND, Woessner, JF. (2004) *Handbook of Proteolytic Enzymes*, 2nd Ed. (Barratt, A., Rawlings, ND, Woessner, JF, Ed.), 2, Elsevier Academic Press, London
59. Eakin, A. E., Mills, A. A., Harth, G., McKerrow, J. H., and Craik, C. S. (1992) *J Biol Chem* **267**, 7411-7420
60. Mach, L., Mort, J. S., and Glossl, J. (1994) *J Biol Chem* **269**, 13036-13040
61. McIntyre, G. F., and Erickson, A. H. (1991) *J Biol Chem* **266**, 15438-15445
62. McIntyre, G. F., Godbold, G. D., and Erickson, A. H. (1994) *J Biol Chem* **269**, 567-572
63. Huete-Perez, J. A., Engel, J. C., Brinen, L. S., Mottram, J. C., and McKerrow, J. H. (1999) *J Biol Chem* **274**, 16249-16256
64. Coombs, G. H. a. M., J.C. (1997) *Trypanosomiasis and Leishmaniasis: Biology and Control* (Hide, G., Mottram, J. C., Coombs, G. H., and Holmes, P. H., eds, Ed.), CAB International, Oxford, U. K.
65. Mottram, J. C., North, M. J., Barry, J. D., and Coombs, G. H. (1989) *FEBS Lett* **258**, 211-215
66. Brooks, D. R., Tetley, L., Coombs, G. H., and Mottram, J. C. (2000) *J Cell Sci* **113 (Pt 22)**, 4035-4041
67. Nishizawa, K., Maruyama, N., Satoh, R., Fuchikami, Y., Higasa, T., and Utsumi, S. (2003) *Plant J* **34**, 647-659
68. Varughese, K. I., Ahmed, F. R., Carey, P. R., Hasnain, S., Huber, C. P., and Storer, A. C. (1989) *Biochemistry* **28**, 1330-1332
69. Cygler, M., Sivaraman, J., Grochulski, P., Coulombe, R., Storer, A. C., and Mort, J. S. (1996) *Structure* **4**, 405-416
70. Illy, C., Quraishi, O., Wang, J., Purisima, E., Vernet, T., and Mort, J. S. (1997) *J Biol Chem* **272**, 1197-1202
71. Musil, D., Zucic, D., Turk, D., Engh, R. A., Mayr, I., Huber, R., Popovic, T., Turk, V., Towatari, T., Katunuma, N., and et al. (1991) *Embo J* **10**, 2321-2330
72. Day, P. M., Yewdell, J. W., Porgador, A., Germain, R. N., and Bennink, J. R. (1997) *Proc Natl Acad Sci U S A* **94**, 8064-8069
73. Honey, K., Nakagawa, T., Peters, C., and Rudensky, A. (2002) *J Exp Med* **195**, 1349-1358
74. Nakagawa, T., Roth, W., Wong, P., Nelson, A., Farr, A., Deussing, J., Villadangos, J. A., Ploegh, H., Peters, C., and Rudensky, A. Y. (1998) *Science* **280**, 450-453
75. Nakagawa, T. Y., and Rudensky, A. Y. (1999) *Immunol Rev* **172**, 121-129
76. Brasch, F., Ten Brinke, A., Johnen, G., Ochs, M., Kapp, N., Muller, K. M., Beers, M. F., Fehrenbach, H., Richter, J., Batenburg, J. J., and Buhling, F. (2002) *Am J Respir Cell Mol Biol* **26**, 659-670

77. Lloyd, J., Mason, RW. (1996) *Biology of Lysosomes: subcellular Biochemistry* (Lloyd, J., Mason, RW, Ed.), 27, Plenum Press, New York
78. Halangk, W., Lerch, M. M., Brandt-Nedelev, B., Roth, W., Ruthenbuerger, M., Reinheckel, T., Domschke, W., Lippert, H., Peters, C., and Deussing, J. (2000) *J Clin Invest* **106**, 773-781
79. Guicciardi, M. E., Deussing, J., Miyoshi, H., Bronk, S. F., Svingen, P. A., Peters, C., Kaufmann, S. H., and Gores, G. J. (2000) *J Clin Invest* **106**, 1127-1137
80. Stoka, V., Turk, B., Schendel, S. L., Kim, T. H., Cirman, T., Snipas, S. J., Ellerby, L. M., Bredesen, D., Freeze, H., Abrahamson, M., Bromme, D., Krajewski, S., Reed, J. C., Yin, X. M., Turk, V., and Salvesen, G. S. (2001) *J Biol Chem* **276**, 3149-3157
81. Mai, J., Finley, R. L., Jr., Waisman, D. M., and Sloane, B. F. (2000) *J Biol Chem* **275**, 12806-12812
82. Mai, J., Waisman, D. M., and Sloane, B. F. (2000) *Biochim Biophys Acta* **1477**, 215-230
83. Lah, T. T., Buck, M. R., Honn, K. V., Crissman, J. D., Rao, N. C., Liotta, L. A., and Sloane, B. F. (1989) *Clin Exp Metastasis* **7**, 461-468
84. Buck, M. R., Karustis, D. G., Day, N. A., Honn, K. V., and Sloane, B. F. (1992) *Biochem J* **282 (Pt 1)**, 273-278
85. Gong, Q., Chan, S. J., Bajkowski, A. S., Steiner, D. F., and Frankfater, A. (1993) *DNA Cell Biol* **12**, 299-309
86. Campo, E., Munoz, J., Miquel, R., Palacin, A., Cardesa, A., Sloane, B. F., and Emmert-Buck, M. R. (1994) *Am J Pathol* **145**, 301-309
87. Rescheleit, D. K., Rommerskirch, W. J., and Wiederanders, B. (1996) *FEBS Lett* **394**, 345-348
88. Stanley, S. L., Jr., Zhang, T., Rubin, D., and Li, E. (1995) *Infect Immun* **63**, 1587-1590
89. Que, X., and Reed, S. L. (2000) *Clin Microbiol Rev* **13**, 196-206
90. Reed, S. L. (1995) *Clin Infect Dis* **21 Suppl 2**, S182-185
91. Bruchhaus, I., Loftus, B. J., Hall, N., and Tannich, E. (2003) *Eukaryot Cell* **2**, 501-509
92. Frame, M. J., Mottram, J. C., and Coombs, G. H. (2000) *Parasitology* **121 (Pt 4)**, 367-377
93. Alderete, J. F., Provenzano, D., and Lehker, M. W. (1995) *Microb Pathog* **19**, 93-103
94. Reed, S. L., Ember, J. A., Herdman, D. S., DiScipio, R. G., Hugli, T. E., and Gigli, I. (1995) *J Immunol* **155**, 266-274
95. Salas, F., Fichmann, J., Lee, G. K., Scott, M. D., and Rosenthal, P. J. (1995) *Infect Immun* **63**, 2120-2125
96. Shenai, B. R., Sijwali, P. S., Singh, A., and Rosenthal, P. J. (2000) *J Biol Chem* **275**, 29000-29010
97. Caffrey, C. R., McKerrow, J. H., Salter, J. P., and Sajid, M. (2004) *Trends Parasitol* **20**, 241-248
98. Delcroix, M., Sajid, M., Caffrey, C. R., Lim, K. C., Dvorak, J., Hsieh, I., Bahgat, M., Dissous, C., and McKerrow, J. H. (2006) *J Biol Chem*

99. Sharma, M., Hirata, K., Herdman, S., and Reed, S. (1996) *Exp Parasitol* **84**, 84-91
100. Makioka, A., Kumagai, M., Kobayashi, S., and Takeuchi, T. (2005) *Exp Parasitol* **109**, 27-32
101. Villalobo, E., Moch, C., Fryd-Versavel, G., Fleury-Aubusson, A., and Morin, L. (2003) *Eukaryot Cell* **2**, 1234-1245
102. Ward, W., Alvarado, L., Rawlings, N. D., Engel, J. C., Franklin, C., and McKerrow, J. H. (1997) *Cell* **89**, 437-444
103. Turk, B., Turk, V., and Turk, D. (1997) *Biol Chem* **378**, 141-150
104. Touz, M. C., Nores, M. J., Slavin, I., Carmona, C., Conrad, J. T., Mowatt, M. R., Nash, T. E., Coronel, C. E., and Lujan, H. D. (2002) *J Biol Chem* **277**, 8474-8481
105. Alberts, B. (2002) *Molecular biology of the cell*, Garland Science, New York
106. Dacks, J. B., Davis, L. A., Sjogren, A. M., Andersson, J. O., Roger, A. J., and Doolittle, W. F. (2003) *Proc Biol Sci* **270 Suppl 2**, S168-171
107. Marti, M., Regos, A., Li, Y., Schraner, E. M., Wild, P., Muller, N., Knopf, L. G., and Hehl, A. B. (2003) *J Biol Chem* **278**, 24837-24848
108. Langford, T. D., Silberman, J. D., Weiland, M. E., Svard, S. G., McCaffery, J. M., Sogin, M. L., and Gillin, F. D. (2002) *Exp Parasitol* **101**, 13-24
109. Lanfredi-Rangel, A., Attias, M., de Carvalho, T. M., Kattenbach, W. M., and De Souza, W. (1998) *J Struct Biol* **123**, 225-235
110. Kartenbeck, J., Stukenbrok, H., and Helenius, A. (1989) *J Cell Biol* **109**, 2721-2729
111. Gagnon, E., Duclos, S., Rondeau, C., Chevet, E., Cameron, P. H., Steele-Mortimer, O., Paiement, J., Bergeron, J. J., and Desjardins, M. (2002) *Cell* **110**, 119-131
112. Sandvig, K., and van Deurs, B. (2002) *FEBS Lett* **529**, 49-53
113. Touret, N., Paroutis, P., Terebiznik, M., Harrison, R. E., Trombetta, S., Pypaert, M., Chow, A., Jiang, A., Shaw, J., Yip, C., Moore, H. P., van der Wel, N., Houben, D., Peters, P. J., de Chastellier, C., Mellman, I., and Grinstein, S. (2005) *Cell* **123**, 157-170
114. Gillin, F. D., Reiner, D. S., Gault, M. J., Douglas, H., Das, S., Wunderlich, A., and Sauch, J. F. (1987) *Science* **235**, 1040-1043
115. Gillin, F. D., Boucher, S. E., Rossi, S. S., and Reiner, D. S. (1989) *Exp Parasitol* **69**, 164-174
116. Reiner, D. S., Douglas, H., and Gillin, F. D. (1989) *Infect Immun* **57**, 963-968
117. Kulda, J. a. N., E. (1995) *Giardia in humans and animals.*, 2 Ed. Parasitic protozoa (Kreier, J., Ed.), 10, Academic Press, San Diego
118. Benchimol, M. (2004) *Parasitol Res* **94**, 254-264
119. Mottram, J. a. S., M. (2004) *Trichomonad and Giardia Cysteine Endopeptidases.* Handbook of Proteolytic Enzymes (Barrett, A., Rawlings, ND and Woessner, JF, Ed.), Chapter 36, Academic Press, London
120. Touz, M. C., Kulakova, L., and Nash, T. E. (2004) *Mol Biol Cell* **15**, 3053-3060
121. Turk, V., Turk, B., and Turk, D. (2001) *Embo J* **20**, 4629-4633
122. Porter, K. R. (1953) *J Exp Med* **97**, 727-750
123. Soltys, B. J., Falah, M., and Gupta, R. S. (1996) *J Cell Sci* **109 (Pt 7)**, 1909-1917

124. Federovitch, C. M., Ron, D., and Hampton, R. Y. (2005) *Curr Opin Cell Biol* **17**, 409-414
125. Towler, M. C., Gleeson, P. A., Hoshino, S., Rahkila, P., Manalo, V., Ohkoshi, N., Ordahl, C., Parton, R. G., and Brodsky, F. M. (2004) *Mol Biol Cell* **15**, 3181-3195
126. Benchimol, M., Piva, B., Campanati, L., and de Souza, W. (2004) *J Struct Biol* **147**, 102-115
127. Morgan, G. W., Hall, B. S., Denny, P. W., Carrington, M., and Field, M. C. (2002) *Trends Parasitol* **18**, 491-496
128. Perret, E., Lakkaraju, A., Deborde, S., Schreiner, R., and Rodriguez-Boulan, E. (2005) *Curr Opin Cell Biol* **17**, 423-434
129. Tai, J. H., Ong, S. J., Chang, S. C., and Su, H. M. (1993) *Exp Parasitol* **76**, 165-174
130. Gething, M. J., and Sambrook, J. (1992) *Nature* **355**, 33-45
131. Paulsson, K., and Wang, P. (2003) *Biochim Biophys Acta* **1641**, 1-12
132. Nishikawa, S., Brodsky, J. L., and Nakatsukasa, K. (2005) *J Biochem (Tokyo)* **137**, 551-555
133. Lord, J. M., and Roberts, L. M. (1998) *J Cell Biol* **140**, 733-736
134. Bourne, H. R., Sanders, D. A., and McCormick, F. (1990) *Nature* **348**, 125-132
135. Novick, P., and Zerial, M. (1997) *Curr Opin Cell Biol* **9**, 496-504
136. Takai, Y., Sasaki, T., and Matozaki, T. (2001) *Physiol Rev* **81**, 153-208
137. Pfeffer, S. R. (2001) *Trends Cell Biol* **11**, 487-491
138. Zerial, M., and McBride, H. (2001) *Nat Rev Mol Cell Biol* **2**, 107-117
139. Segev, N. (2001) *Sci STKE* **2001**, RE11
140. Pereira-Leal, J. B., and Seabra, M. C. (2001) *J Mol Biol* **313**, 889-901
141. Loftus, B., Anderson, I., Davies, R., Alsmark, U. C., Samuelson, J., Amedeo, P., Roncaglia, P., Berriman, M., Hirt, R. P., Mann, B. J., Nozaki, T., Suh, B., Pop, M., Duchene, M., Ackers, J., Tannich, E., Leippe, M., Hofer, M., Bruchhaus, I., Willhoeft, U., Bhattacharya, A., Chillingworth, T., Churcher, C., Hance, Z., Harris, B., Harris, D., Jagels, K., Moule, S., Mungall, K., Ormond, D., Squares, R., Whitehead, S., Quail, M. A., Rabbinowitsch, E., Norbertczak, H., Price, C., Wang, Z., Guillen, N., Gilchrist, C., Stroup, S. E., Bhattacharya, S., Lohia, A., Foster, P. G., Sicheritz-Ponten, T., Weber, C., Singh, U., Mukherjee, C., El-Sayed, N. M., Petri, W. A., Jr., Clark, C. G., Embley, T. M., Barrell, B., Fraser, C. M., and Hall, N. (2005) *Nature* **433**, 865-868
142. Lal, K., Field, M. C., Carlton, J. M., Warwicker, J., and Hirt, R. P. (2005) *Mol Biochem Parasitol* **143**, 226-235
143. Pereira-Leal, J. B., and Seabra, M. C. (2000) *J Mol Biol* **301**, 1077-1087
144. Pfeffer, S. (2005) *Biochem Soc Trans* **33**, 627-630
145. Temesvari, L. A., Harris, E. N., Stanley, S. L., Jr., and Cardelli, J. A. (1999) *Mol Biochem Parasitol* **103**, 225-241
146. Dhir, V., Goulding, D., and Field, M. C. (2004) *Mol Biochem Parasitol* **137**, 253-265
147. Stenmark, H., and Olkkonen, V. M. (2001) *Genome Biol* **2**, REVIEWS3007
148. Ackers, J. P., Dhir, V., and Field, M. C. (2005) *Mol Biochem Parasitol* **141**, 89-97
149. Saito-Nakano, Y., Nakazawa, M., Shigeta, Y., Takeuchi, T., and Nozaki, T. (2001)

Mol Biochem Parasitol **116**, 219-222
150. Field, H., Ali, B. R., Sherwin, T., Gull, K., Croft, S. L., and Field, M. C. (1999) *J Cell Sci* **112 (Pt 2)**, 147-156
151. Bourne, H. R. (1988) *Cell* **53**, 669-671
152. Plutner, H., Cox, A. D., Pind, S., Khosravi-Far, R., Bourne, J. R., Schwaninger, R., Der, C. J., and Balch, W. E. (1991) *J Cell Biol* **115**, 31-43
153. Tisdale, E. J., Bourne, J. R., Khosravi-Far, R., Der, C. J., and Balch, W. E. (1992) *J Cell Biol* **119**, 749-761
154. Seabra, M. C., Mules, E. H., and Hume, A. N. (2002) *Trends Mol Med* **8**, 23-30
155. Urbe, S., Huber, L. A., Zerial, M., Tooze, S. A., and Parton, R. G. (1993) *FEBS Lett* **334**, 175-182
156. Ullrich, O., Reinsch, S., Urbe, S., Zerial, M., and Parton, R. G. (1996) *J Cell Biol* **135**, 913-924
157. Chen, W., Feng, Y., Chen, D., and Wandinger-Ness, A. (1998) *Mol Biol Cell* **9**, 3241-3257
158. Ren, M., Xu, G., Zeng, J., De Lemos-Chiarandini, C., Adesnik, M., and Sabatini, D. D. (1998) *Proc Natl Acad Sci U S A* **95**, 6187-6192
159. Wilcke, M., Johannes, L., Galli, T., Mayau, V., Goud, B., and Salamero, J. (2000) *J Cell Biol* **151**, 1207-1220
160. Moore, R. H., Millman, E. E., Alpizar-Foster, E., Dai, W., and Knoll, B. J. (2004) *J Cell Sci* **117**, 3107-3117
161. Nepomuceno-Silva, J. L., de Melo, L. D., Mendonca, S. M., Paixao, J. C., and Lopes, U. G. (2004) *Gene* **327**, 221-232
162. Berriman, M., Ghedin, E., Hertz-Fowler, C., Blandin, G., Renauld, H., Bartholomeu, D. C., Lennard, N. J., Caler, E., Hamlin, N. E., Haas, B., Bohme, U., Hannick, L., Aslett, M. A., Shallom, J., Marcello, L., Hou, L., Wickstead, B., Alsmark, U. C., Arrowsmith, C., Atkin, R. J., Barron, A. J., Bringaud, F., Brooks, K., Carrington, M., Cherevach, I., Chillingworth, T. J., Churcher, C., Clark, L. N., Corton, C. H., Cronin, A., Davies, R. M., Doggett, J., Djikeng, A., Feldblyum, T., Field, M. C., Fraser, A., Goodhead, I., Hance, Z., Harper, D., Harris, B. R., Hauser, H., Hostetler, J., Ivens, A., Jagels, K., Johnson, D., Johnson, J., Jones, K., Kerhornou, A. X., Koo, H., Larke, N., Landfear, S., Larkin, C., Leech, V., Line, A., Lord, A., Macleod, A., Mooney, P. J., Moule, S., Martin, D. M., Morgan, G. W., Mungall, K., Norbertczak, H., Ormond, D., Pai, G., Peacock, C. S., Peterson, J., Quail, M. A., Rabbinowitsch, E., Rajandream, M. A., Reitter, C., Salzberg, S. L., Sanders, M., Schobel, S., Sharp, S., Simmonds, M., Simpson, A. J., Tallon, L., Turner, C. M., Tait, A., Tivey, A. R., Van Aken, S., Walker, D., Wanless, D., Wang, S., White, B., White, O., Whitehead, S., Woodward, J., Wortman, J., Adams, M. D., Embley, T. M., Gull, K., Ullu, E., Barry, J. D., Fairlamb, A. H., Opperdoes, F., Barrell, B. G., Donelson, J. E., Hall, N., Fraser, C. M., Melville, S. E., and El-Sayed, N. M. (2005) *Science* **309**, 416-422
163. El-Sayed, N. M., Myler, P. J., Bartholomeu, D. C., Nilsson, D., Aggarwal, G., Tran, A. N., Ghedin, E., Worthey, E. A., Delcher, A. L., Blandin, G., Westenberger, S. J., Caler, E., Cerqueira, G. C., Branche, C., Haas, B., Anupama, A., Arner, E., Aslund, L., Attipoe, P., Bontempi, E., Bringaud, F., Burton, P.,

Cadag, E., Campbell, D. A., Carrington, M., Crabtree, J., Darban, H., da Silveira, J. F., de Jong, P., Edwards, K., Englund, P. T., Fazelina, G., Feldblyum, T., Ferella, M., Frasch, A. C., Gull, K., Horn, D., Hou, L., Huang, Y., Kindlund, E., Klingbeil, M., Kluge, S., Koo, H., Lacerda, D., Levin, M. J., Lorenzi, H., Louie, T., Machado, C. R., McCulloch, R., McKenna, A., Mizuno, Y., Mottram, J. C., Nelson, S., Ochaya, S., Osoegawa, K., Pai, G., Parsons, M., Pentony, M., Pettersson, U., Pop, M., Ramirez, J. L., Rinta, J., Robertson, L., Salzberg, S. L., Sanchez, D. O., Seyler, A., Sharma, R., Shetty, J., Simpson, A. J., Sisk, E., Tammi, M. T., Tarleton, R., Teixeira, S., Van Aken, S., Vogt, C., Ward, P. N., Wickstead, B., Wortman, J., White, O., Fraser, C. M., Stuart, K. D., and Andersson, B. (2005) *Science* **309**, 409-415

164. Brauers, A., Schurmann, A., Massmann, S., Muhl-Zurbes, P., Becker, W., Kainulainen, H., Lie, C., and Joost, H. G. (1996) *Eur J Biochem* **237**, 833-840
165. Gonzalez, L., Jr., and Scheller, R. H. (1999) *Cell* **96**, 755-758
166. Segev, N., Mulholland, J., and Botstein, D. (1988) *Cell* **52**, 915-924
167. Zahraoui, A., Touchot, N., Chardin, P., and Tavitian, A. (1989) *J Biol Chem* **264**, 12394-12401
168. Jedd, G., Richardson, C., Litt, R., and Segev, N. (1995) *J Cell Biol* **131**, 583-590
169. Saraste, J., Lahtinen, U., and Goud, B. (1995) *J Cell Sci* **108 (Pt 4)**, 1541-1552
170. Saraste, J., and Kuismanen, E. (1992) *Semin Cell Biol* **3**, 343-355
171. Hauri, H. P., Kappeler, F., Andersson, H., and Appenzeller, C. (2000) *J Cell Sci* **113 (Pt 4)**, 587-596
172. Klumperman, J. (2000) *Curr Opin Cell Biol* **12**, 445-449
173. Lippincott-Schwartz, J., and Zaal, K. J. (2000) *Histochem Cell Biol* **114**, 93-103
174. Hammond, A. T., and Glick, B. S. (2000) *Mol Biol Cell* **11**, 3013-3030
175. Stephens, D. J., Lin-Marq, N., Pagano, A., Pepperkok, R., and Paccaud, J. P. (2000) *J Cell Sci* **113 (Pt 12)**, 2177-2185
176. Martinez-Menarguez, J. A., Geuze, H. J., Slot, J. W., and Klumperman, J. (1999) *Cell* **98**, 81-90
177. Horstmann, H., Ng, C. P., Tang, B. L., and Hong, W. (2002) *J Cell Sci* **115**, 4263-4273
178. Sannerud, R., Saraste, J., and Goud, B. (2003) *Curr Opin Cell Biol* **15**, 438-445
179. Sannerud, R., Marie, M., Nizak, C., Dale, H. A., Pernet-Gallay, K., Perez, F., Goud, B., and Saraste, J. (2006) *Mol Biol Cell* **17**, 1514-1526
180. Palokangas, H., Ying, M., Vaananen, K., and Saraste, J. (1998) *Mol Biol Cell* **9**, 3561-3578
181. Haubruck, H., Prange, R., Vorgias, C., and Gallwitz, D. (1989) *Embo J* **8**, 1427-1432
182. Zuber, C., Fan, J. Y., Guhl, B., Parodi, A., Fessler, J. H., Parker, C., and Roth, J. (2001) *Proc Natl Acad Sci U S A* **98**, 10710-10715
183. Ying, M., Sannerud, R., Flatmark, T., and Saraste, J. (2002) *Eur J Cell Biol* **81**, 469-483
184. Blaustein, M. P., and Golovina, V. A. (2001) *Trends Neurosci* **24**, 602-608
185. Tisdale, E. J., and Balch, W. E. (1996) *J Biol Chem* **271**, 29372-29379
186. Short, B., Preisinger, C., Korner, R., Kopajtich, R., Byron, O., and Barr, F. A.

(2001) *J Cell Biol* **155**, 877-883
187. Satoh, A., Wang, Y., Malsam, J., Beard, M. B., and Warren, G. (2003) *Traffic* **4**, 153-161
188. Saito-Nakano, Y., Loftus, B. J., Hall, N., and Nozaki, T. (2005) *Exp Parasitol* **110**, 244-252
189. Sun, C. H., McCaffery, J. M., Reiner, D. S., and Gillin, F. D. (2003) *J Biol Chem* **278**, 21701-21708
190. Benli, M., Doring, F., Robinson, D. G., Yang, X., and Gallwitz, D. (1996) *Embo J* **15**, 6460-6475
191. Jedd, G., Mulholland, J., and Segev, N. (1997) *J Cell Biol* **137**, 563-580
192. Chen, S. H., Chen, S., Tokarev, A. A., Liu, F., Jedd, G., and Segev, N. (2005) *Mol Biol Cell* **16**, 178-192
193. McGugan, G. C., Jr., and Temesvari, L. A. (2003) *Mol Biochem Parasitol* **129**, 137-146
194. Jeffries, T. R., Morgan, G. W., and Field, M. C. (2001) *J Cell Sci* **114**, 2617-2626
195. Grunfelder, C. G., Engstler, M., Weise, F., Schwarz, H., Stierhof, Y. D., Morgan, G. W., Field, M. C., and Overath, P. (2003) *Mol Biol Cell* **14**, 2029-2040
196. Hall, B. S., Smith, E., Langer, W., Jacobs, L. A., Goulding, D., and Field, M. C. (2005) *Eukaryot Cell* **4**, 971-980
197. Cyr, D. M., Langer, T., and Douglas, M. G. (1994) *Trends Biochem Sci* **19**, 176-181
198. Nepomuceno-Silva, J. L., De Melo, L. D., Mendonca, S. M., Paixao, J. C., and Lopes, U. G. (2004) *Parasitology* **129**, 325-333
199. Yuasa, Y., Gol, R. A., Chang, A., Chiu, I. M., Reddy, E. P., Tronick, S. R., and Aaronson, S. A. (1984) *Proc Natl Acad Sci U S A* **81**, 3670-3674
200. Riederer, M. A., Soldati, T., Shapiro, A. D., Lin, J., and Pfeffer, S. R. (1994) *J Cell Biol* **125**, 573-582
201. Owada, M., and Neufeld, E. F. (1982) *Biochem Biophys Res Commun* **105**, 814-820
202. Kirsch, T., Paris, N., Butler, J. M., Beevers, L., and Rogers, J. C. (1994) *Proc Natl Acad Sci U S A* **91**, 3403-3407
203. Marcusson, E. G., Horazdovsky, B. F., Cereghino, J. L., Gharakhanian, E., and Emr, S. D. (1994) *Cell* **77**, 579-586
204. Turk, D., Podobnik, M., Kuhelj, R., Dolinar, M., and Turk, V. (1996) *FEBS Lett* **384**, 211-214
205. Coulombe, R., Grochulski, P., Sivaraman, J., Menard, R., Mort, J. S., and Cygler, M. (1996) *Embo J* **15**, 5492-5503
206. Marti, M., and Hehl, A. B. (2003) *Trends Parasitol* **19**, 440-446
207. Yang, X., Matern, H. T., and Gallwitz, D. (1998) *Embo J* **17**, 4954-4963
208. Pitts, K. R., Yoon, Y., Krueger, E. W., and McNiven, M. A. (1999) *Mol Biol Cell* **10**, 4403-4417
209. Li, H., Han, Z., Lu, Y., Lin, Y., Zhang, L., Wu, Y., and Wang, H. (2004) *Biochem Biophys Res Commun* **320**, 664-671
210. Lalle, M., Salzano, A. M., Crescenzi, M., and Pozio, E. (2006) *J Biol Chem* **281**, 5137-5148

211. Moorhead, G., Douglas, P., Cotelle, V., Harthill, J., Morrice, N., Meek, S., Deiting, U., Stitt, M., Scarabel, M., Aitken, A., and MacKintosh, C. (1999) *Plant J* **18**, 1-12
212. Pozuelo Rubio, M., Geraghty, K. M., Wong, B. H., Wood, N. T., Campbell, D. G., Morrice, N., and Mackintosh, C. (2004) *Biochem J* **379**, 395-408
213. Jin, J., Smith, F. D., Stark, C., Wells, C. D., Fawcett, J. P., Kulkarni, S., Metalnikov, P., O'Donnell, P., Taylor, P., Taylor, L., Zougman, A., Woodgett, J. R., Langeberg, L. K., Scott, J. D., and Pawson, T. (2004) *Curr Biol* **14**, 1436-1450
214. Al-Khedery, B., Barnwell, J. W., and Galinski, M. R. (1999) *Mol Biochem Parasitol* **102**, 117-130
215. Nelson, N., and Harvey, W. R. (1999) *Physiol Rev* **79**, 361-385
216. Nishi, T., and Forgac, M. (2002) *Nat Rev Mol Cell Biol* **3**, 94-103
217. Klausner, R. D., Donaldson, J. G., and Lippincott-Schwartz, J. (1992) *J Cell Biol* **116**, 1071-1080
218. Lahtinen, U., Dahllof, B., and Saraste, J. (1992) *J Cell Sci* **103 (Pt 2)**, 321-333
219. Enenkel, C., Lehmann, A., and Kloetzel, P. M. (1998) *Embo J* **17**, 6144-6154
220. Vashist, S., Kim, W., Belden, W. J., Spear, E. D., Barlowe, C., and Ng, D. T. (2001) *J Cell Biol* **155**, 355-368
221. Chang, H. C., and Lindquist, S. (1994) *J Biol Chem* **269**, 24983-24988
222. Caplan, A. J. (1999) *Trends Cell Biol* **9**, 262-268
223. Haug, G., Leemhuis, J., Tiemann, D., Meyer, D. K., Aktories, K., and Barth, H. (2003) *J Biol Chem* **278**, 32266-32274
224. Haug, G., Wilde, C., Leemhuis, J., Meyer, D. K., Aktories, K., and Barth, H. (2003) *Biochemistry* **42**, 15284-15291
225. Sandvig, K., and Olsnes, S. (1980) *J Cell Biol* **87**, 828-832
226. Wesche, J., Elliott, J. L., Falnes, P. O., Olsnes, S., and Collier, R. J. (1998) *Biochemistry* **37**, 15737-15746
227. Nothwehr, S. F., Ha, S. A., and Bruinsma, P. (2000) *J Cell Biol* **151**, 297-310
228. Arighi, C. N., Hartnell, L. M., Aguilar, R. C., Haft, C. R., and Bonifacino, J. S. (2004) *J Cell Biol* **165**, 123-133
229. Seaman, M. N. (2004) *J Cell Biol* **165**, 111-122
230. Seaman, M. N. (2005) *Trends Cell Biol* **15**, 68-75
231. Nakada-Tsukui, K., Saito-Nakano, Y., Ali, V., and Nozaki, T. (2005) *Mol Biol Cell* **16**, 5294-5303
232. Ghosh, P., and Kornfeld, S. (2003) *J Cell Biol* **160**, 699-708
233. Bonifacino, J. S., and Traub, L. M. (2003) *Annu Rev Biochem* **72**, 395-447
234. Ohno, H., Fournier, M. C., Poy, G., and Bonifacino, J. S. (1996) *J Biol Chem* **271**, 29009-29015
235. Ohno, H., Stewart, J., Fournier, M. C., Bosshart, H., Rhee, I., Miyatake, S., Saito, T., Gallusser, A., Kirchhausen, T., and Bonifacino, J. S. (1995) *Science* **269**, 1872-1875
236. Brodsky, F. M., Chen, C. Y., Knuehl, C., Towler, M. C., and Wakeham, D. E. (2001) *Annu Rev Cell Dev Biol* **17**, 517-568
237. Zheng, Q. S., Braunfeld, M. B., Sedat, J. W., and Agard, D. A. (2004) *J Struct Biol* **147**, 91-101